The Development and Application of Design and Optimization Methods for Energy Intensive Mechanical Systems for Challenging Environments as Applied to a Concentrated Solar Power Particle Lift System

A Dissertation
Presented to
The Academic Faculty

By

Kenzo K. D. Repole

In Partial Fulfillment
Of the Requirements for the Degree
Doctor of Philosophy in the
George W. Woodruff School of Mechanical Engineering

Georgia Institute of Technology
May 2019

The Development and Application of Design and Optimization Methods for Energy Intensive Mechanical Systems for Challenging Environments as Applied to a Concentrated Solar Power Particle Lift System

Approved By:

Dr. Sheldon M. Jeter, Co-Chair (ME)
G. W. Woodruff School of Mechanical Engineering
Georgia Institute of Technology

Dr. Said I. Abdel-Khalik, Co-Chair (ME)
G. W. Woodruff School of Mechanical Engineering
Georgia Institute of Technology

Dr. William R Callen Jr, (ECE)
School of Electrical and Computer Engineering
Georgia Institute of Technology

Dr. Hany Al-Ansary, (ME)
Department of Mechanical Engineering
King Saud University

Dr. Roger Jiao (ME)
G. W. Woodruff School of Mechanical Engineering
Georgia Institute of Technology

Date Approved: March 13, 2019

ACKNOWLEDGEMENTS

This thesis has been a great journey and test of my tenacity, confidence and belief. I would not have been able to complete it without the help of so many.

I would like to thank the One who knows which I know not. My parents, even though they are no longer with us, but it was their encouragement and sacrifices that made me appreciate the journey more. Especially and ironically the fact that my father had to ride a mine hoist to work while in university in order to provide for his young family. To my family for their encouragement, patience and sacrifices they made.

I would like to thank and acknowledge with great appreciation and gratitude; my faculty advisors Dr. Sheldon Jeter and Dr. Said Abdel-Khalik, for giving me the opportunity to work on their team and mentoring me both inside and outside the classroom. Their kindness, wisdom and patience are greatly noted.

I appreciate the time and effort my thesis committee has taken in guiding my work, giving me perspectives, I would not have thought about or encountered otherwise.

As for the unsung heroes who have helped me not sweat the small stuff but made this journey successful like Glenda Johnson, Dr. Paul Neitzel, Todd Kennedy, and Steve Bednarz. I cannot thank you enough.

Part of this work was supported by the US Department of Energy through the Sun Shot Program's project for the "Development of a High Temperature Falling Particle Receiver" (Project ID: DE-AC04-94L85000). The Prime Contractor is Sandia National Laboratories, and the Sandia's PI is Dr. Clifford K Ho. The financial and programmatic support is recognized and greatly appreciated.

TABLE OF CONTENTS

LIST OF TABLES

LIST OF FIGURES

NOMENCLATURE

A_w = sum of the nominal metallic cross-section areas of all wires in the rope (mm^2)

A_r = the circumscribed area of the rope based on the nominal diameter d (mm^2)

β = scaling factor for component

C = the nominal metallic cross-sectional area factor

CB = Cold Bin

C_c = current component cost

C_0 = base cost for component

CRPT = Central Receiver Power Tower

CSP = Concentrated Solar Power

d_{nom} = nominal wire rope diameter (mm)

DM = Design Matrix

DP = Design Parameters

DSM = Dynamic simulation model

EES = Engineering Equation Solver

EIPS = Extra Improved Plow Steel

EEIPS = Extra Extra Improved Plow Steel)

f = fill factor

F_{min} = minimum breaking force of wire rope (N)

FR = Functional Requirements

FS = Factor of Safety

HB = Hot Bin

HTF = Heat Transfer Fluid

IPS = Improved Plow Steel

IWRC = Independent Wire Rope Core

k_s = spinning loss factor

KEM = Kinetic EES based model

KS = Kimberly skip

MS = molten salts

MT = metric ton

MWth = MW-thermal

OLDS = Olds Elevators

PHR = Particle Heating Receiver

PL=Payload

PS-FR = Pseudo-Functional Requirements

R = rating factor for component

R_0 = base rating factor for component

R_g = Rope grade (N/ mm^2)

SC = Standard Rope Cores

SS 316 = 316 Stainless Steel

SSM = Spreadsheet based model

TES = Thermal Energy Storage

VFD = variable frequency driven

SUMMARY

This thesis investigated improved methods and tools for the design and optimization of energy intensive mechanical systems with specific application to high temperature particle transport for use in a particle heating receiver based concentrated solar power system. This form of concentrated solar power uses solid particles to capture the solar energy and then use it for power generation or store it as thermal energy for later use. The particle lift system is a critical component that must transport the particles from the lower temperature storage bin back to the particle heating receiver. This research is the integration and development of design and analysis tools for such energy-intensive mechanical systems and their demonstration in the conceptual design followed by the design development and optimization. The conceptual design employs an innovative multi-stage structured design process. For optimization, a unique performance and cost model based on first principles and standard cost engineering is used to generate efficiency and cost estimates. The design development, modeling, and optimization methods developed herein, while demonstrated for a particular system, are generally applicable to any energy intensive materials handling system, especially one developed for operation in a challenging environment such as the high temperature particle-laden environment in this application. This research furthers the development of design and analysis tools and the methods available for developing such energy intensive systems and the development of basic design methods. It helps ensure that potentially effective conceptual design approaches are not overlooked and that the most promising concepts are selected and developed and implemented with a minimum investment in the design and engineering effort.

CHAPTER 1. INTRODUCTION

Central Receiver Power Tower (CRPT) with Concentrating Solar Power (CSP) systems use multiple heliostats to focus solar energy on single collection location. This technology allows for more efficiently thermal to electrical energy conversion and more cost-effective thermal energy storage capacity in comparison to other solar energy solutions. CSP can be applied through different technologies that are currently employed in electricity production. Current or proposed CSP technologies range from direct heat conversion using arrays of dishes with individual gas cycle engines [1] to CRPT systems using direct steam generation [2], molten salts (MS), thermochemical storage [3] or more recently Particle Heating Receiver (PHR) technology [4].

PHR systems main characteristic is having the concentrated solar energy from a field of heliostats focus on a falling curtain of solid particles at the power tower aperture. By using these solid particles, integration of thermal energy storage is becoming economical, and higher temperatures can be reached than in existing MS systems [5].

The PHR-based CSP system is among the most promising alternatives as a cost-effective producer of renewable electric energy or process heat. However, it is generally recognized that the particle lift in such a system presents a special and interesting challenge to engineering design, analysis, and optimization making this subsystem worthy of engineering research as discussed in the earliest relevant research by Hruby [6] and Falcone et al [7]. Even though hoist skip systems have been suggested both earlier and after recent research, potential improvements and alternatives exist. Therefore, the design methodology in this research will demonstrate a method to give an independent unbiased solution neutral design whether it is a hoist skip system or another solution such as an innovative bucket elevator. In particular, the development of such a system presents a

promising opportunity for research on innovative design and systems engineering. This research and development are inherently multidisciplinary: involving conceptual design methodology; tribology, machine and structural design; mechanical, electrical, and thermal modeling; control system theory, cost engineering, and engineering optimization. In the balance of this thesis certain aspects especially relevant to a skip hoist are discussed in detail; nevertheless, other design options including innovative options will be considered and the analogous aspects of any viable alternatives will be similarly addressed.

This development must address several important criteria, constraints, and conditions. (1) Unlike many other lifts, the energy consumption of this lift is economically significant, and its energy efficiency is recognized as being so important that a high target efficiency has been assigned by potential users. (2) Another nearly unique consideration is that, unlike in most lifts, the particulate load is continually recycled with life spans of many years. As in the case with use of particles in challenging environments used on an industrial scale, wear due to excessive abrasion by the particulates during transport must be avoided. (3) Also, the extreme operating environment due to the high temperature of the load is a challenge. This condition affects the conceptual design, the choice and configuration of the materials of construction, insulation, and demands consideration of the heat leak from the lift. (4) Furthermore, with respect to the impact on design optimization, is the situation that some important practical design parameters must be critically reconsidered with respect to this design. Some examples are, the determination for the appropriate factor of safety for this application, the appropriate maximum speed of the lift, and the operating temperature limits of lubricants. (5) Design optimization also differed from usual practice in thermal systems engineering is the evident lack of suitable generic cost models to facilitate the simple but accurate life cycle cost calculations needed for design optimization. (6) Finally, the

calculation of energy efficiency for a skip hoist in particular requires a cyclical analysis fundamentally more complicated than the multiple factor models found to be common in mechanical applications [8].

The requirements for excellent energy efficiency, high temperature operation, and handling of the particulate puts great demands on the basic conceptual design of the system. A poor conceptual design cannot be engineered into an effective practical system. These requirements have necessitated a thorough technology review and required development and execution of an effective conceptual design process. The proposed strategy is the nuanced use of multiple matrix-based design methods and integrating them with thermal system design methods in order to achieve functional and economical best solutions. The use of multiple methodology design processes developed and demonstrated in this research should be applicable to other similar challenging conceptual design problems. This process is intended to be a new paradigm useful in designing systems that will operate in extreme or unusual environments as in applications where conventional design rules that overly limit design alternative should be identified and redefined, if appropriate.

Moreover, this thesis reveals a situation worthy of general design related research where inappropriate design decisions presented as general functional requirements, such as unusually large factors of safety, are found to exist. To achieve a truly optimal system, the design process should not be overly constrained by such arbitrary limits. Such suspicious or faulty “rules of thumb” must be identified and critically reviewed and either adopted or if necessary modified after thorough engineering analysis. This is especially important when the problematical rules have been embedded in standards or regulations. This thesis will demonstrate the identification of such parameters and illustrate how they can be modified or adapted to this design problem. A prime

example of such a dubious parameter is the factor of safety for lifting rope, which exists for mining applications where uncontrolled overloads can occur and human life is at risk. This high factor should not be inappropriately applied to this highly-controlled industrial application where overloads can always be prevented, and human life is never at risk during normal operation.

As with any project, cost models are used with the appropriate scaling rules that can easily be adapted and employed in optimization. Some systems-level cost models will be shown to exist even in the lift industries, but system-level models are not useful for design optimization. Furthermore, very detailed cost models are known to exist in the general machine design industries, and some even exist in the public domain [9]. However, these detailed cost models typically require not only a detailed design but also a detailed Bill of Materials and Work Breakdown Statement [10]. This level of detail is neither necessary nor desirable or even feasible for system level design and optimization. This thesis will demonstrate how the cost models similar to those used in thermal systems engineering can be developed and applied in this interdisciplinary design. It is proposed to develop a cost model flexible enough to generate unbiased cost estimates for systems as different as a skip hoist, a bucket elevator, and a friction drive device known as the Olds Elevator (OLDS).

The penultimate new research in this thesis is the development of a cyclic efficiency model for the lift system. Any highly efficient lift will surely exploit every opportunity to minimize work inputs and recover stored kinetic and potential energy. It must be noted that in this respect the challenge is greater due the two forms of mechanical energy that must be considered whereas in thermal systems the only stored energy is usually internal thermal energy. The available literature typically reports simple multiple factor models with some of the factors such as motor efficiency, easy to accept and quantify. Such models can be adapted in this research to continuously operating

lifts such as bucket elevator. In contrast with cyclic lifts, other factors, such as energy recovery factors, are much less definite.

This thesis includes the development of a component-based system model that can address this deficiency in energy modeling for cyclic lifts. Each component is modeled independently by application of first principles with a minimum of experimental information. Normally, the component models are implemented as subprograms in a simulation program or even more conveniently as functional block in a GUI-based simulation system. Numerous simple components can then readily be assembled into relatively complex system models, and the system models can be made more complex as necessary. Finally, a supervisory program will manage the transient simulation and record the results.

The simulation model can and must be used by the optimization process to develop efficiency and energy consumption data. At least two approaches are possible (1) the optimization program can execute the simulation for a point design or (2) the simulation program can be executed independently to generate needed data. As an example, an energy efficiency factor can be used in a product formula for the system efficiency. In this thesis, the efficiency investigation is implemented using the simulation model in the well-regarded Simulink platform. The result of this phase of the research is a suitable performance model. Subsequently, design tools being developed in the proposed research will represent a new approach to systematically incorporating simulation results into systematic design.

Figure 1 Proposed particle skip design charging [11].

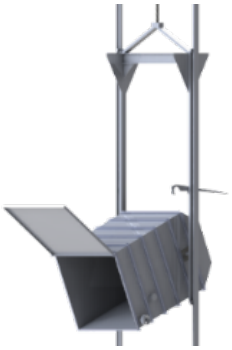

Figure 2 Proposed particle skip design discharging [11].

Figure 3 Conventional mining skip [12].

A skip hoist has been proved to be feasible in earlier research, and some specific aspects of skip hoists are addressed in some detail below. Nevertheless, all feasible designs including innovative designs will be considered. Once a suitable conceptual design, based on skips such as seen in Figure 1 and Figure 2 [11] has been generated, and cost and performance models have been developed, a suitable optimization procedure must be developed to generate an optimal design. In comparison to designs similar to a mining skips as seen in Figure 3, the conceptual design is better suited to high temperature operation. The usual criterion will be minimization of life cycle cost within the necessary constraints. New aspects of optimization include critical evaluation of constraints and thorough evaluation of the life cycle costs. New features of the life cycle cost include the cyclic simulation program and consideration of parasitic power and in a new feature the consideration of the impact of heat leak on life cycle design.

This thesis will ultimately use a proposed commercial scale 460 MW-thermal (MWth) CSP system as the proposed design, which is on the scale of other thermal conversion commercial plants. It is important to note that a completed initial conceptual design process has independently

selected the mining-type skip hoist as the best conceptual design in agreement with other research [6]. Furthermore, an initial preliminary design process has identified a particular simple drum and skip combination as the preferred embodiment. A mining hoist, especially any commercial design, is not necessary the obvious choice especially since (1) energy efficiency is barely considered commercially, (2) skip and drum designs are typically optimized for much longer lifts, and (3) heat lost is almost never a consideration. Interestingly, while the selected drum or winder design is commonly used, the preferred skip design is a type developed independently of the designs found in the initial technical review. This result demonstrates the advantages of a solution-neutral structured design. A solution-neutral design is one where the resulting design is based solely on the design process and not based on any preconceived bias. Ultimately, the lift design resulting from the overall initial design process is an innovative energy-efficient skip hoist adapted to high temperature operation.

As in any non-trivial engineering process, an early part of this and any similar design process was a literature review structured to reveal the important practices, constraints, and potential design approaches. This review is summarized in the next chapter.

CHAPTER 2. LITERATURE REVIEW

For PHR CSP systems to be successful, the means of transporting the solid particles to the power tower aperture is essential. Unlike transportation of other bulk materials such as an industrial lift or a mine hoist; the operating conditions for the solid particles is unique due to the need to transport the particles vertically to a high elevation while maintaining an elevated temperature. The elevation required would be greater than typical height when an industrial lift is employed and much shorter in length as compared to the depths experienced in a mine hoist operation.

2.1. CONCENTRATED SOLAR POWER

Concentrated Solar Power (CSP) is the method of collecting solar energy in the form of thermal energy usually to be used in the process of electric power generation in comparison photovoltaic panels convert solar energy directly into electrical energy.

In CSP, usually one of three methods are used to concentrate the solar energy and convert it to electric power. The first method is distributed collection and conversion typically using a paraboloidal dish with a Sterling heat engine or some other gas cycle engine located at the focus. A second method is distributed collection and central conversion, typically with parabolic troughs and a central steam plant.

The third method is to use a field of heliostats to concentrate the solar energy on one central location or power tower. At the power tower, the concentrated solar energy is captured today by indirect absorption into steam or molten salts [13]; however, direct absorption by solid particles [14] is currently being researched and developed. As reviewed below, this method now appears to

be potentially the most cost effective; therefore, the design of such particle lifts became available as suitable example for the approaches developed in this thesis.

2.1.1. SOLID PARTICLE CSP

Molten salts are currently the heat transfer fluid of choice used in CSP with Thermal Energy Storage (TES); however, there has been a new push to use solid particles as an HTF. Solid particles, have the advantage of being easily available [15], they do not have the problem of solidification around 240°C like molten salts [16], nor do they have the degradation of conventional molten salts around 565°C [15]. Solid particles can used in CSP applications up to 1,000°C; their life span of use extends over many years; and they can be used both as the HTF and in the TES without heat exchange thus increasing the efficiency of the thermal side of the CSP power plant [14].

The particles considered in this study are solid ceramic particles identified as ID-50 that is primarily alumina based [17]. It was decided to consider ID-50 herein, since it has been studied and used in two CSP Particle Receiver prototypes [18], [19]. Other particles and natural sands are being considered, but all are basically similar to the ID-50 beads.

2.2. DESIGN METHODOLOGIES

A challenging design should employ the best available tools including conceptual design tools. When developing and generating design concepts, many different design methodologies can be used. These methodologies can be categorized mainly into three groups of conventional methods, systematic methods, and intuitive methods [20]. As described below, several of these methods were found to be useful in this design process and would be useful in similar applications.

Conventional methods are well suited to adapting or applying existing technology or for product improvement [21]; especially for products already being mass produced. These methods can encompass analysis of existing systems, literature and patent reviews, using analogies for

design formulation, or analysis of natural systems [22]. This method is adequate for many non-challenging situations.

Systematic methods use a structured process, which uses a solution-neutral design analysis to arrive to a solution while giving allowance for both conventional and intuitive designs. Two such processes are the Axiomatic design method [23] and the Morphological Chart method [24]. The structure encourages creative but appropriate and cost-effective design.

Intuitive methods are probably better suited for product invention or innovation. Processes such as brainstorming [25] or similar methods that encourage freedom in design have been promoted to support this method. The 635 Method [26] to encourage teaming and the mind mapping [27] process to employ a visual aid fall within this group. Intuitive approaches should definitely be integrated into any attempt to develop and deploy a disruptive technology such as PHR based CSP. Indeed, a suitable mind map that visually interconnects the various considerations such as the requirements, physical constraints, application challenges, and possible lift options will be shown to be useful in promoting innovative conceptual designs.

This research will show that strategically interweaving the different design methodologies, which are further discussed below, with emphasis on systematic methods will promote the definition of a suitable unbiased solution-neutral design with a reduction in the time and resources needed to elucidate such a design.

2.2.1. THE PUGH METHOD

The Pugh method is acknowledged as one of the “best practices” in the design process method since it encourages a solution-neutral design analysis [21]. Once the initial functional requirements (FR) and selection criteria have been developed, the Pugh method can be applied to the different design concepts that have been generated to select the most suited solution-neutral

design option. During the process, one of the generated concepts is considered to be the reference design. This selection can be arbitrarily or based on experience but is ultimately immaterial. All remaining design are then compared with respect to the reference and then first scored using equally weighted selection criteria. Each design is then ranked based on their respective scores. The design with the largest scores is then compared for a second round using unevenly weighted criteria. The winning design would then be developed into a more detail design. It will be shown in this thesis how adaptable and well suited this method is for energy intensive systems to be used in challenging environments.

2.2.2. AXIOMATIC METHOD

In the Axiomatic Design method (AD), the vector of functional requirements [28] is mapped to design parameters $\{DP\}$ by the design matrix [DM]. The design parameters are the range of values required to meet the functional requirements. The parameters become the basis for a more detailed set of functional requirements from which the next level of detailed design parameters is developed. Iteration is essential until a sufficiently detailed level of parameters have been achieved to allow the design to be physically implemented [29]. The initial relationship (identified by subscript "1") can be represented by the following matrix equation.

$$\{\mathrm{FR}\}_1 = [\mathrm{DM}]_1\{\mathrm{DP}\}_1 \quad (1)$$

Here $[\mathrm{DM}]_1$ represents the first iteration of the design matrix, and $[\mathrm{DM}]_1$ may be square or rectangular. In the case of a square [DM], the [DM] may be diagonal, triangular, or fully populated. A rectangular [DM] is highly likely and deserves further attention if a robust design is to be developed. It is desired to have a one to one mapping or a square [DM], however as in many physical systems a rectangular [DM] will result. A rectangular [DM] indicates that the design has inherent redundancy, which by a case to case basis could be desirable. As the design process

continues, the requirements, the design parameters, and the corresponding design matrix will be refined and extended. As shown by Gonçalves-Coelho et al., [30] it is possible to refine or further develop the FR and thereby elucidate additional FRs that couple more directly to the DPs. Indeed, after some generations a square or nearly square DM may result. There are theorems and corollaries as mentioned by Suh [31] on how to use AD in different situation. Moreover, others like Thompson [23], who have recommend of adding non-FRs and constraints to each domain to address the need of stake holders whom might have a direct hand in the design process. Thompson also recommends having a selection criteria and optimization criteria added to the domains to also address indirect stakeholder needs. While it is important to be aware of these considerations, their implementation was not found to be necessary in this application.

Information Axiom and Independence Axiom theory [31] can now be applied to the sets of functional requirements and design parameters. They are used to determine a robust design considering the interactions between different functional requirements, different design parameters, and between the two sets. Illustrating these interactions, for use with the Independence Axiom, can be performed in a matrix form after k iterations.

$$\{\mathrm{FR}\}_k = [\mathrm{DM}]_k\{\mathrm{DP}\}_k \tag{2}$$

The ideal design solution would be a diagonal design matrix. Each functional requirement would be independent of the other functional requirements. This ideal solution is called an uncoupled design. It can be easily optimized since modification of a functional requirement can be done independent of the other requirements. Such a situation may be present in some product designs but may not be feasible in a challenging energy-intensive design.

The least desirable design would be a design matrix that produces a nearly full or full matrix. This resulting design matrix solution would be related to a coupled design. It is the most difficult

design to optimize or change since the full matrix is an indication that every functional requirement is linked or coupled to all other functional requirements. A common design matrix is a triangular matrix. This matrix form indicates that the functional requirements are coupled to each other at interfaces of different parts of the design architecture. This is known as decoupled design.

As recommend by Tseng and Jiao, [32], if the elements of the design matrix was replaced by 0-1 elements or other binary elements then visually or by using pattern recognition software module, clusters could be identified and identifying possible potential modules and module interfaces in the design. This approach was found useful and was applied in the identification of interfaces and the identification of the final selected concept.

2.2.3. DESIGN FOR MANUFACTURING

There are times when a product design is modified to increase the ease of manufacturing. This design for manufacturing normally results in more efficient assembly, cost reductions, standardized parts, or dimensions that allow for ease of transport based on the method of transportation available to the costumer [33]. In addition to the application specific requirements discussed above, every design must eventually consider manufacturing, and designs for extreme environments this requirement is especially significant. Ultimately, such considerations were important in this application illustrating that manufacturing opportunities and constraints must be considered early in the design.

2.2.4. CUSTOMER NEEDS

The initial customer needs are based on the need to transport particles for a PHR system exemplified by the specifications in US Department of Energy’s Sun Shot Program project for the "Development of a High Temperature Falling Particle Receiver". Typically, the project specifications only require the lift to (1) ensure a constant mass flow rate and (2) handle the

particles as temperatures close to or exceeding 300°C. All functional requirements and design parameters needed to define the practical design were developed based on these broadly defined needs. It must be noted that during the research process additional customer needs were added. These customer needs generally relate to having a power tower that has an operating particle temperature with a range between 700°C and 1,000°C. Also, they wanted to have the ability to upgrade their system from a cold bin particle temperature system of 300°C to one of a cold bin temperature of 700°C.

2.3. HOISTING SYSTEMS

Since hoists were an early suggested design[6], and they have been shown by recent research to have special advantages, this type has been given initial emphasis to emphasize this systematic design approach. Hoisting systems are used to transport broken material in containers lifted by ropes through shafts. Skips are the name of the conveyances used to transport ore or material in the shaft. Other components of the hoisting system are the loading stations, hoist drum, wire ropes, and electric drive motors. The particular hoist system is normally named after one of the two main classification of skip drum configurations commonly in use currently. The two main classifications of hoists are the winder drum hoist system or the friction hoist system [34] as described and distinguished below.

2.3.1. WINDER DRUM HOISTS

In winder drum hoists systems, the hoist rope is stored on a rotating drum. The drum is typically driven by an electric motor. The two most favored drum hoist systems used in large industrial applications are the Double Drum and the Double Drum Blair type. The characteristic advantage of the Double Drum Blair type has over the ordinary Double Drum is its ability to have

larger payloads due its ability of having multiple ropes per drum [34] by subdividing the basic drum into two or more sections.

These configurations, especially the Double Drum Blair type, also have the advantages of using the opposite skip as a counterweight and that each drum can be individually engaged enabling it to continue to operate if the other drum is unavailable. This advantage in potential energy recovery is obvious.

2.3.2. FRICTION HOISTS

Friction hoists consists of a large drum that has grooved liners to allow multiple rope attached to the skip to move due to the large amount of friction generated between liner and the hoist ropes. The ropes are not stored or attached to the drum. The ropes are connected to two skips on either side, thus the resulting imbalance is the payload [34]. The most common friction hoist in use is called the Koepe hoist, that was developed in 1877.

Some of the advantages of the drum hoist system are that they are best suited for high payloads at shallow depths, Blair type double drums with two ropes have a greater depth capacity compared to single rope or friction hoist, and drum hoist rope maintenance is less intensive compared to friction hoist systems.

Some advantages, of the friction hoist system, are that with multi-rope configurations have higher payload and output tonnage rates for shaft depths down to 1,520 m, have lower peak power and light power supply requirements, and they are said to be simpler to operate with lower inertia as compared to drum-based hoist systems. Both types should be considered in a solution-neutral approach.

2.3.3. WIRE ROPE

Since skip hoists are readily identified as a suitable solution, it follows that the lifting rope is the critical component. Consequently, the wire rope should be carefully evaluated and modeled. This feature is an example of how and why significant manufacturing and materials issues must be identified early in the design process. As seen as an example in the following schematic, Figure 4, wire rope is made of metal wires combined in the form of strands, and these strands are then combined to surround a fiber or another wire strand as its core. Furthermore, wire ropes can be made from either alloy steel or non-alloy steel. Consequently, different configurations and alloys are available for disparate applications.

Rope characteristics are exemplary of a critical design parameter or feature that must be identified early in the design process to have a successful result. Also, in applying the mind map method, the possibility of eliminating or replacing the lifting rope should be a consideration; thereby introducing the possibility of a truly revolutionary design in the future.

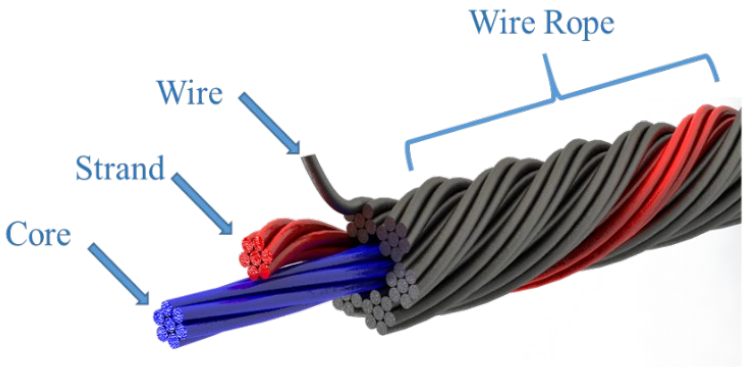

Figure 4 Illustrative diagram showing the different parts of a wire rope.

2.3.4. WIRE ROPE STRENGTH

Wire ropes can come in many different configurations however the two most common classifications are ropes with fiber cores also known as Standard Cores (SC) and ropes with Independent Wire Rope Cores (IWRC). Fiber cores are normally made from natural or synthetic fibers.

The material most commonly used for wires are low carbon steel that meet the strength values stipulated in the federal standard RR-W-410G [35]. Different forms of alloys or stainless steel can be used depending on their operational needs; for example, corrosive environments or the need for non-magnetic properties. The range of wire tensile strengths for low carbon steel are given in Table 1 and the rope grade designations used in industry seen in Table 2.

Table 1 Tensile strength grades [36].

Rope Grade	Range of tensile strength grades (N/ mm^2)
1570	1370 to 1770
1770	1570 to 1960
1960	1770 to 2160
2160	1960 to 2160

Table 2 Rope grade equivalents [36].

Rope Grade Designation	Equivalent Rope Grade
Improved Plow Steel (IPS)	1770
Extra Improved Plow Steel (EIPS)	1960
Extra Extra Improved Plow Steel (EEIPS)	2160

It must be noted that these values are determined for cold drawn wire and not the bulk material. As an example in the standard RR-W-410G [35] the value required for 316 Stainless Steel (SS 316) to meet is 1206 N/ mm^2 while the bulk ultimate strength is 517 N/ mm^2 [37]. While Carbon Steel AISI 1065 has a bulk ultimate strength of 635 N/ mm^2 in comparison to Extra Improved Plow Steel wire that has an ultimate strength of 1960 N/ mm^2. These differences indicate

that even an apparently simple feature may have practical implications that must be identified early.

Wire ropes come in different configurations of strand and wire combinations. These configurations and combinations help determine if the wire rope is more suitable for stationary guys or for hoisting, considering the rotational properties, flexibility, and abrasive resistance.

The wire rope fill factor, f, is a correction factor that represents the percentage of aggregated cross-sectional area of the actual wire strands with respect to the nominal wire rope cross sectional area. The difference between the theoretical fill factor value and the values used industry can be attributed to the fact that the theoretical fill value is for a combination of different congruent circles, that means groups of circles where each group of inner circles all have the same diameter. While in the wire rope industry, a 6 x 37 wire rope means that the number of wires in each of the 6 strands could actually range from 27 wires up to 49 wires per strand in a specific design for a nominal count of 37 wires[38]. In hoisting, a 6 x 37 configuration is used; since in general it offers rope flexibility while maintaining abrasive resistance and rotational resistive characteristics. As a result, the fill factor cannot be uniquely fixed during the design and optimization process. Never the less, it will be shown that the rope diameter can be optimized, noting that the final rope configuration and fill factor will be decided in the detail design phase.

Another factor that needs to be considered with wire ropes is the spinning loss factor, k_s. The spinning loss is due to the construction and spinning process of the wire rope during manufacturing. It takes into account the ratio between the calculated minimum breaking force of the rope and the manufacturer's specified aggregate breaking force of the wire rope [39]. Its value ranges from 0.72 for 18x7 configuration to 0.96 for Spiral 3 or 7 strands [40]. For spiral strands of 37 wires the value used is 0.94 [40].

By knowing the nominal metallic cross section area factor, the fill factor, the spinning loss factor and the rope grade, the minimum breaking force of the wire rope, $F_{\min}$ can be determined. The standardized wire rope grade values used in the wire rope industry are defined in federal specifications RR-W-410G [35]. In Equation (3), the "rope grade" is effectively the maximum allowable tensile stress in N/area.

$$F_{\min} = \frac{\pi}{4}\, k_s\, f\, R_g\, {d_{\text{nom}}}^2 \tag{3}$$

Obviously, the strength of the wire rope material is critical to the allowable load and has been addressed by a thorough literature review and analysis as presented in the next section.

2.3.5. TEMPERATURE EFFECTS ON WIRE ROPE MATERIAL

As with all mechanical systems, temperature can affect the operation and life of the machine. In the case of wire rope, the strength can drop very quickly with the increase of temperature. As seen in, Figure 5, the tensile strength of the cold drawn wires is much higher than the bulk materials, but as the temperature approaches 300°C, the advantage of cold drawing begins to vanish [41, 42]. However, the wire rope will maintain its strength to which it was relaxed to during the initial conditioning as long as the temperatures do not exceed that initial conditioning temperature [43].

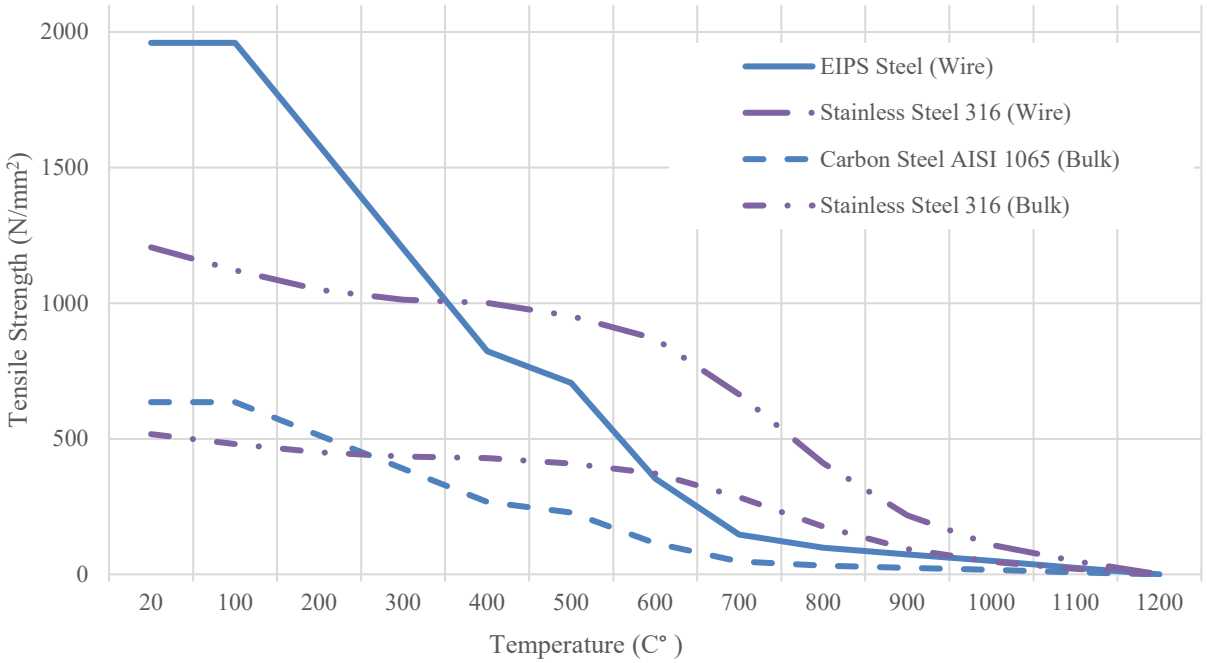

Figure 5 Temperature effects on tensile strength [35].

To summarize, the design processes, material properties and wire rope theory will all play major roles in defining a solution-neutral design for the particle lift that is an energy intensive mechanical system that has to operate in extreme temperatures. These concepts are laying the foundations for novel processes and concepts that will be presented in subsequent chapters.

CHAPTER 3. DESIGN ANALYSIS

Chapter 3 gives an example of defining the needs of the customer and the process of translating them into functional requirements and then into design parameters. From there, the design analysis is illustrated by beginning with a survey of current solutions similar to what is desired. The resulting solutions will be analyzed by different techniques such as the Pugh selection method and the Axiomatic design methods, and novel approaches that will be presented throughout the chapter. Ultimately, the determined design parameters will be used in developing a dynamic model and a cost model in the following chapter.

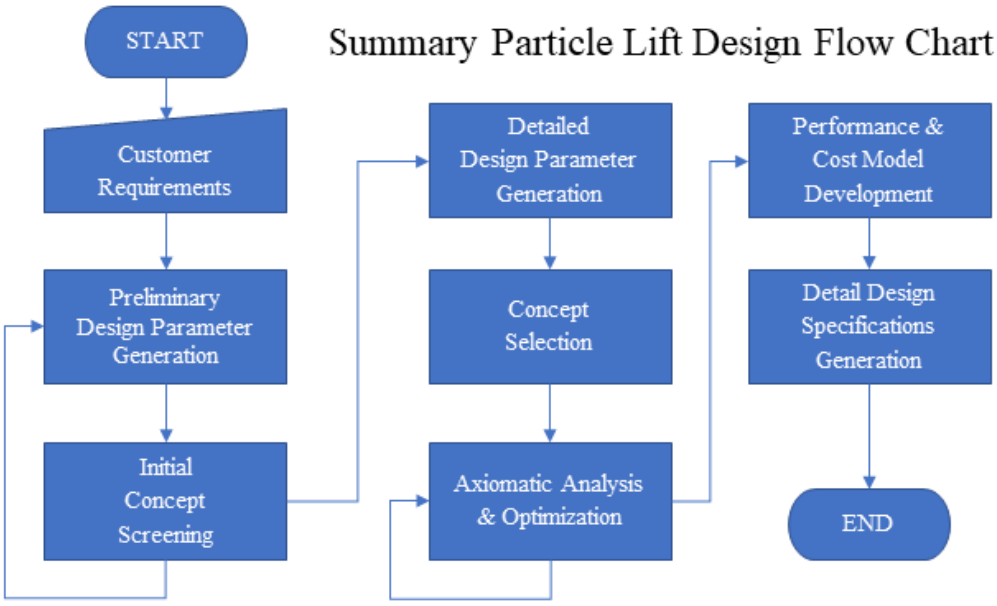

Figure 6 Summary particle lift solution design process flow.

Typically, and expectedly, the exact needs of the customer usually cannot all be specified initially. As a result, neither the FR nor the DP are usually initially defined well enough to implement the design or even support more than an initial scenario for the AD. Therefore, it was

decided to use design elicitation to develop the first level functional requirements. Moreover, in order to stay within budgetary and time constraint, a sequence of different design methodologies, as seen in Figure 6, were developed as to arrive at a viable set of design solutions for the preliminary design development for the particle lift.

3.1. FUNCTIONAL REQUIREMENTS GENERATION

As mentioned above, the customer needs could not be directly used as a set of performance specifications. Therefore, it was decided to begin the elicitation by investigating how other components of the project interfaced with the particle lift. Using this information as a basis for the design and using basic requirements as a starting point, the functional requirements seen in Table 3 were developed by identifying both internal and external constraints.

Table 3 First level functional requirements [44].

FR#	FR Description
FR01	Be able to transport vertically large number of small particulates.
FR02	Be able to maintain temperature environment <= 150°C.
FR03	Be able to operate with minimal heat loss.
FR04	Be able to operate with minimum particulate spillage.
FR05	Be able to resist wear regardless of size or hardness of particles.
FR06	Be able to have an overall energy efficiency of 75%.
FR07	Be able to have dimension that allow transportation on rail and shipping containers.
FR08	Be able to meet safety factor minimum for industry related standard.

Once the preliminary FRs were developed; the patent and literature reviews were conducted in order to find any current solutions or investigate possible designs that can aid in a viable solution-neutral design for the customer. This step completes the identification of FRs that will allow the design process to proceed to the next step, that is the patent search and literature review related to the customer needs.

3.2. PARTICLE TRANSPORTATION OPTIONS

With the first level functional requirements as a guide, conventional design methods of literature and patent reviews were conducted. This process generated particle transport options that could possibly meet the functional requirements.

3.2.1. Patent and Scientific Literature review

During the particle lift solution search, different methods were used. These included a patent search, scientific literature reviews, web reviews, industry standards, and currently known “in use” solutions. This experience indicates the range of sources needed for a successful design.

The initial result of patent searches using the terms “bulk material handling” yielded over 500,000 results. Due to this large number of results, the search results were narrowed down as much as possible trying to get useful results and seeking a solution-neutral design or not biasing the search results. The resulting search terms finally used were “bulk granular material handling” and “bulk granular material conveying systems”. These search terms resulted in a combined list of 216,104 results. From these results, which included patents from the United States, China, France, and Germany, only five results where applicable to the intended customer requirements. Most results, including the filtered results, were just an improvement or combination of different ubiquitous known solutions for bulk granular material handling. Except for the five filtered solutions the remainder of the result were intended to solve short distance transport problems.

To filter the search results, the title was first reviewed to understand the patent. If the title indicated the patent was not appropriate, that result was discarded. Next a review of the images describing the patent was reviewed. If the image indicated the patent was not related, then it was discarded. Finally, abstracts of the remaining results were reviewed, and only the most relevant results were kept. Examples of some relevant results are shown in Table 4.

Table 4 Examples of filtered patent and literature search results.

Patent Number	Patent Title
US-4195724-A	Belt elevator with staggered edge rollers
US-2009145514-A1	Aerator device inducing cyclonic flow
US-5240355-A	Dense phase transporter pneumatic conveying system
US-3982626-A	Belt elevator for bulk material
US-5076704-A	Methods of and apparatus for blending and elevating materials

3.2.2. Web Search

The search for solutions was then turned to web searches. Different search engines were used. However, most of them did not give very relevant results except for the Google search engine. The results of this search engine were used in the process. The search terms used in the patent search were used with the search engine. This resulted in a search result of 5,070,000 listings. Many of these were listings for companies and the products they sold. However, all these results were able to be classified into different categories. The categories were conveyor belts, screw conveyors, tubular drag conveyors, moving floors, top loaders, stackers, reclaimers, bucket elevators, truck dumpers, railcar dumpers, wagon tipplers, ship loaders, hoppers, pneumatic conveyors, hoists. [45]. Of this list, the relevant solution categories were chosen as seen in Table 5.

Table 5 Categories for grouping bulk material handling related to the design criteria.

Category Number	Solution Category
1	Conveyor Belts
2	Screw Conveyors
3	Tubular Drag Conveyors
4	Bucket Elevators
5	Pneumatic Conveyors
6	Hoist
7	Olds Elevator

After the categories were determined, metrics were developed to be able to compare the different solutions; especially since the different solution options have very different methods of transporting the particles. Some of the metrics were subjective, based on experience, such as the ease of installation of the option. An example of a very intensive installation would be of a very tall bucket elevator where the requirements call for a special foundation in order that the top of the bucket elevator does not tilt more than a few degrees during its service life. A very easy installation would be one that required minimal planning and tools or other resources in to install the machinery.

Other metrics were objective, such as the cost indicator, which should not be confused with a cost index. The cost indicator is defined to be a value related to capacity, height and cost which can be used to compare different solution on a level playing field. The metrics for profiling the solution categories are seen in Table 6.

Table 6 List of criteria for comparing the different categories of solutions.

Profile Criteria	Description	Score Range
Installation Ease	Can the solution be easily installed? For example, can it be assembly on the spot with the minimum amount of additional infrastructure or does additional infrastructure need to be installed for the solution to operate?	1 – very easy to 5 – very intensive
Cost Indicator $ /(mt/h-m)	The cost approximation of an option that is similar in size to design criteria divided by the product of the industry standard operating rate in metric tonnes per hour and the height used to determine the approximate cost.	
Temperature Factor	The subjective ease at which the option could be modified to operate at higher temperature to reduce the heat loss of the particles during transportation.	1 – very easy to 5 – very intensive
Operating Capacity (mt/h)	The industry standard capacity range closest to the solution capacity requirement	e.g. 700 mt/h to 1000 mt/h
Operating Temperature	The industry standard temperature operating range closest to the solution temperature requirements.	e.g. 100°C to 500°C
Maintenance Ease	Can the solution be easily maintained? For example, can it be maintained on the site with the minimum number of additional tools or does the solution need specialized equipment or need to be taken off site for maintenance?	1 – very easy to 5 – very intensive
Transport Ease	Can the solution be easily transported to the site? For example, can it be transported intact or with minimal assembly required using standard forms of transport or does require a team of specialized technicians, specialized transport and changes to infrastructure to transport it to the site?	1 – very easy to 5 – very intensive
Compatibility (with other systems)	Can the solution easily be integrated with another solution in the list? This is generalized and not specific to a one to one match with another particular option.	1 – very easy to 5 – very intensive
Quoted Height (m)	The height used or referenced related to the approximated option cost. For example, the shortest height found with a similar operating capacity as the design criteria for a Hoist system.	
Cost @ Quoted Height ($)	The approximated system cost with respect to the quoted height and operating capacity that could be determined by literature or a cost index.	

The fully populated table for the different categories solutions is seen in Table 7.

Table 7 Category comparison table.

Name	Conveyor Belts	Screw Conveyors	Tubular Drag Conveyors	Bucket Elevators	Pneumatic Conveyors	Hoist	Olds Elevator
Installation Ease	2	2	1	4	2	5	3
Cost Indicator $ /(mt/h-m)	21.1	8.6	18.9	3.6	2,940.0*	0.1	8.3
Temperature Factor	4	3	2	1	4	1	3
Operating Capacity (mt/h)	7200	304	136	1600	3	6000	7000
Operating Temperature	400°C	650°C	300°C	> 300°C	> 700°C	> 200°C	650°C
Maintenance Ease	2	2	2	4	2	5	4
Transport Ease	2	3	2	5	3	5	3
Compatibility	1	1	1	1	1	5	1
Quoted Height (m)	138	43	120	30	144	630	11
Cost @ Quoted Height ($)	5,233,000	37,000	206,000	175,000	317,520	246,300	206,000
• This value has been verified.							

Once the profile table was developed, then the different categories were compared using the functional requirements that were elicited from the customer needs. These functional requirements were then augmented to enhance the ability to compare the different categories on a more level playing field. As mentioned by Tseng and Jiao, [46] functional requirements can be heavily dependent on the designer's insight about a design and as suggested by Thompson [23], that non-functional requirements are sometimes needed. The additional functional requirements coined here as Pseudo-Functional requirements (PS-FR) are not elicited from the customer needs and will not be used after the category comparison but are vital to make the comparison as solution-neutral as

possible. This novel approach of using these PS-FR are based on the subjective and objective metrics developed above. The full list of functional requirements is listed in Table 8.

Table 8 The functional requirements used in the comparison of solution categories.

FR#	Description
FR01	Be able to transport vertically large number of small particulates.
FR02	Be able to maintain temperature environment <= 150°C.
FR03	Be able to operate with minimal heat loss.
FR04	Be able to operate with minimum particulate spillage.
FR05	Be able to resist wear regardless of size or hardness of particles.
FR06	Be able to have an overall energy efficiency of 75%.
FR07	Be able to have dimension that allow transportation on rail and shipping containers.
FR08	Be able to meet safety factor minimum for industry related standard.
PS-FR09	Be able to resist frictional effects due to properties of particles
PS-FR10	Cost Indicator metric
PS-FR11	Ease of modifying for high temperature operation
PS-FR12	Ease of Installation
PS-FR13	Ease of Maintenance

The Pugh Matrix, as seen in Table 9, was then used to narrow down the most viable option. The Olds Elevator was used as the reference design during the Pugh method since it was used in the only existing PHR prototypes [47].

Olds Elevators [48], are devices that drive the particles by friction and are similar in appearance to screw augers and provide a continuous mass flow at low but usually acceptable efficiency. As the lift height and operating temperature requirements increase so does the cost increases.

Specialized bucket elevators have the ability at temperature greater than 200°C [49]. The drawback of using a bucket elevator is that the shaft transporting the particles would have to be kept close to or at the same temperature as the particles to maintain an acceptable heat loss. Furthermore, due to the methods of charging and discharging the buckets, this system would experience a high spillage rate compared to other options. Nevertheless, the bucket elevator retains advantages.

Conveyer belts, unlike the bucket elevators, have little spillage but they are not able to convey particles without a large heat loss. In addition, they are difficult to integrate into tall towers.

The Pugh method was applied to these options, as illustrated in Table 9, resulting in the bucket elevator solution being the most suitable of the different options to pursue into greater preliminary detail.

However, this analysis should not be considered the final step in selecting a viable option since defining FRs, as mentioned above, are based on experience and for a need to have a systematic and repeatable selection process that considers key factors that sometimes cannot be directly included into option comparison or even a weighted option comparison.

Table 9 Pugh Analysis of Concepts using Pseudo-Functional Requirements

FR#	Conveyor Belts	Screw Conveyors	Tubular Drag Conveyors	Bucket Elevators	Pneumatic Conveyors	Hoist	Olds Elevator (reference)
FR01	+	-	-	-	-	-	0
FR02	-	0	-	0	+	-	0
FR03	-	0	+	+	-	+	0
FR04	+	0	+	+	+	+	0
FR05	+	0	+	+	-	+	0
FR06	0	0	+	+	-	+	0
FR07	0	0	0	0	0	0	0
FR08	0	0	0	0	0	0	0
PS-FR09	+	0	-	+	-	+	0
PS-FR10	-	-	-	+	-	+	0
PS-FR11	-	0	+	+	-	+	0
PS-FR12	+	0	+	-	+	-	0
PS-FR13	+	+	+	0	+	-	0
Sum +	6	1	7	7	4	7	0
Sum 0	3	10	2	4	2	2	13
Sum -	4	2	4	2	7	4	0
Net Score	2	-1	3	5	-3	3	0
Rank	4	6	2	1	7	2	5

Therefore, by using a novel approach, the options were further analyzed by penalizing each ranking based on the values in the profile table, Table 7, in a second and third round of comparisons. The penalty was conducted by multiplying each option rank by its respective table value. After that each option was then re-ranked.

This method was chosen since having a weighted comparison again draws in the subjectivity in assigning the value or percentage assigned to each FR. Moreover, using this novel approach, by penalizing each ranking, the comparison process can address factors that might not seem obvious in the beginning but can have major consequences for the design.

Table 10 Final ranking of each concept after 3 rounds of comparison.

	Comparison Rounds					
Particle Lift Options	1 (Pugh)	2 (Cost)	3 (Temp.)	Avg. of Rounds	Final Rank	Pareto Choice
Conveyor Belts	4	6	6	5.3	6	
Screw Conveyors	6	5	4	5.0	5	
Tubular Drag Conveyors	2	3	3	2.7	3	
Bucket Elevators	1	2	2	1.7	2	✓
Pneumatic Conveyors	7	7	7	7.0	7	
Hoist	2	1	1	1.3	1	✓
Olds Elevator	5	4	5	4.7	4	

As seen in Table 10, where the column labeled 1 is the considered round 1 where the Pugh selection analysis was conducted. Round 2 is, shown in the following column labeled 2, where the cost metric indicator from Table 7 is used as a penalty value and multiplied with each option's corresponding rank value from round 1. The respective option product values were then re-ranked.

Once the options were re-ranked after round 2, another round of penalization and ranking was conducted. In round 3, the column labeled as 3 in Table 10 the options were then subjected to the penalty of the temperature factor and re-ranked based on the resulting score. Without using a temperature penalty, a possible design that excels at cost and mass flow capacity could be selected as a favorable design, even if its temperature factor was weighted poorly against other FRs. However, after material transport capability, temperature plays a major role in successfully accomplishing the customer needs. Temperature performance can be dominating in this and similar design for extreme environments.

The resulting score based on averaging all round scores, and then each option obtained a final rank. The Pareto principle [50], also commonly known as the 80/20 rule was applied to these ranking and the top 20% options were selected for a final analysis and comparison.

The Pareto principle was applied based on the concept that the top 20% of the options will address at least 80% of any unknown unknowns, famously coined by Joseph Luft and Harrington Ingham [51] in their development of the Johari window and then subsequently adapted for risk management in NASA and in general by the field of risk management [52].

By applying this novel use of the Pareto principle, it ensures in having at least 2 options at the end, this ranking process helps to reduce any issues that could arise that have not been anticipated or any unknowns so early in the design process without the need to develop a more detailed level of design options.

The top two options, of the Bucket Elevator and the Hoist, were compared for their pros and cons and the net was evaluated with again the Hoist being the favored solution-neutral viable option as seen in Table 11.

Table 11 Pro and Con analysis of top 2 rank concept solutions.

	Bucket Elevators	Hoist
Pros	Can produce continuous flow of particles.	Less sensitive to vertical angle.
	Possibly can operate with little to no lubrication in main casing.	Easier to insulate particle to the environment.
	Can have multiple working together	Can have multiple working together.
	Can operate close to operating temp of 300°C or higher.	Maintenance is cheaper since main maintenance part will be the rope replacement.
	In general, efficiency is around 85%	Can be integrated into structure.
		Easier to insulate the shaft to maintain a higher environmental temperature to reduce heat loss to the surroundings.
		In general, efficiency is around 95% with some form of counter weight.
Total Pros	5	7
Cons	Need to have a specialized and expensive foundation built to reduce vibration and not have the bucket elevator tilt more than a few degrees. Very difficult for desired height.	Particle flow is intermittent.
	Encasing for Bucket elevator has large surface area to prevent heat loss.	Particle charging, and discharging may cause flow shock to the system.
	Can carry small bucket loads but overall vertical plus chain and bucket will be very large.	Wire rope will need lubrication to prevent martensite from forming in rope during operation by helping to redistribute heat due to friction.
	Maintenance will be more expensive.	Rope strength decreased due to operating temperature.
	Cost per linear meter will be more expensive.	Might need to operate below typical lubrication flame temperature of 200°C.
Total Cons	5	5
Net	0	2

3.3. COMBINATORIC OPTIMIZATION OPTIONS

In general, most customer needs are intended to be fulfilled using a single design, however there are times in which there is a possibility where a combination of different options produce a more viable solution to the customer. Therefore, the option selection process was reconducted with this combinatorial concept in mind.

The exact method of combinatorial analysis and optimization depends greatly on the nature of the solution use and design characteristics of each possible solution option. For example, are the solution combinations a discrete combination or a continuous range of combinations? Or do the combinations follow a linear pattern or exponential scale? Some optimization methods considered were the simplex method [53], the Nelder-Mead optimization [54], greedy methods [55], etc.

3.3.1. Optimization Options

Preliminary combinatorial optimization was conducting using the simplex and the Nelder-Mead optimization methods. The Nelder-Mead optimization method is a modified faster version of the simplex method. The greedy methods were not used since they are known to be exceptional in finding local minimums or maximums but fail at finding a global minimum or maximum.

The optimization was based on finding the best combination of solutions that minimized the overall cost of the solution. The optimization was conducted in the Engineering Equation Solver (EES) program and the results were not realistic where the optimization would suggest a half unit of one option at 137.5 m in height with 0.5 m of a single unit of another option. Only after

eliminating some of the options did the optimization converge onto a single hoist system running the full length of travel.

Randomly eliminating options is an unsatisfactorily means of optimization and the entire purpose of the combinatorial optimization is to develop a systematic and reproduceable method in finding a solution. Therefore, the novel approach developed was to first use information from the profile table, as seen in Table 7, and develop an inter-compatibility matrix as seen in Figure 7 to be used to develop any relationship between the different options in order to optimize on solution cost.

Options	Conveyors Belts	Screw Conveyor	Tubular Drag Conveyor	Bucket Elevator	Pneumatic Conveyor	Hoist	Olds Elevator
Conveyors Belts	●	○	○	○	○	•	○
Screw Conveyor	○	●		○		•	
Tubular Drag Conveyor	○		●	○		•	
Bucket Elevator	○	○	○	●		•	○
Pneumatic Conveyor	○				●	•	
Hoist	•	•	•	•	•	●	•
Olds Elevator	○			○		•	●
LEGEND	● Very Compatible		○ Compatible		• Small or Difficult Compatibility		

Figure 7 Matrix for analysis of the inter-compatibility of solution concepts.

Next, the concept of having pictorial representation of the optimization combinations, examples are seen in Figure 8. This concept was used in facilitating the selecting of the most viable

combinations with the aid of using the Taguchi method and other design of experiment techniques in order to reduce the number of combinations to a viable few.

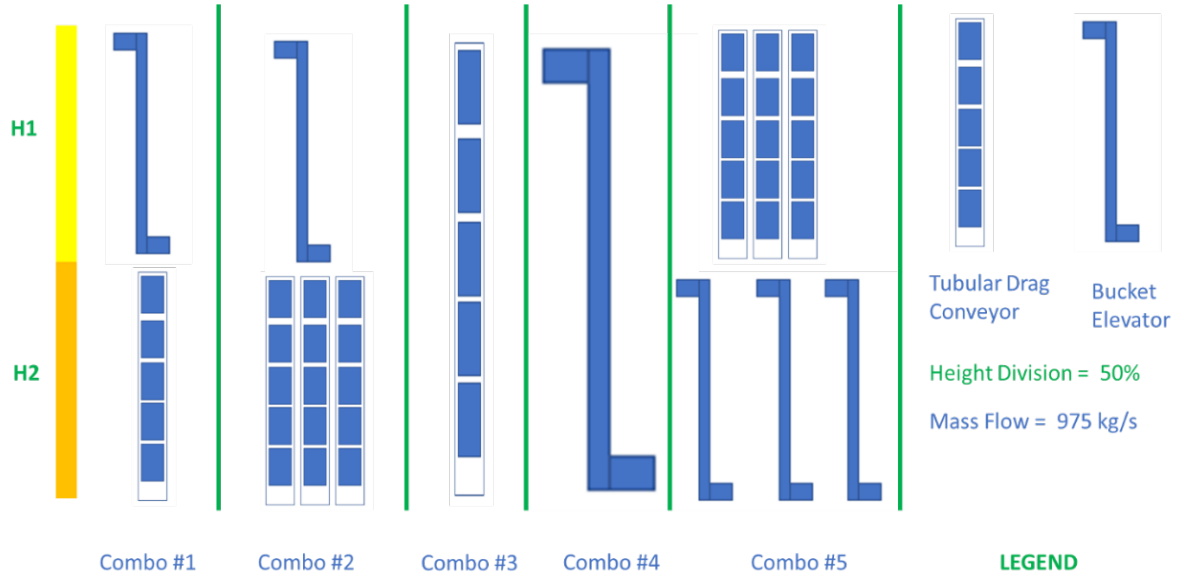

Figure 8 Concept combination for optimization analysis using pictographs

The reduced set of combinations are represented in Table 12 and in Table 13. In Table 12, only single solutions with different quantities running the full length of travel were considered.

Table 12 Group 1 of reduce list of concepts for combination analysis.

Options	Combinations		
Tubular Drag Conveyor	1	2	3
Bucket Elevator	1	2	3
Hoist	1	2	3
Height = 100% (Each cell is one combination)			

While in Table 13, combinations of the three most viable inter-compatible solutions where considered with the half way mark of travel used as the transition point between solutions. Any other combination of the transition point was not considered since there is an inherent and unfavorable base cost for short lifts in each proposed solution.

Table 13 Group 2 of reduce list of concepts for combination analysis.

Options	Combinations					
Tubular Drag Conveyor	1	2	3	0	0	3
Bucket Elevator	2	2	1	1	2	0
Hoist	0	0	0	1	2	2
Height = 50% (Each column is one combination)						

The combinational optimization was then conducted by solving for the cost indicator. The resulting cost values were then normalized, as seen Table 14, since this value was not representative of the actual cost of the solution but used merely to determine the most cost-effective combination of solutions. As with the preliminary results, the single hoist system running the full length of travel was determined to be the most cost-effective combination of solutions.

Table 14 Normalized Cost comparison for different solution combinations

Tubular Drag Conveyors	Bucket Elevators	Hoist	Height (%)	Normalized Cost
0	0	1	100	1
0	0	2	100	2
0	0	3	100	3
0	1	0	100	66
0	2	0	100	132
0	3	0	100	198
1	0	0	100	232
2	0	0	100	464
3	0	0	100	697
0	1	1	50	34
0	2	2	50	67
1	2	0	50	232
2	2	0	50	298
3	0	2	50	349
3	1	0	50	381

3.4. SKIP LIFT ALTERNATIVES

The Pugh analysis and the novel combinational optimization analysis both determined that the Lift Hoist System was the best solution for the given first level functional requirements when compared to the other transportations system. Next, the different types of hoist systems were investigated and based on the characteristics of each system and functional requirements, a more detailed level of design parameters were developed. These design parameters aided in deciding which hoist design was best suited to achieve the customer needs.

The main hoist systems used in mass transport of materials are employed in the mining industry. The systems currently in use are Front Dump skips, Bottom Dump skips, Arc Gate skips and overturning skips, that are more commonly known as Kimberly skips (KS). Our earliest design favored a top loading bottom dump skip [56] since it maintains the vertically downward flow of particles; however, the later solution-neutral design shows that the overturning skip has several advantages.

The main basis that determined which skip is used for a particular application are, (1) the ease of high temperature operation, (2) maintenance requirements, (3) effective thermal insulation capability, (4) height required for operation, and (5) amount of spillage during operation.

Front Dump skips have a vertical sliding gate as part of the lower section of the skip. This gate is oriented on the vertical side that is facing towards the discharge chute. This skip is charged from above and then discharged from this lower trap door type gate. It is suspected that there will be a high spillage rate due to the fine size of the solid particles to be used in the PHR. These particles have the size of approximately 250 nm. Front Dump skips are known to be able to carry large volumes while putting the least amount of stress on the headframe [57].

Bottom Dump skips are similar to Front Dump skips where they are charged from above. As the name suggests, they are discharged via a gate as a trap door located on the bottom of the skip. This skip design has the advantages of being rugged, light weight, and in comparison, with other skip types does not require excessive additional operation height during use. The disadvantage is the large about of spillage expected due to the location of the discharge exit and the nature of the solid particles in use.

Arc Gate skips are comparably rugged and more safe in comparison to the other skip types [57]. As with the other skips they are charged from above and then discharged from the side of the lower section. The discharge exit is an "arc gate" or a pivoting gate. As with the Bottom Dump skip and the Front Dump skip, this design will also have issues with large amount of spillage during operation. The many moving parts of the skip puts its design at a disadvantage with regards to the high temperature and fine particle environment that would increase the risk of failure or fouling.

Kimberly skips, unlike the other skip designs, are charged and discharged from a single entrance at the top of the skip. During charging, the skip is in a vertical position. Once the skip reaches its discharge location, the skip's set of scroll wheels engages with the guide scrolls located on the shaft walls. This allows a controlled rotation of the skip through the dump zone. At full discharge the skip has rotated to approximately 120° with respect to its original vertical position.

In general, KS are known to have initial lower cost, lower maintenance cost and higher service lives when compared to other skip designs [57]. An advantage KS have over the other skips designs is that it would have a lower spillage rate due to its design. The disadvantages of the KS design are that it requires greater width clearance, larger headroom, and exerts larger amounts of headframe stress due to the need to rotate the skip during discharge [34, 58]. As a result, Bottom

Dump and Arc Gate skips are more widely used than KS, but the KS is more compatible with CSP applications.

In work conducted [56] prior to this thesis, two skip designs appear to be the most promising solutions. These skip types were the Arc Gate and the Kimberly skips. This experience illustrates the advantage of mock ups or early concept prototyping, which may be a way to encourage solution-neutral designs. Therefore, scale models were developed for qualitative comparison. The results of the comparison indicated that the KS would be the easier to effectively insulate and give the most reliable service during high temperature operation.

3.5. HOIST SYSTEM ALTERNATIVES

The hoist winding drum system is an important subsystem of the particle lift. As mentioned above, there are two main types of hoists in wide use, the drum hoist and the Koepe friction hoist. The friction hoist is an attractive solution due to its low cost and wide use, however it was eliminated in the initial selection process due to concerns about its reliability to maintain friction during high temperature operation. As a result, the Blair drum hoist system was considered.

After using the Pugh method to select the hoisting lift system for the particle lift design a mind map as seen in Figure 9 was used to elicit or organize the different aspects of the design that needs to be accounted for in the design parameters. It needs to be noted that as in the preliminary selection process and in the above mind map of Figure 9, temperature and heat loss were found to be major issues that need to be investigated during the design process. This resulted in a more detailed level of the DP. At this point the Independence Axiom analysis would be employed.

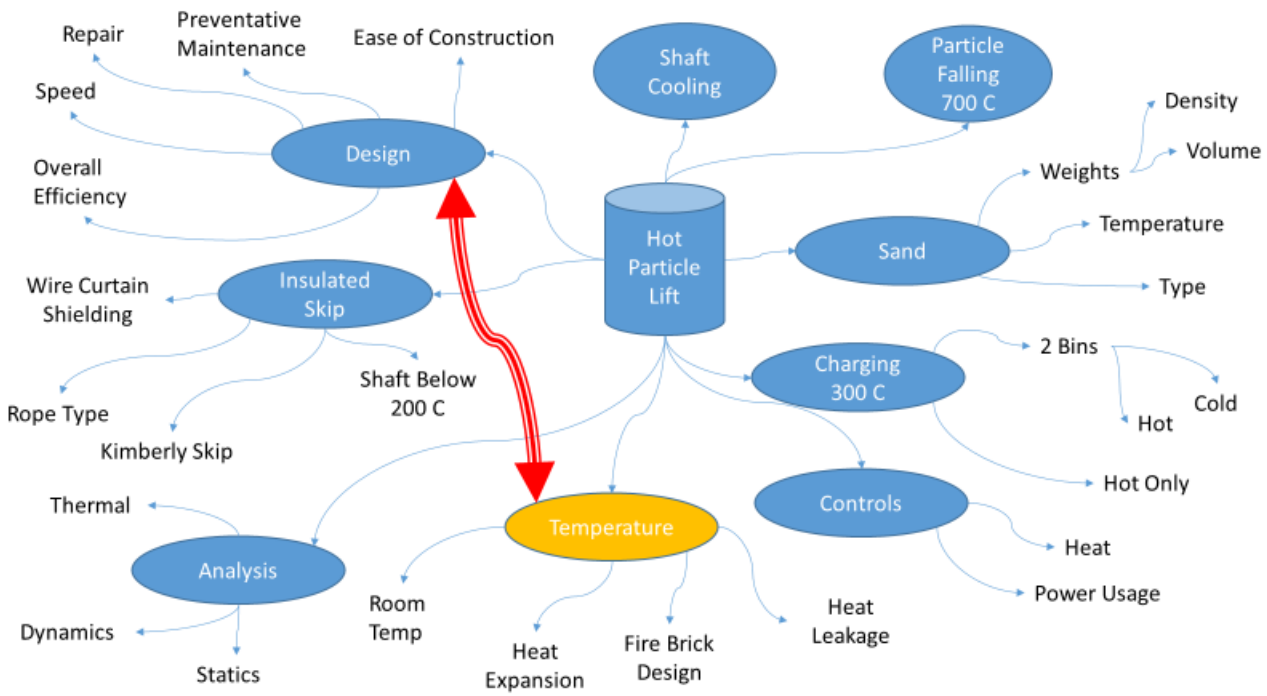

Figure 9 Kimberly Skip Mind map for drill-down of FR.

Table 15 Detailed functional requirements [44]

FR#	Description
FR01-01	Be able to transport 250 nm size particulates.
FR01-02	Be able to transport particulates up to 140 m.
FR01-03	Be able to transport 20000 kg per minute.
FR02-01	Material must be able to maintain desired in 200°C shaft.
FR02-02	Lubricants must tolerate temperatures up to 150 to 200°C.
FR03-01	Skip must be insulated.
FR04-01	Overall system must have less than 1% spillage recovery.
FR05-01	Impact surfaces must resist abrasion.
FR05-02	All moving parts and ropes need to resist or avoid abrasion.
FR06-01	Be able to have an overall energy efficiency of 75%.
FR07-01	Skip maximum dimension must not exceed container size.
FR08-01	Single rope preliminary factor of safety 5 [59].
FR08-02	Rope nominal diameter cannot be > 76 mm.
FR08-03	Rope core rope must withstand shaft temperatures.
FR08-04	Overall system should have factor of 5 [60, 61].

This required that, based on the mind mapping results, a drill-down (meaning a more detailed in a design context) version of the FR was developed as seen in Table 15 and the corresponding drill down DP as seen in Table 16. The Axiomatic analysis for the combination of the KS and the Blair drum indicated that it is a highly suitable design but not an uncoupled design. Coupled designs are expected in energy-intensive applications, so this feature is not a disqualification.

Table 16 Detailed design parameters [44]

DP#	Description
DP01-01	Kimberly skip design.
DP01-02	Blair drum type.
DP01-03	AC Electric drive motor.
DP02-01	Metal for skip is of SS 316-H material 3 mm thick.
DP02-02	Lubricant with NLGI No 2 and flash point over 200°C.
DP03-01	Suitable fire brick with needed properties identified.
DP04-01	Olds Elevator in sump to remove spillage.
DP05-01	Loading and unloading angles greater than 20 degrees.
DP05-02	Bearing and joint material with Hardness > ID-50K.
DP06-01	Lift efficiency > 75%
DP07-01	Skip dimensions L x W x H is (2 m x 2 m x 12 m).
DP08-01	Revised rope safety factor of 3.
DP08-02	Rope diameter between 31.7 mm and 50.8 mm.
DP08-03	Rope is EIPS 6x37 IWRC
DP08-04	Rope safety factor > 3 & skip safety factor > 5.

3.5.1. REFINING PARTICLE LIFT DESIGN

The resulting axiomatic matrix, as seen in Figure 10, is approximately a triangular matrix indicating that the design is largely decoupled. The coupled portion of the matrix is clustered around the FR of temperature and rope selection. Therefore, these criteria are critical for a successful design.

A novel method was developed in which AD benefits are incorporated in a systematic approach with reproducible results. As such this means that any critical aspects and issues identified during the AD process need to be addressed. This is especially true for complex designs. Suh asserts that this process encourages better solution-neutral designs that have increased quality and reliability [29]. In an attempt to increase reliability of complex systems Shao et al., [62] advocates AD as early in the selection and design process as possible. Attempts made by Nepal et al., [63] have focused on identifying failure modes using AD with regards to the complex interactions between assemblies and sub-assemblies and by Sy et al., [64] in developing a failure coefficient in order to reduce risk in designing components and the interactions. However, these attempts are applied only during the later stages of the design process such as the embodiment design or detail design. This delay results in an increased risk of failure and failure modes already built into the solution. Applying AD early as in this application avoids this failure mode.

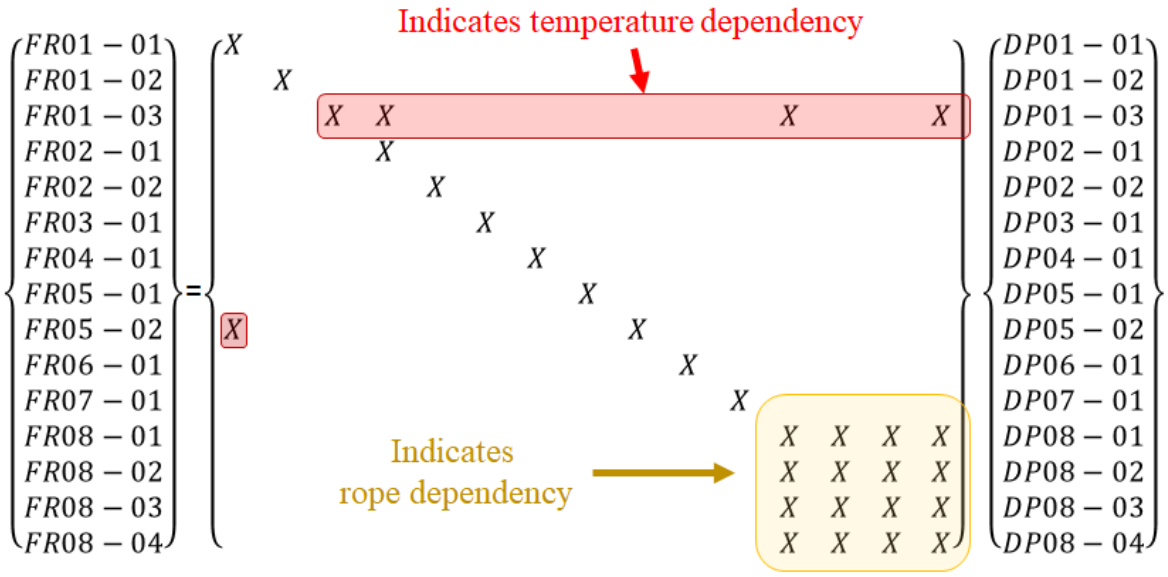

Figure 10 Independence Axiom Matrix analysis for KS with Blair drum [44].

These issues were addressed they by identifying them in the AD process: therefore, analysis is conducted on the proposed components of the system in earlier stages of design where modifications are easier and more cost effective. As seen in Table 17, potential environmental effects that could lead to failure in components was conducted using a ranking system. Where each effect was ranked from having no to minimum effect to having major influence on the particular component. The rankings are then summed. The Pareto principle was used to identify the most at-risk components and the effect that has the most influence on possibly failures during the life of the solution.

In the case of this design process, the Drums, Rope and Skip were identified as the components most susceptible to failure and that temperature being the greatest influencer on failure.

Table 17 Analysis of environmental effects on components for selected concept.

Components	Chemical	Temperature	Wear	Friction	∑ Failure Types
Power	0	3	0	0	3
Drums	1	3	0	1	5
Rope	1	3	1	1	6
Bail	1	1	0	0	2
Skip	1	5	1	0	7
∑ Components Effects	4	15	2	2	
Effect Ranking	0 – None to minimum effect, 1 – Moderate, 3 – Considerable, 5 - Major				

Next the failure modes due to temperature where investigated, as seen in Table 18 and ranked in a deeper analysis based on ranking and the Pareto principle. This resulting in the rope and skip designs being influenced the greatest by temperature and that the generalized temperature failure modes should all be addressed.

Table 18 Deeper analysis of thermal effects on components of selected solution.

Components	Thermal Fatigue	Thermal Expansion	Heat Transfer	Strength	∑ Thermal Effects
Power	0	0	3	0	3
Drums	0	1	1	1	3
Rope	3	3	3	5	14
Bail	1	1	1	1	4
Skip	5	5	5	5	20
∑ Components Effects	9	10	13	12	
Effect Ranking	0 – None to minimum effect, 1 – Moderate, 3 – Considerable, 5 - Major				

3.6. COMMERCIAL SCALED PARTICLE LIFT REQUIREMENTS

Based on the information gathered from the Axiomatic design matrix and analysis, concept drawings were developed in order to see how the design would integrate into a CSP tower, to develop and optimize a model for material specification and rope selection, and to develop ultimate design specifications catering to the proposed commercial scaled, 460 MWth CSP tower. The concept integration and design concept drawings with method of operation are shown in Figure 11 and Figure 12. The success of the earlier design steps is illustrated and demonstrated by the ease with which the selected particle lift solution and design can be integrated into the overall system. The ultimate optimization of the design specifications is addressed in CHAPTER 4.

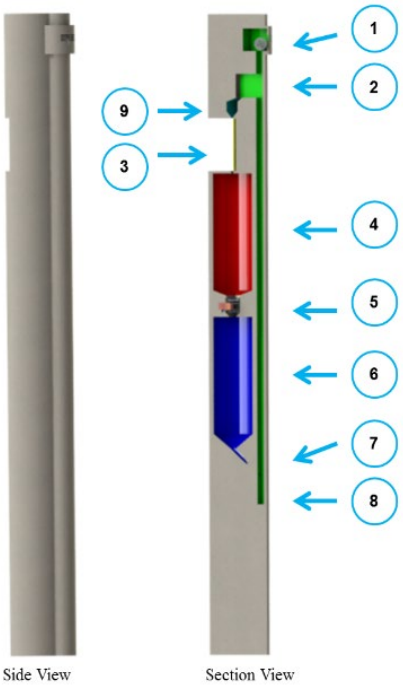

No.	Name
1	Lift Machine Room
2	Lift Discharge Chute
3	Particle receiver
4	High Temperature TES Bin
5	PWF Heat Exchanger
6	Low Temperature TES Bin
7	Lift Charge Chute
8	Lift Shaft
9	Top hopper

Figure 11 Overall schematic [65].

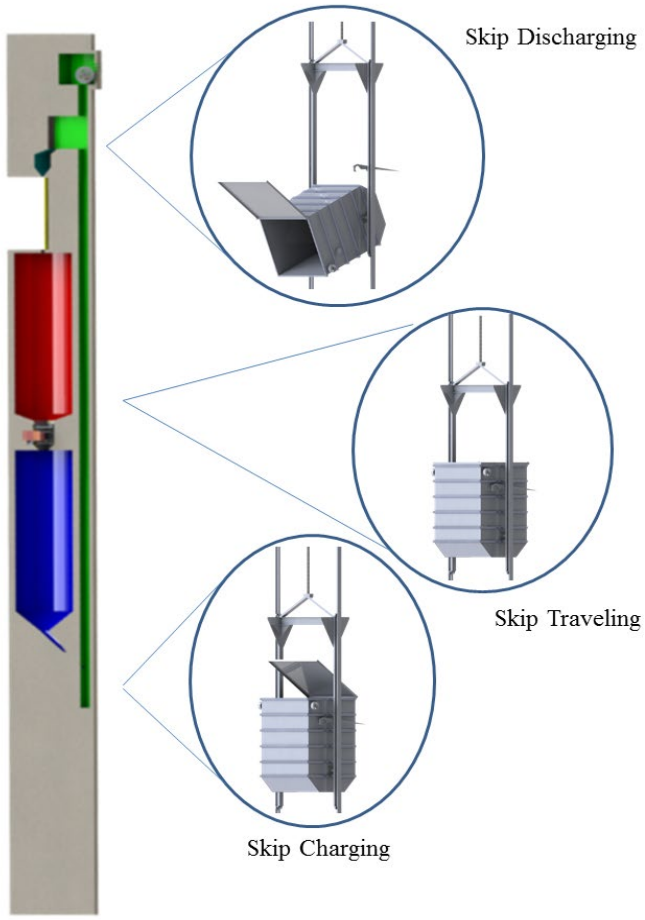

Figure 12 Conceptual insulated Kimberly skip operating positions [65].

It must be noted that to reduce heat loss; an insulated top hatch for the skip was included in the design. SS 316 wire rope was initially selected for its high temperature strength, corrosion resistance, and durability. However, upon further analysis EIPS was considered due to its lower comparative cost and high strength up to 250°C. The resulting commercial particle lift design specifications are seen in Table 19. These design specifications are for both designs the customer requested.

Table 19 Commercial particle lift design specifications [44].

Design Specification	Value (300°C)	Value (700°C)
Power Capacity of Tower	460 MWth	460 MWth
Cold Bin Temp	300°C	700°C
Shaft Temperature	150°C	150°C
System Mass Flow	979 kg/s	979 kg/s
Skip installed	2 skips	2 skips
Estimated Skip Dimensions (L x W x H)	2m x 2m x 8.5m	2m x 2m x 11.5m
Ropes in use per skip	2 ropes per skip	2 ropes per skip
Rope Type	EIPS 6x37 IWRC	EIPS 6x37 IWRC
Rope Diameter	44.5 mm (1 3/4 in.)	50.8 mm (2 in.)
Drum to Rope Diameter Ratio	80	80
Rope wraps (including dead wraps)	20	20
Electric Motor	AC Induction Motor	AC Induction Motor
Motor Size	2100 kW	2800 kW
Overall Safety Factor	3	3

A factor of safety of 3 was used for the tensile strength of the wire rope. The reason is that the particle lift, and the wire rope should be considered as an industrial application since there is no direct human interaction as opposed to an elevator or a mine skip with a miner cage attached to it. Therefore, the FS was based on the government regulations for industrial applications such as steel pipes [66]. Otherwise, the factor of safety would have to range between 7 to 8 for skips that have direct human interaction [61] or the FS would have the industry accepted value of 5 [59].

As a result, the nominal rope size of 44.5 mm (1 3/4 inch), was selected for a two-rope skip configuration for a CB temperature of 300°C design and the nominal rope size of 50.8mm (2 inch), was selected for a two-rope skip configuration for a CB temperature of 700°C design.

The top hatch was designed to be very simple in order to increase its reliability during operation at high temperature. The design was developed based on physical models and investigating similar applications such as dump truck operations. The hatched is opened or closed by the skip motion in relation to the location in the shaft. This eliminates the need for hydraulic or mechanical actuators to operate in an extreme environment. The design is intended to make

leakage negligible and reduce temporary spillage during charging and discharging to much less than 0.1%.

To summarize, this chapter shows with the aid of a novel solution-neutral design process, how an energy intensive extreme environment design solution can be developed. The process spans collecting customer requirements, to developing functional requirements and design parameters through axiomatic analysis until a final concept is developed.

It was shown in the transformation of the customer requirements to the development of the design parameters, that different successful novel approaches were used. As an example, in the literature reviews and patent searches, the novel method of using simple methods of result elimination and reduction through the use of scanning titles, then reviewing descriptive images and finally reviewing detailed abstracts.

Once the initial functional requirements could be successfully defined and the possible generalized solutions identified then a novel method of developing datum criteria was employed to compare the solutions in an initial concept screening. Firstly, a cost indicator was developed in order to allow a fair comparison between possible solutions that ordinarily would be difficult to compare. Next, using the Pugh method of screening with the novel approach of penalty ranking, then applying the Pareto principle two general solutions were identified. This process has the intention of reducing the influence of unknown bias in the selection and accounting for unknown unknowns that can never be fully accounted for in such novel designs.

In some design situations, a single solution might not be the most cost effective of optimized solution. Therefore, a novel approach was developed and applied to determine the most combinational optimized solution. This process applied optimizations such as Nelder-Mead Simplex method, to Taguchi methods with the aid of matrix analysis and pictorial organization for

the reduction of options. Both novel methods resulted in the same generalized solution-neutral option.

Finally, with a single solution identified, mind-mapping and axiomatic analysis were applied to identified interfaces in the systems, coupled portions of the design and aid with the optimization of design parameters needed for the optimal successful design. With this information available, further optimization, manufacturability analysis, and cost analysis could be conducted that is presented in the following chapter.

CHAPTER 4. MODELING AND OPTIMIZATION

The preceding chapter described the design process that developed and assessed various design options resulting in the selection of a preferred option for further development and optimization. This current chapter presents the development of the performance modeling and cost analysis tools needed and their use that is required in supporting the optimization of this energy intensive mechanical system. It will be shown that a series of models of increasing complexity are needed to support this design and in fact other similar design requirements.

Initially, a traditional design selection and sizing tool used in industry was consulted. For purposes of studying the actual engineering design process in use, this tool was superseded by a more efficient spreadsheet based proprietary preliminary design tool. This spread-sheet tool was developed as part of this research but based on the pre-existing industrial tool, that was useful in preliminary design. Both of these tools are, however, essentially heuristic and not reliable or detailed or flexible enough to help complete the optimal design of this uniquely challenging energy-intensive system.

The final optimization and more detailed design were both supported by two models that are important results of this research. The first can be called a kinematic model; in that it assumes reasonable accelerations and computes the resulting velocity and position profiles without regard to the necessary drive and control systems needed to actually implement a proposed skip cycle. Such a model will be shown to be capable of computing nearly all the important system characteristics, such as loading and stresses, needed to support the detailed design analysis.

Moreover, the kinematic model was shown to be adequate to address the design modifications needed for system efficiency, manufacturability, and acceptable thermal heat loss.

4.1. SYSTEM OPTIMIZATION

Since an acceptable energy-intensive design requires optimization, a rather detailed cost model was also developed and integrated with the kinematic model. Although the kinematic model is reasonably well detailed and is ideal for preliminary design, it cannot be conclusive especially about details of the drive train and control system. Consequently, the kinematic model was supplemented by a rather complex dynamic simulation model of the particle lift system. Together, these methods and models were used to determine the final characteristics of the drive and lift system.

The first design tool used was the traditional handbook method employed by industry [58] used in characterizing a hoist system. This model is essentially a guide that outlines the basic lift specifications as usually encountered. Consequently, this traditional method is essentially heuristic and requires the designer to personally predetermine certain critical hoist characteristics such as skip weight, payload weight, mass of the rope in operation of the conveyance, rope diameter, drum size, skip velocity, speed reducer gear ratio, and mass flow rates. Then using basic engineering calculations, the starting and standing torque, power requirements, and finally the motor capacity are determined. This method is a good example of the sort of tool needed early in any design process.

The traditional method has given rise to a simple spreadsheet computer-based model (SSM) as seen in Figure 13. This version was based on interactions with industry and appears to be similar to the design tools used currently used in industry as confirmed by private correspondence [67] with a leading international mining hoist manufacturer. This model is still very limited by relying on the judgment of the designer to specify the basic design. The SSM is an improvement over the traditional method with its ability to calculate and compare more than one scenario very quickly.

	Inputs	Outputs				Inputs	Outputs									
Power Requirements				Speed Profile												
Power Tower (MWth)	460			Max Rope Speed (m/s)		4										
Electric Power (MWelec)		220.0957		Skip Acceleration (m/s2)		0.5										
				Skip Decceleration (m/s2)		0.5										
				Creep Out Speed (m/s)		0.5										
Temperature				Creep In Speed (m/s)		0.5										
High Temperature C	700			Creep Distance (m)		1.5										
Low Temperature C	300			Charge Time (s)		15										
Delta Temp		400		Drum Interia (kg/m3)		1500000										
				Angular Velocity (rad/s)			6									
Mass Flow (Apeture) (kg/s)		978.7234														
Mass Flow (Per Skip) (kg/skip)		58845.74														
				Velocity Profile	Delta Time	Start Time (s)	End Time (s)	Velocity (m/s)	Acceleration	Start Distance (m)	End Distance (m)	Delta Distance	Angular Velocity	Angular Acc		
Particle Lift				Charging	15	0	15	0	0	0	0	0	0	0		
Number of Skips (Total)	2			Creep Out	1	15	16	0.5	0.5	0	0.75	0.75	0.75	0.75		
Number of Skips Per Direction		1		Accelearation	7	16	23	4	0.5	0.75	41	40.25	6	0.75		
				Constant Speed	14.125	23	37.125	4	0	41	97.5	56.5	6	0		
Displacement (m)	138			Decceleration	7	37.125	44.125	7.5	-0.5	97.5	137.75	40.25	11.25	-0.75		
				Creep In	1	44.125	45.125	0.5	-0.5	137.75	138	0.25	0.75	-0.75		
Skip Tare Weight	41192.02			Discharge	15	45.125	60.125	0	0	138	138	0	0	0		
Payload	58845.74															
				Inertia	Inputs	Outputs										
Rope Characteristics								Load Diagram								
Number of Ropes Per Skip	1			Payload	58845.74468				Payload Mass	Rope Mass	Rope+Rope Mom	Friction	Ang Acc Moment	Torque	Power (kW)	
Rope Diameter (mm)	60			Skips		82384.04255										
Rope Mass/ Length (kg/m)	15.5			Rope		5576.524963		Start Creep Out	58845.74468	2139	60984.74468	7340.31561	1174685.437	1243010	7458.063	
Breaking Force (kN)	2128			Total Payload Mass		146806.3122		End Creep Out	58845.74468	2138.625	60984.74468	7340.31561	1174685.437	1243010	7458.063	
Tensile Strength (MPa)	1760							Start Acceleration	58845.74468	2138.625	60984.36968	7340.31561	1174685.437	1243010	7458.061	
				Drum Inertia	1500000			End Acceleration	58845.74468	2118.875	60984.36968	7340.31561	1174685.437	1243010	7458.061	
Drum Diameter (m)		1.333333		Motor Inertia	1000			Start Constant Speed	58845.74468	2118.875	60964.61968	7340.31561	0	68304.94	409.8296	
Dead Turns	10			Payload Inertia		65247.24987		End Constant Speed	58845.74468	2118.875	56726.86968	7340.31561	0	64067.19	384.4031	
				Total Inertia		1566247.25		Start Deceleration	58845.74468	2118.875	56726.86968	7340.31561	-1174685.437	-1110618	-6663.71	
System Constants								End Deceleration	58845.74468	2138.875	56726.86968	7340.31561	-1174685.437	-1110618	-6663.71	
				Angular Creep Acc M		1174685.437		Start Creep In	58845.74468	2138.875	56706.86968	7340.31561	-1174685.437	-1110618	-6663.71	
Mux	2.09			Angular Creep DEC M		-1174685.437		End Creep In	58845.74468	2139	56706.86968	7340.31561	-1174685.437	-1110638	-6663.83	
Specific Heat (kJ/kg-K)	1.175			Angular Acc Momentum		1174685.437										
Skip/Payload Ratio	0.7			Angular Dec Momentum		-1174685.437		Hoist Capacity	Power Avera	Time		14935.8146				
Drum/Rope Ratio	80			Friction		11010.47341		Creep Out Stage	55622703.51	1	55622703.51					
Friction	0.075			Friction Moment		7340.31561		Acceleration Stage	55622669.94	7	389358689.6					
								Constant Speed Stage	157863.0315	14.125	2229815.32					
								Deceleration Stage	44405024.47	7	310835171.3					
								Creep In Stage	44405824.12	1	44405824.12					
								Average Time		35.125						
								Motor Capacity			4779.708605					

Figure 13 Developed spread-sheet based model (SSM).

The primary benefit of having the SSM is the insight it has given on current industrial practice and is useful at the level of rudimental conceptual design. Furthermore, it shows that a more physics-based model allowing efficient design optimization is necessary for an effective preliminary design.

The newly-developed kinematic model is an improvement over both the traditional method and the spreadsheet model since it requires far fewer predetermined parameters. This model has been developed using a modern equation-based solver. In this case EES was used, but other equation-based environments such as Modelica could be applied. By using the non-linear equation based EES model, the kinematic equation-based model (KEM) can solve for the dependent variables and optimize the values simultaneously. The KEM requires only a few specifications such as a maximum acceleration, a maximum velocity, and a reasonable velocity profile. Also, a cost model for the optimized system has been incorporated into the KEM to display an estimated cost of the system. The information flow deployed in the KEM model is seen in Figure 14.

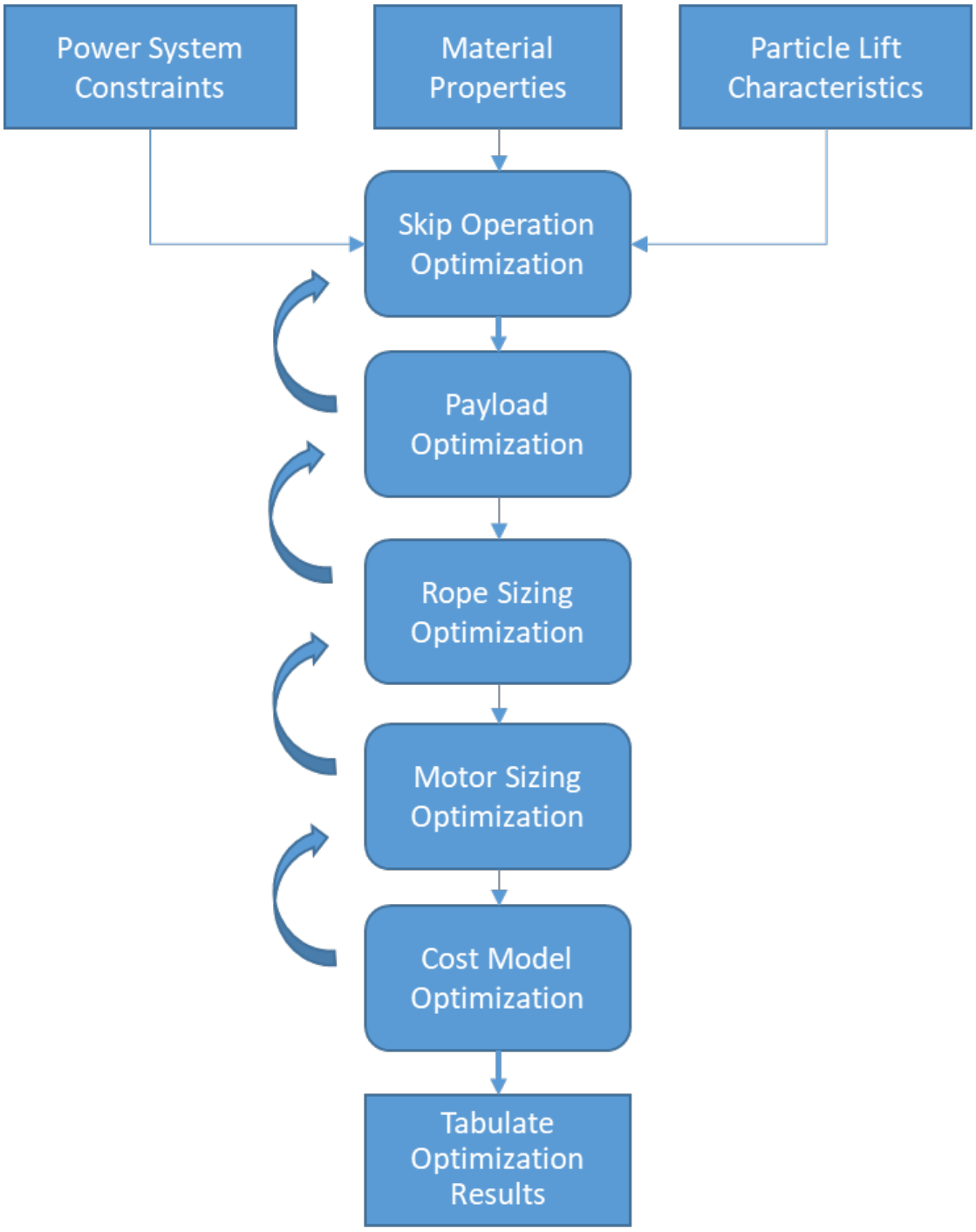

Figure 14 Information for chart for KEM

Alternatively, the cost model can be used to help optimize the system characteristics that minimize the cost and eventually the life cycle cost of the system.

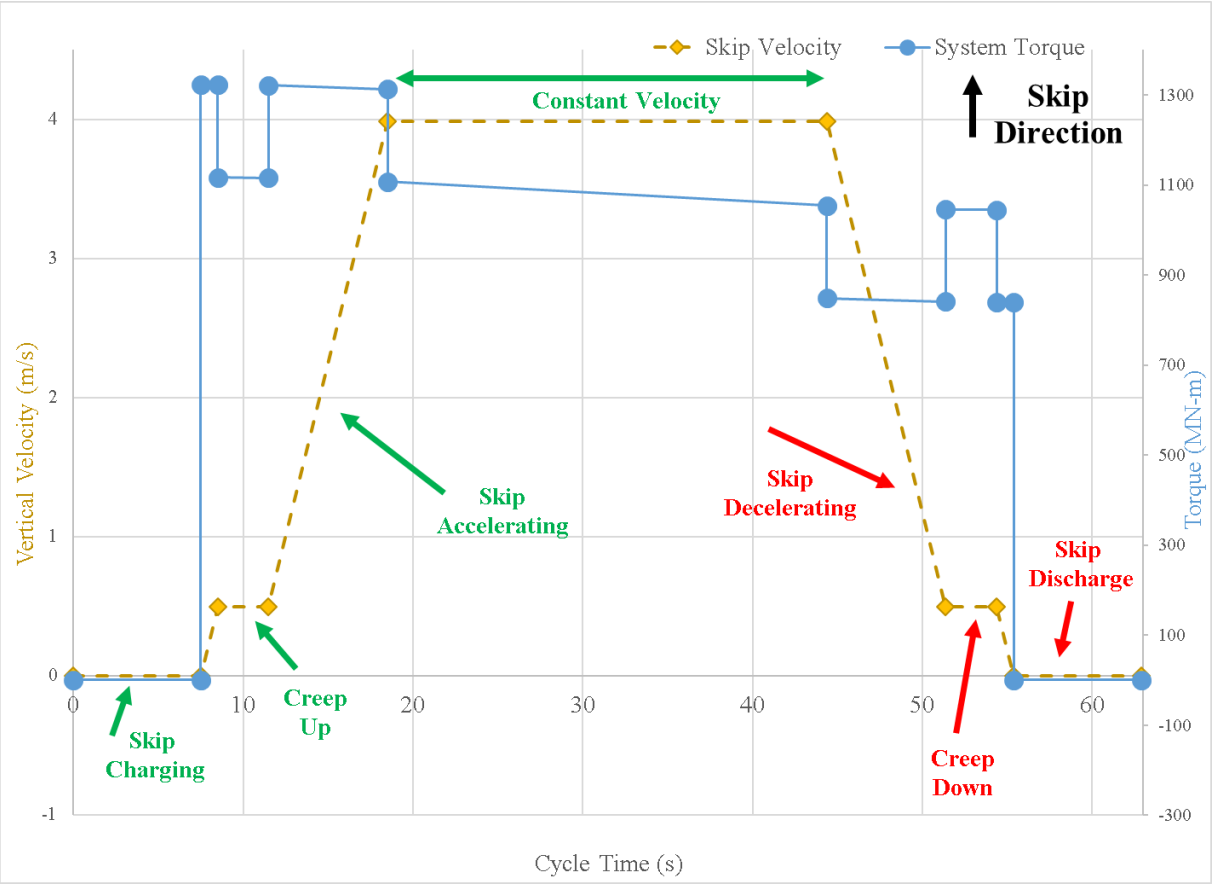

Figure 15 Particle lift kinematic study of torque and vertical velocity (CB = 300°C).

The optimized system, from the KEM, can then produce graphical profiles of the system behaviors such as torque and most importantly velocity and skip displacement profiles as functions of time. These system behaviors are shown in Figure 15 and Figure 16. In Figure 16, the figure includes the relationship between the skip velocity and its vertical displacement.

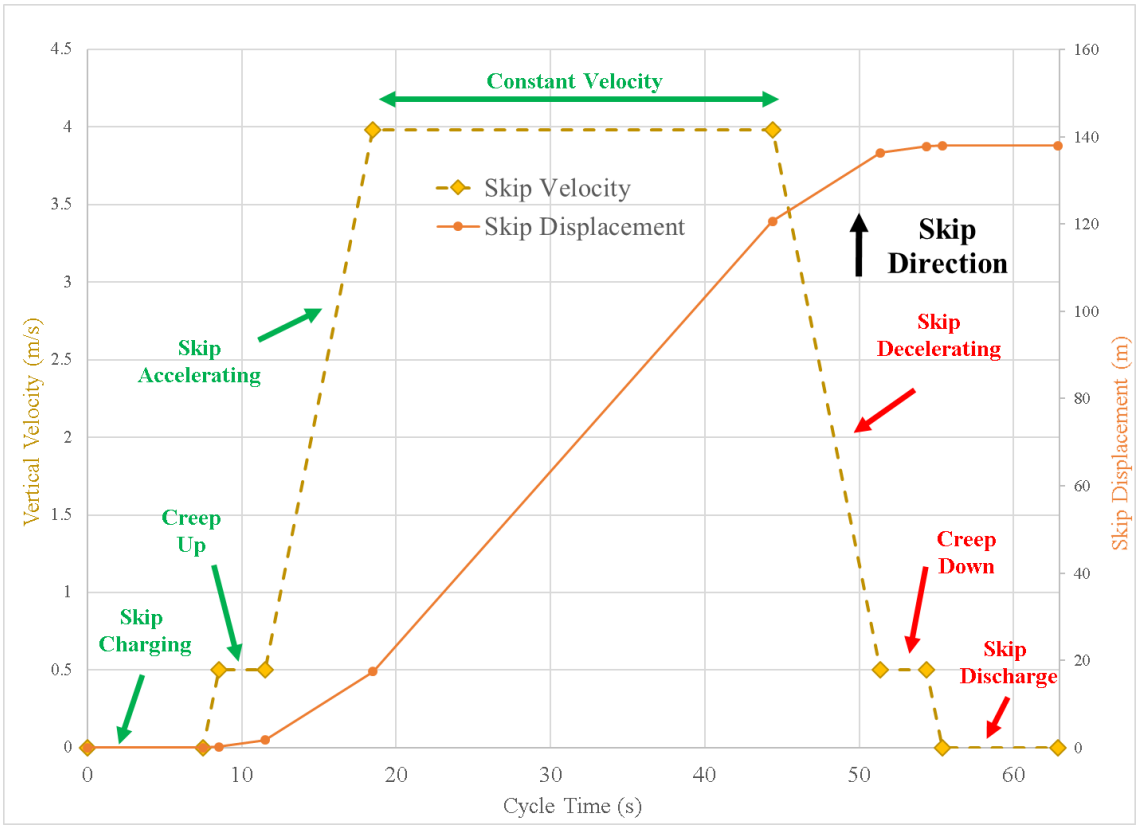

Figure 16 Particle lift KEM of skip velocity and displacement (CB = 300°C)

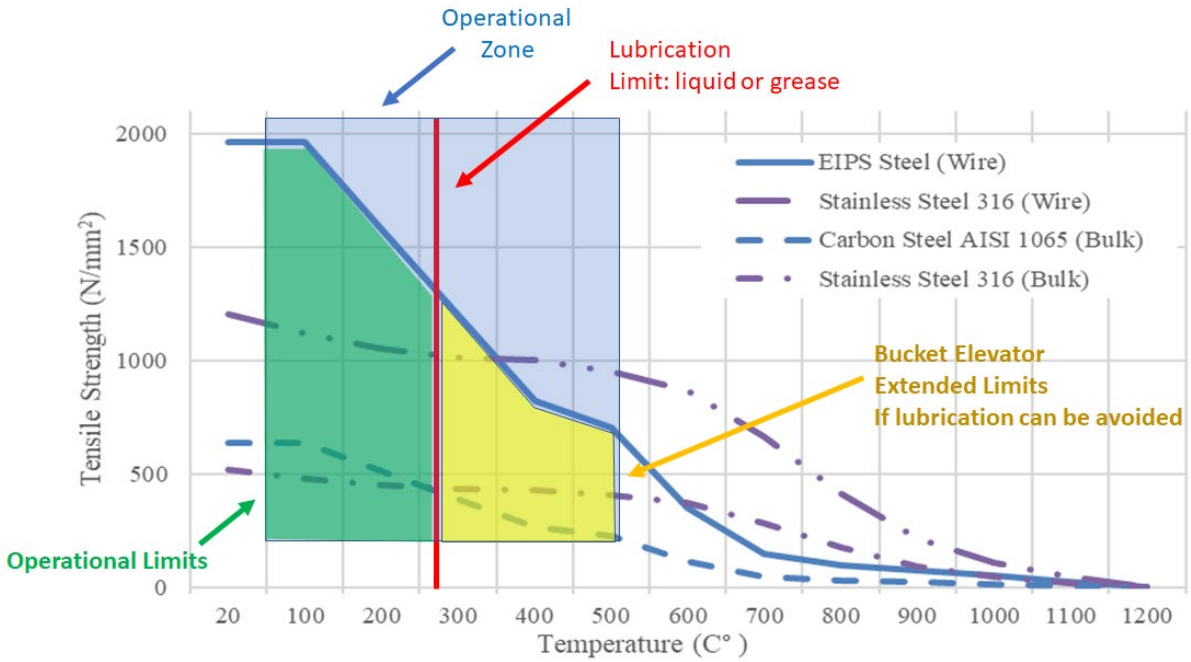

Figure 17 Using the KEM to apply Information AD to optimize the wire rope size.

Besides the ability of the KEM to produce the graphical optimized profiles of the system; is its ability to apply AD actively during the optimization. For example, the KEM used properties and constraints developed from Information AD, to optimize the size of the wire rope and thus determined the skip weights, drum characteristic and ultimately determining the motor capacities and cost of the system. A graphical interpretation of the application of the Information AD is seen in Figure 17. Other constraints and properties developed from Information AD and used in the KEM are the maximum allowable skip velocity, the shaft temperature and the limitations of temperature on not only the wire rope but on other components of the system, such as possible lubricants, to determine the optimized minimum diameter of the wire rope to be able to the carry skip payload and still maintain the pre-determined safety factor.

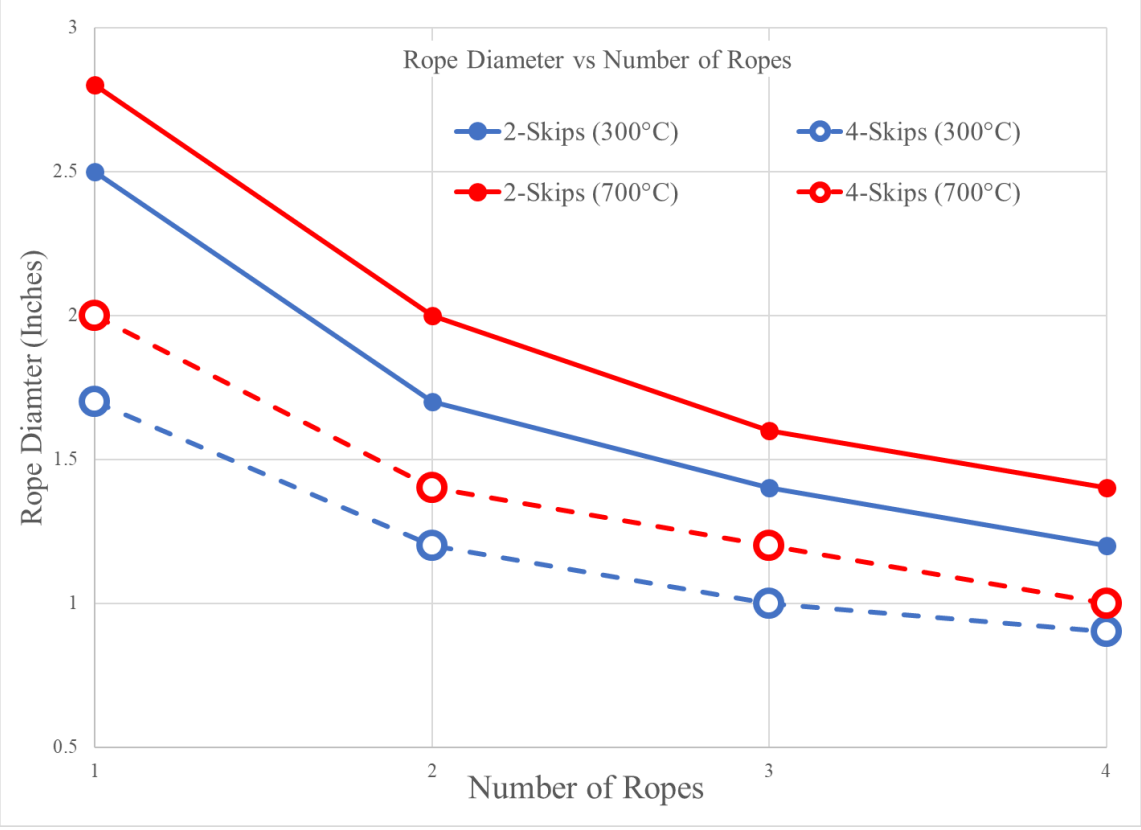

Figure 18 KEM results for rope diameter with respect to number of ropes per skip.

A validation for the KEM can be seen in Figure 18, in this figure only the 2-skips and 4-skips configurations are shown. The figure shows that as the number of skips installed increased or the number of ropes per skip increased; the rope diameters decreased due to the decreased amount of load per skip or per rope. However, some solutions are not physically possible due to the resulting diameters of the ropes. Rope diameters above 2 inches and especially those approaching 3 inches are not recommended for hoisting use [38] since the flexibility of the rope greatly decreases.

The usefulness of the KEM was shown in the defining and optimized design and the optimization of the system operation that can be further refined by the fully dynamic simulation model (DSM). The DSM can be programmed based on the motor torque profile and the desired skip speed profile. The torque profile is key in determining the electric motor performance and rotational speed during operation. The DSM compliments the KEM since it can investigate anticipated transient issues, unlike the KEM, such as when the system's acceleration experiences high rates of change or jerks.

The DSM, as seen schematically in Figure 19, was developed using Matlab Simulink software. Simulink was chosen over other platforms since its ubiquitous presence and use throughout academia and industry. Moreover, it has a well-developed graphical user interface and a large number of libraries of model components and control models used in developing the control system. This advantage of Matlab is that it allows for a control system that can mimic the behavior of the system at specific points in time, automate vital systems like brakes, even simulate possible failure that could be encountered over the life of the operation of the particle lift. This is an important capability since it allows the ability for a more informed prototype to be built and tested at a reduce cost since more issues can be addressed before large amounts of resources are committed to the design cycle of the particle lift.

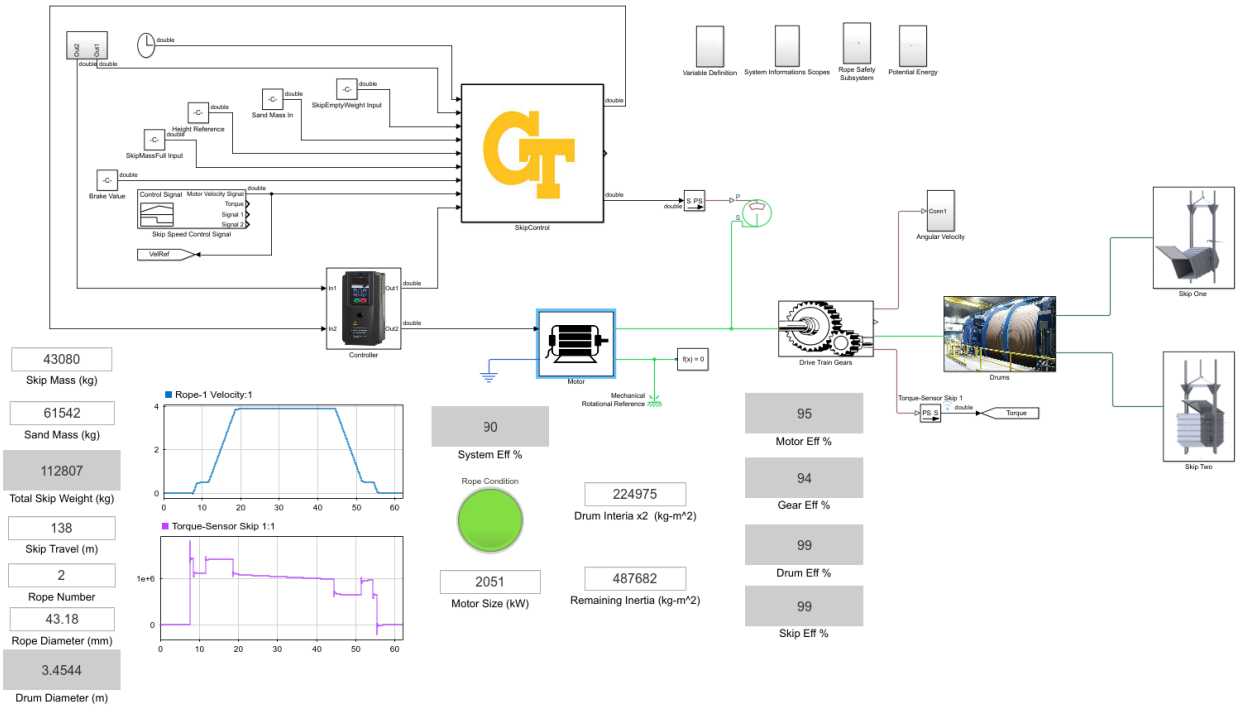

Figure 19 DSM for 2 skip particle lift system (CB = 300°C).

One of the most challenging aspects of developing the DSM is its inherently transient and cyclic nature. This means it is more difficult to model in comparison with thermal systems that are normally modeled and optimized only for steady-state conditions. The DSM is able to simulate torque and forces exerted by and experienced on the different components of the particle lift. The DSM can determine the overall efficiency of the cycle. It represents one cycle of charging a skip while simultaneously discharging the second skip. This model can be easily modified to account for the number of skips and ropes per skip. Moreover, unlike the SSM or the KEM above, the DSM also includes the ability to simulate unexpected events like rope failure or skip malfunction. Thus, the DSM will be a great help both in academia and industry in the analysis and optimizations hoisting systems and similar applications.

The DSM represents a major step forward in research and analysis for lift designs similar to mining hoists. Currently, there are very few, if any dynamic models for mining hoist like systems or applications especially ones that are based off of first principles. Of the existing dynamic models, their primary intent is primarily to analyze the design of the electric motor in the application [68, 69].

The flexibility and realism of the DSM allows the analysis of the transient forces experienced during the different critical stages of operation and parasitic power loads. Different scenarios based on different size and types of electric motors, speed reducer gear ratios, different types of breaking systems, the ability to accurately model frictional forces, and the interjection of unexpected events like rope failure can be easily performed.

In Figure 20, the DSM developed for this thesis, is shown to have four main modules or subsystems. These modules are: (1) Signal Input, System Control and Output, (2) Motor and Gearing module, (3) Double Drum and Axel module, and (4) the Rope and the Skip module containing a filled and empty skip.

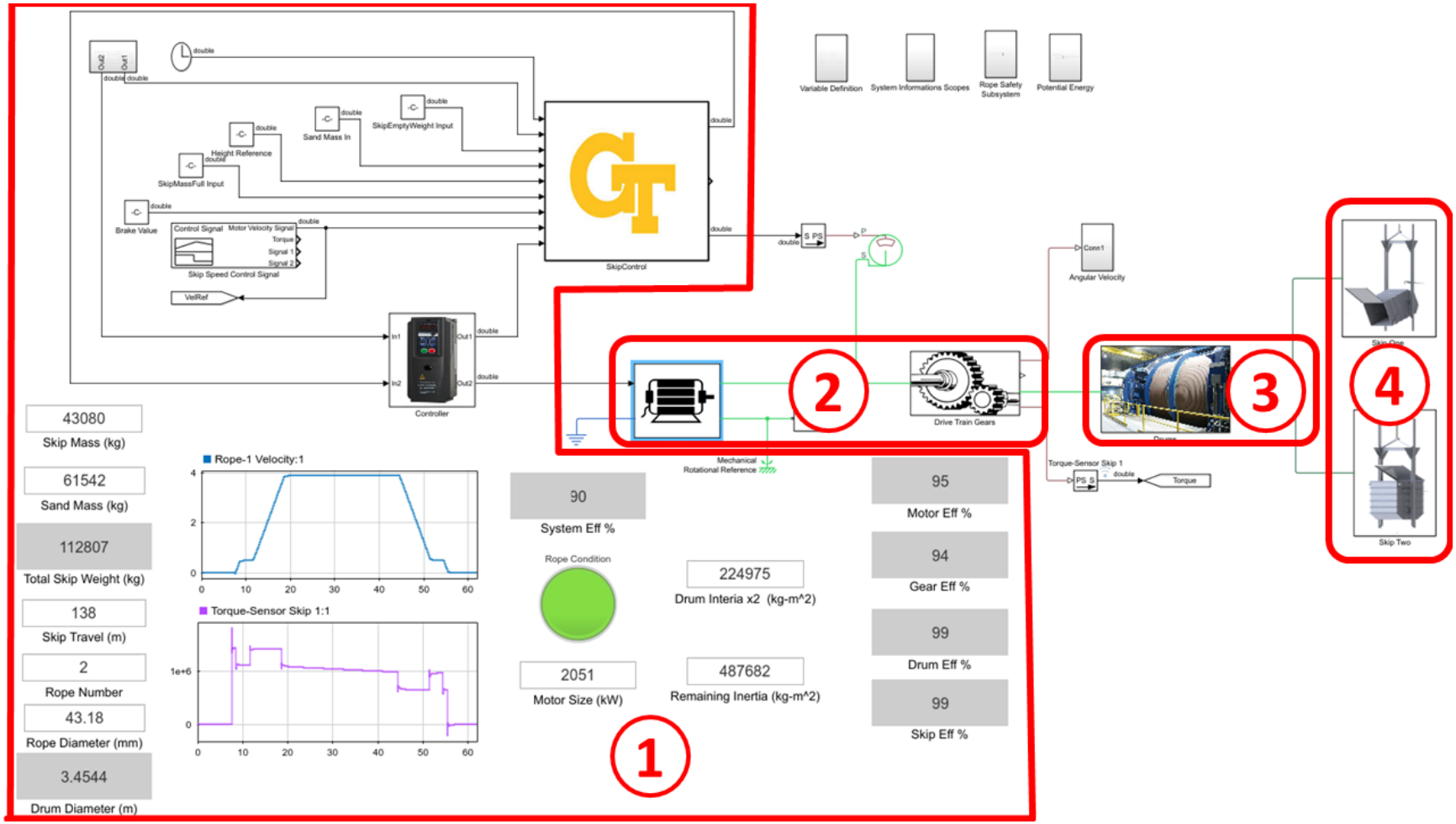

Figure 20 DSM with module labels for 2-skip particle lift system (CB = 300°C).

In module (1) the results from the KEM was used as the basis to signal the needed torque or skip speed for a certain point in time that would be used during the actual operation of a particle lift. This signal is sent to the electric motor or braking system depending on the required operation. Module (1) contains the combination of a custom-built function that controls brake release, timing and has the ability to interject unexpected events into the system. A PID controller is included, where the input signal is converted to a physical signal that controls the motor speed and the brake system. In addition, it also contains rope failure indicator that will permanently switch to red if at any time during the simulation the loads on the rope exceeds it failure limits. Lastly, this module displays the overall efficiency of the system during each time step of the system.

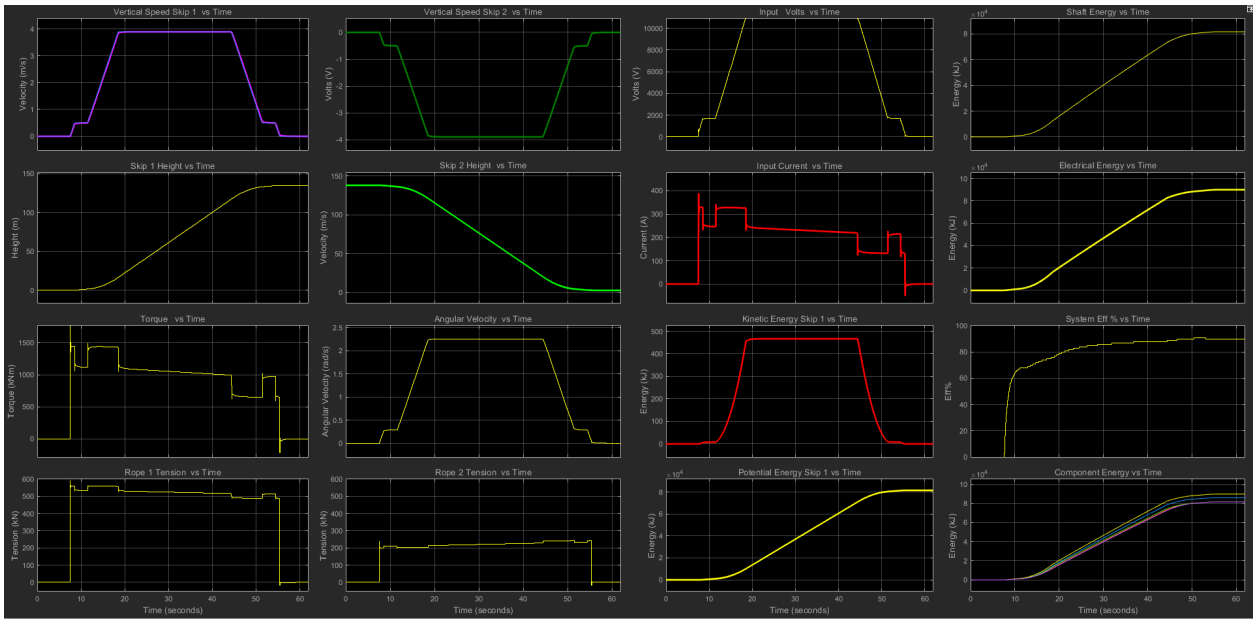

Figure 21 Results from DSM for particle lift (CB = 300°C).

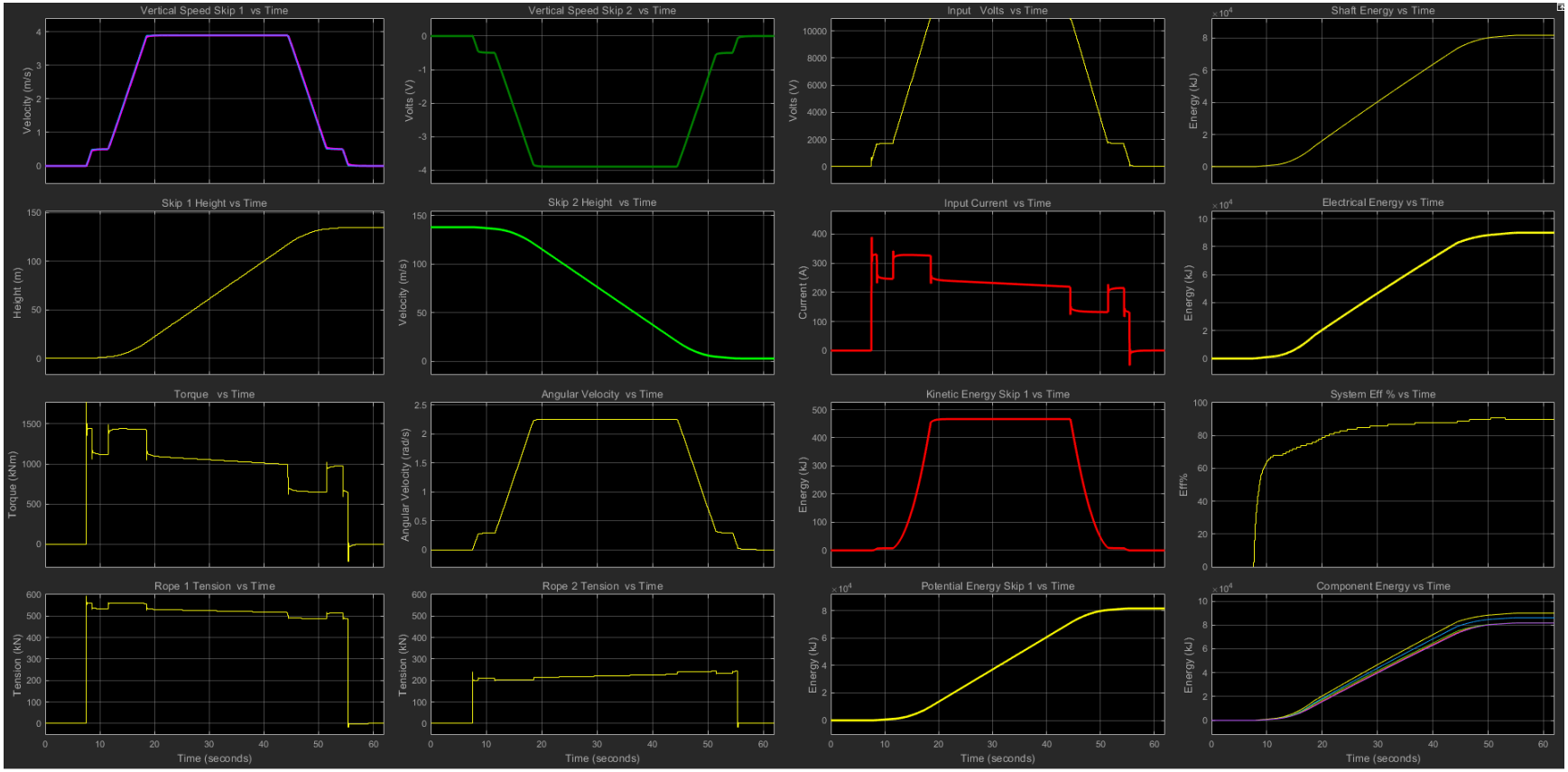

Figure 22 DSM Results for particle lift (CB = 300°C) with corresponding table label.

Table 20 DSM Result labels respective to chart location.

1. Vertical Speed Skip 1 vs Time	2. Vertical Speed Skip 2 vs Time	3. Input Volts vs Time	4. Shaft Energy vs Time
5. Skip 1 Height vs Time	6. Skip 2 Height vs Time	7. Input Current vs Time	8. Electrical Energy vs Time
9. Torque vs Time	10. Angular Velocity vs Time	11. Kinetic Energy Skip 1 vs Time	12. System Eff % vs Time
13. Rope 1 Tension vs Time	14. Rope 2 Tension vs Time	15. Potential Energy Skip 1 vs Time	16. Component Energy vs Time

The output signals are displayed via graphs, as seen in Figure 21, and vary from voltage and current inputs to dynamic loads on the rope, parasitic power, or height and location of the skips at any point in time. In Figure 22, the model outputs are shown with a table, Table 20, which indicates their respective graphs.

The signal is sent from module (1) to module (2), is converted into voltage that controls the torque and speed of the electric DC motor. A DC motor was used since it gives electrical smooth results, easy to implement and reduced the time of the simulation. The motor section of the module was designed so any other motor type can be introduced at a later time. Frictional forces were added to simulate the effects of friction over the life of the system and their contribution to parasitic power loss. The gearing with its frictional and inertial properties is included in this module. It needs to be noted that the type of gears used in the speed reducer affects the efficiency of the speed reducer and thus the overall system. Therefore, it is an imperative to select, based on the most efficient and cost effective, type of gears and ratio value in order to maintain a high torque while reducing the loss in power.

In module (3), the drums for the wire rope and the axel supports are modeled. The weight, dimensions of the drums, inertial properties, torque, and rotational speeds are considered.

Module (4), includes the representation of the charged skip rising towards the PHR or the empty skip being lowered to the charging station near the cold bin. The tare weight of the skip and the presence or lack thereof the payload is considered with this module. In module (4), the inertial properties of the wire rope are modeled, velocity, and tension experienced by the roping during operational conditions. The module has the ability to include simulated protocols related to rope replacement scenarios, different materials and unexpected operational events if needed in a more refined model.

One example of the DSM ability of simulating the realism of the particle lift operation is the worst-case scenario of wire rope failure of the charged skip will in operation. As shown in Figure 23, the Skip One module schematic is shown with the failure event controls that can define if a failure will occur, time of failure in seconds, and the direction of movement will occur.

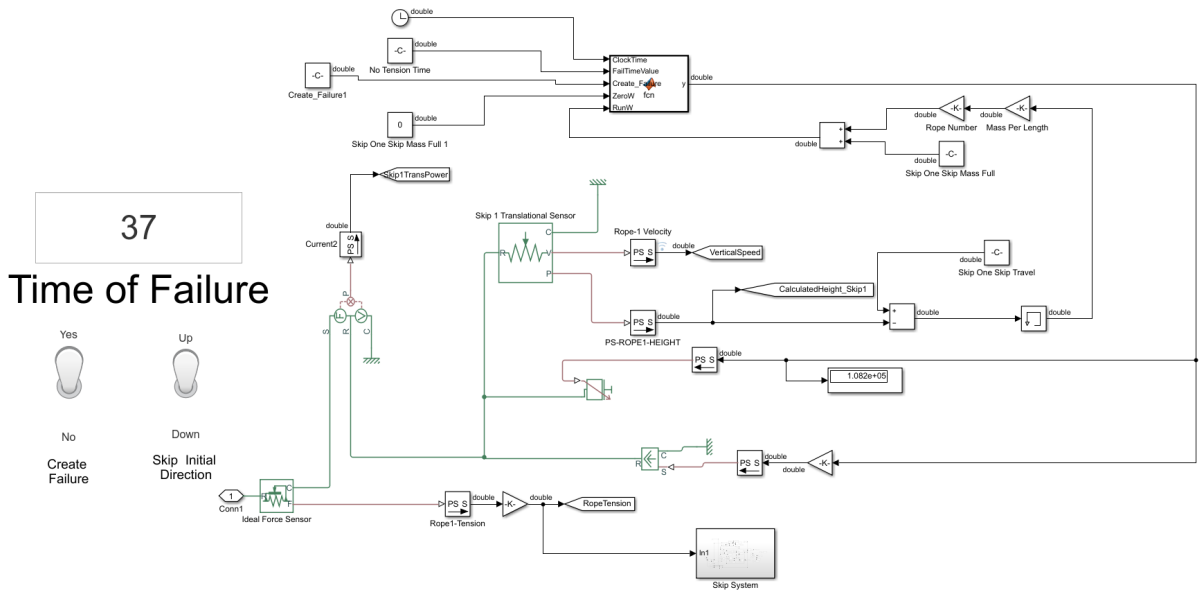

Figure 23 Schematic in the DSM for Skip One showing Failure Event Controls.

In the example shown, the failure will occur at time 37 seconds while the skip is being raised. At that point the rope will fail, and the skip will plunge. The system quickly recovers, as seen in Figure 24, the height and velocity of Skip One are tracked as it plunges. The upper portion of the graph represents the remaining part of the wire rope and drum. It shows a disturbance but quickly recovers. Figure 25 shows a more detailed version of the disturbance and the systems recovery response.

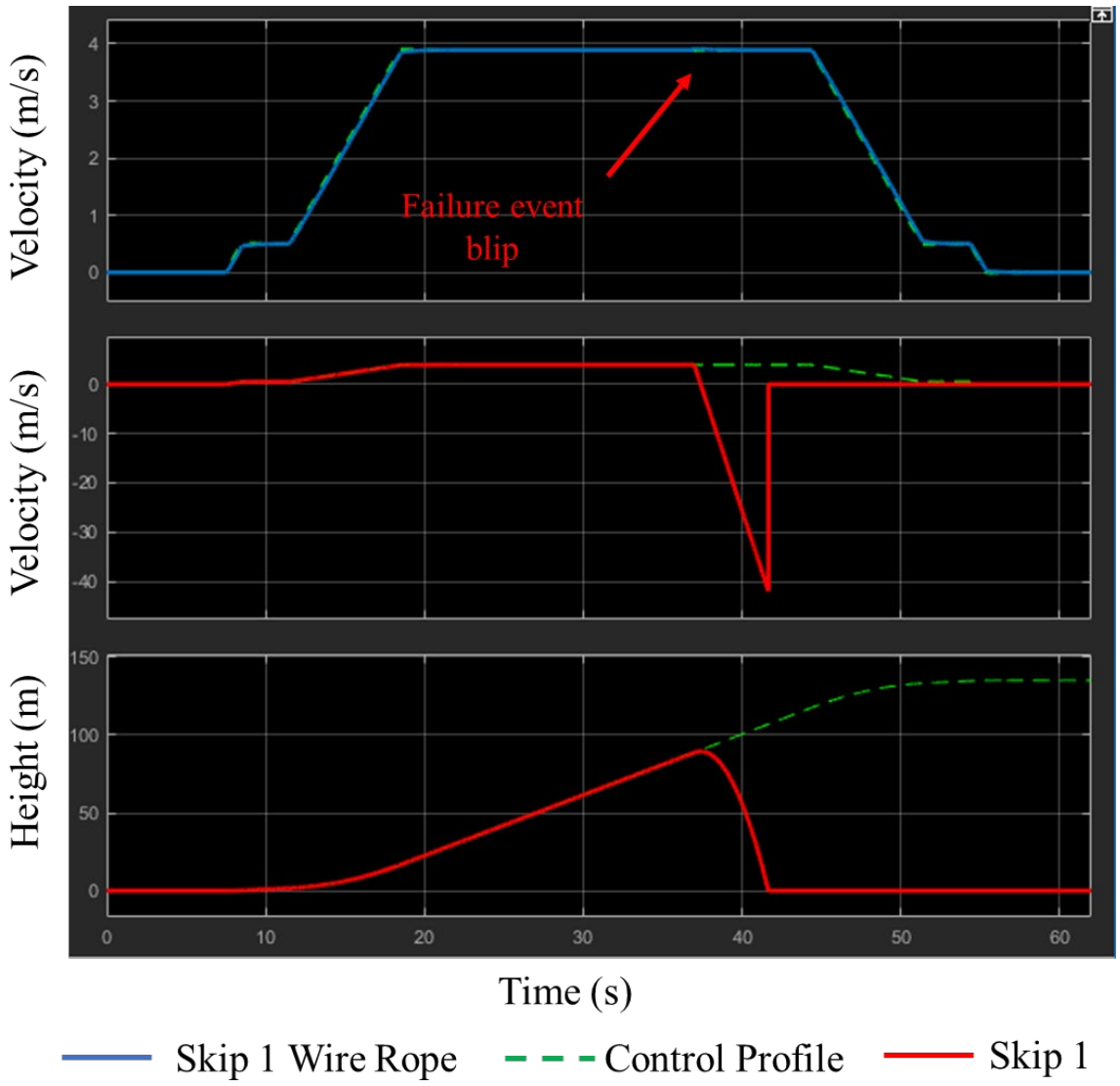

Figure 24 Response of system and Skip One during failure event.

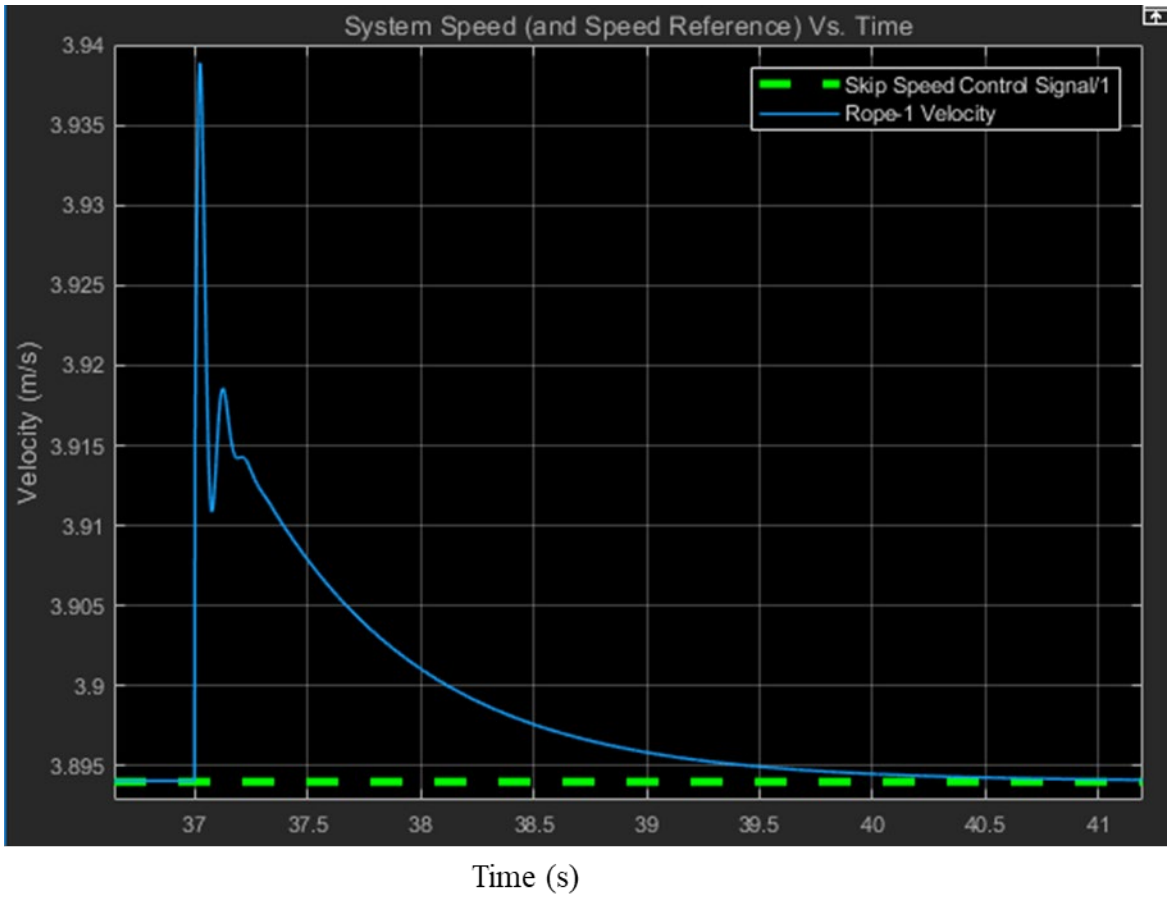

Figure 25 Response and recovery of system during failure event.

The system clearly experiences a sudden jerk as the wire rope fails but is quickly brought back under control by the speed control in approximately four seconds. The model shows that the second skip, Skip2 can quickly recover and continue to function even though Skip One experienced a failure. Figure 26 shows the side by side comparison of both skips during the failure event and the effect of disturbance and subsequent recovery of Skip Two.

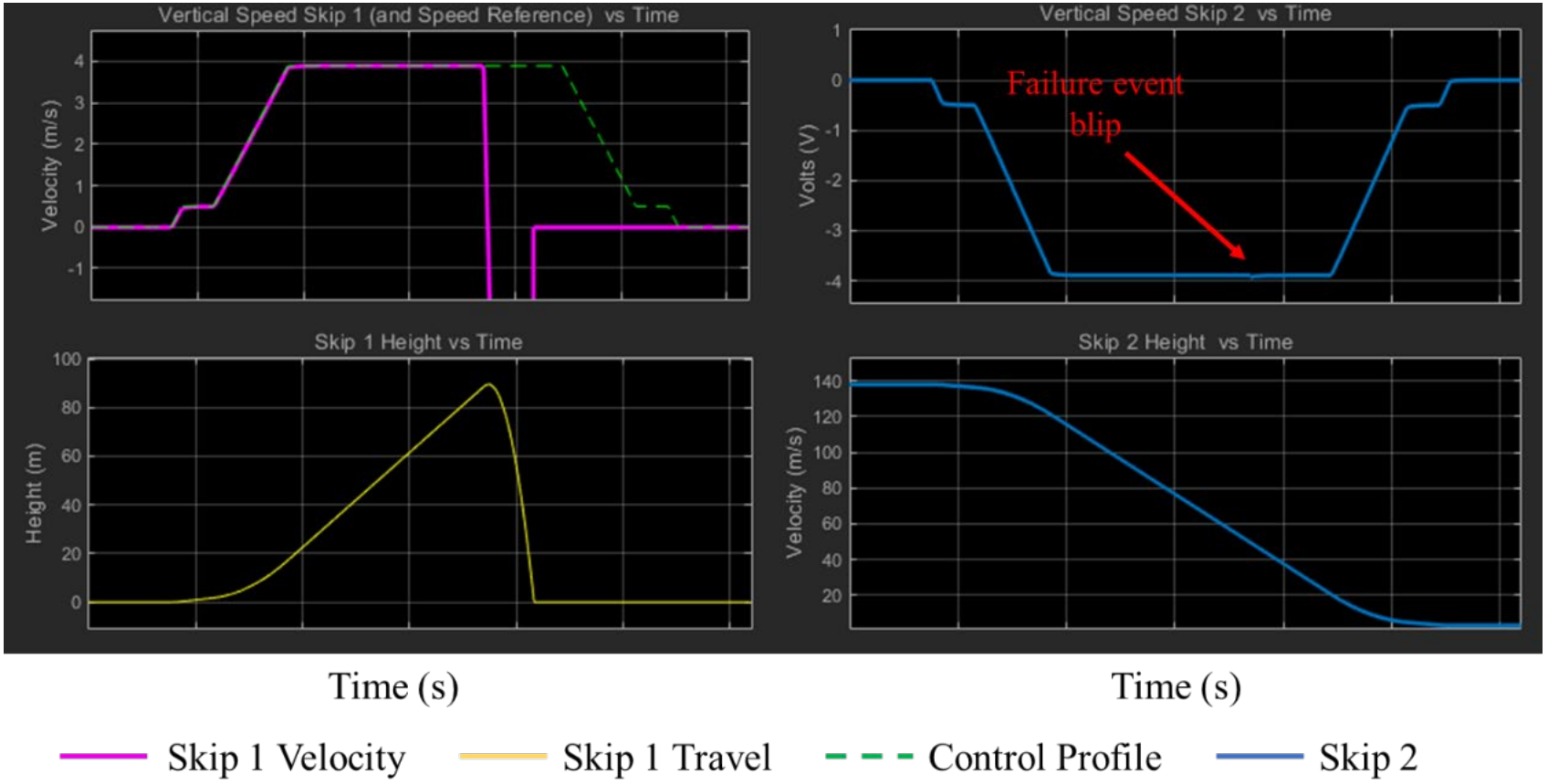

Figure 26 Response of skips during failure event.

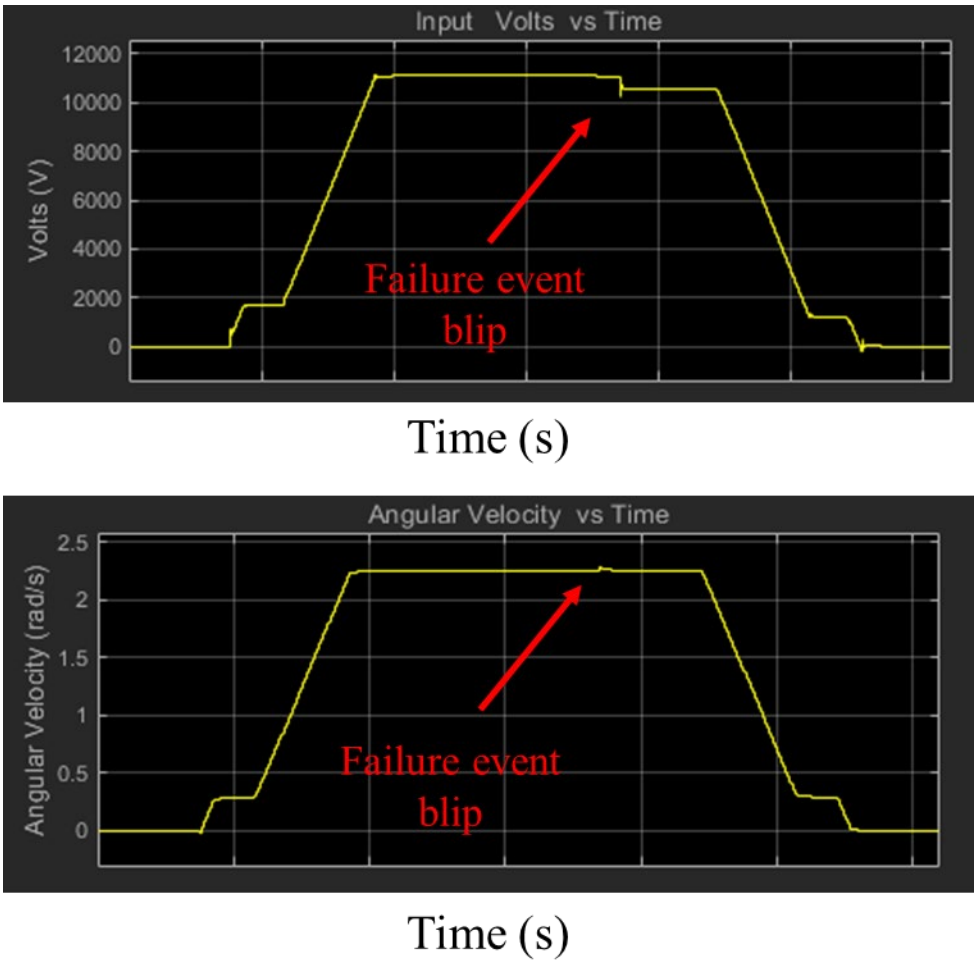

Figure 27 Response and recovery of electrical and angular velocity of system.

The realism of the model can also be seen in Figure 27, where the disturbance effects not only the electrical components of the system but also the angular velocity of the hoist drums.

It must be noted that even though Matlab is a very mature software, it also has its limits. For example, the blocks used to simulate AC Induction motors are geared towards the analysis of its electrical system appear to be too detailed for this application. In additionally, the AC Induction motor or Asynchronous machine, as the termed used in Matlab, are limited to very small sample run times since the accompanying pulse width modulators require steps sizes on the order of 20 μS. Moreover, large torque values in combination with the small step sized resulting in many times

the software crashing. This is another reason why a DC motor was used in the simulation. A suitable AC Induction model is needed but was not part of the scope of this research but is planned to be included in the future.

It is planned in the near future to implement a block that represents the physics of an AC Induction motor on a system without the need to simulate the pulse width modulation or other forms of variable frequency drives (VFD) in minute detail [70].

Lastly, many times nuanced techniques were needed like adding mandatory solver blocks or memory lag block so that the simulation could run. Even with these issues the KEM and DSM are invaluable tools that can be used to quickly define, refine, optimize, and simulate a particle lift of an energy intensive system using fewer resources. However, even with optimized designs simple facts like transportability or standards could cause the adoption a less optimized design. This is where design for manufacturability needs to be considered.

4.1.1. DESIGN FOR MANUFACTURABILITY MODIFICATION

Using the information deemed from the FR, DP, the optimization values from the KEM and the results of the DSM; a first set of drawings and specification were completed. These drawings and specification were then sent to a company familiar with industrial lift manufacture and steel fabrication. They were consulted to see the feasibility of the initial design. This company indicated that the design would be an easy fabrication. However, they noted that some minor changes should be made to the skip dimensions in order for the skip to be able transported inside a shipping container. These changes were made enabling the skip to be able to reach more destinations around the world at a reasonable cost. Without taking design for manufacturability into consideration, a simple intractable dimension or other specification could cost vast amounts of wasted resources in

the need of specialized transportation or the inability to manufacture a realistic design even though the models show it as an optimized design.

As with the consideration of manufacturability, a prominent skip-hoist supplier was informally consulted on the feasibility of installation. They commented that our design was feasible to install. However, they indicated that the Koepe hoist and bottom dump skip should still be considered. Their reasoning was that the Koepe hoist is a simpler design, less expensive, and has a lower drum inertia thus reducing the deceleration losses and dynamic loads. Therefore, future investigations will reconsider these options.

It must be noted for the Koepe hoist, that special consideration with regards to the tail ropes interacting with spillage of heated particles or the increased thermal effects on the guide rope due to the increased shaft temperatures. These interactions and thermal effects can lead to higher maintenance cost or rope failure. Another, special consideration is the friction required between the groove liner and the wire rope for the proper operation of the hoist. The need to maintain adequate friction between the drums and ropes which are greatly temperature dependent and is difficult to maintain in an extreme operating environment. These and other temperature related aspects need to be well addressed for a successful implementation of a Koepe hoist system[70].

Another important aspect of the drive system is the energy recovery of the lift system that have been investigated in [71] and [72]. Within the realm of energy recovery; the special topic of an energy storage accumulator is addressed in [73]. Energy storage accumulators is best suited for this type of energy intensive system. However, it would increase they cost of the particle lift for a small rise in efficiency. Their use is more seen in small industrial lifts or elevator applications that are either high speed or have multiple stops.

It must be noted that in the publications mentioned in the preceding paragraph; tend to be more focused towards small industrial applications as elevators or cranes while the particle lift is of a larger scale and much more energy intensive. One work-around in industry to mitigate the large need for energy during use is to use a two-skip counter balanced configuration that can adequately be used in the recovery of both kinetic and potential energy stored in the skips. This is important since efficiency of the optimized design is critical and will be addressed in the following section.

4.2. DESIGN EFFICIENCY ANALYSIS

An initial efficiency analysis was conducted based on using reasonable lift and energy recovery values in the energy flow analysis. These values are seen in Table 21 for a commercial scale design. The initial analysis was done by component block modeling where each component used industry acceptable efficiency values. The lift efficiency is the efficiency of the mine hoist without regards to the energy needed to operate the lift. The recovery efficiency is related to the recoverable potential energy from lift the payload (PL). The tare ratio plays an important role in the recovery efficiency. The tare ratio is the ratio between the weight of the skip and the weight of the payload (in this case the heated particles). Minimizing the skip's mass compared to the PL is important because the mass of the rope and skip represent the tare mass that contributes to the potential energy of the system. During the process energy is loss not only through heat loss but also through inertial and frictional effects. These losses are expected to account for the parasitic fraction loss of the system.

Table 21 Estimated efficiency for particle lift design [74].

Description	Efficiency
Ratio: Tare/PL	0.70
Lift Efficiency	0.85
PE Recovery Efficiency	0.93
Overall Efficiency	0.79
Parasitic Fraction	0.0086

It is expected that the overall energy efficiency, as seen in Table 22, is less than the basic lift efficiency since not all the potential energy is recovered.

Table 22 Estimate of lift component efficiency for lift design [74].

Component	Efficiency
VFD	0.96
Electric Motor	0.95
Gearing, 2 Stage	0.98 x 0.99 = 0.97
Rope/Drum Efficiency	0.98
Overall Lift Efficiency	0.83 to 0.87

In the estimation of the overall efficiency a value of 85% was used for the important lift efficiency parameter that is based on values published in different standards and models [75]. These values were estimated for use in modeling the components as seen in Table 22. These values were used in the KEM. A more refined set of estimates were determined from the DSM, by taking into consideration transient effects and by having smaller step sizes. This is a very important advantage the DSM has for the traditional method, SSM or the KEM.

Table 23 System efficiency results based on KEM vs DSM studies.

System Properties	Cold Bin Temp	
	300°C	700°C
Rope Dia.” (in)	1.7	2.0
Rope Dia.” (mm)	43.2	50.8
Rope #	2	2
Motor Size (kW)	2,059	2,742
Cost ($/MW)	6,970	8,950
System Efficiency (%) - KEM	88.3	88.5
System Efficiency (%) - DSM	90.0	89.0

The DSM's determined efficiency results were compared to the KEM, as seen in Table 23. They system efficiency values, ranged from 88.3% to 88.5 % in the KEM and from 89.0% to 90.0% in the DSM that confirms the values in the KEM and with better estimates of frictional losses.

The deviation of values between the two models can be attributed to the fact that the DSM can account for information related to its ability to determine systems values in smaller step sizes than the KEM. Also, the dynamic model can more accurately simulate frictional and inertial properties of the system. Lastly, the KEM does not take into account the motor no-load speed that comes in specific ranges due to the number of available poles in the motor or speed reducer gear ratios and thus affect its efficiency.

The efficiencies determined by the KEM and DSM are part of the overall efficiency of the particle lift however the overall operating efficiency must take into account energy lost in the form of heat due to the skip parasitic heat loss. Therefore, a heat loss analysis is needed to investigate how the parasitic heat lost affects the system.

4.3. SKIP HEAT TRANSFER LOSS ANALYSIS

As per the customer needs, a requirement was to have a skip parasitic heat loss of less than 1%. In general, other goals can be considered A heat loss analysis was conducted for a skip design that was internally insulated with fire bricks and externally insulated with mineral wool or an alternative insulation with a comparative R-value.

Using insulated fire bricks protects the skip material from excess direct exposure from the heated particles. But the fire bricks affect the internal volume of the skip and thus it's carrying capacity. Therefore, the use of the internal fire bricks is limited. This volume dependency on the

size of fire bricks used and thus the design of the rope size is a great example of a coupled design that should be avoided or at least minimized.

Therefore, by supplementing the insulation of the internal fire bricks with the more flexible use of externally placed mineral wool; a more suitable value of heat loss is feasible. The application of the mineral wool externally is a good example of an uncoupled or at worst a decoupled design since its change in thickness minimally affects the other parts of the design especially the skip volume or rope sizing.

The analysis found that for both design types (particles of 300°C and 700°C) and fabricated material metal types (i.e. Stainless Steel 316 and AISI 1065) for the skip the parasitic losses fall well below the desired goal of heat loss as seen in Table 24. Therefore, the current design can well achieve the desired heat loss goal and without greatly affecting the overall cost of the optimized design.

Table 24 Parasitic Heat Transfer Loss analysis for Skips of varying metals.

Material	Temp			
	300°C	700°C	300°C	700°C
Mineral Wool Thickness (mm)	150	150	25	25
Material = Steel	0.0013 %	0.0047 %	0.0069 %	0.0251%
Material = SS316	0.0013 %	0.0047 %	0.0068%	0.0251%

4.4. DESIGN COST ANALYSIS

For successful optimization for the design; capital cost needs to be determined. Even though there are no directly applicable cost models for this design there were some beneficial cost formulas found in literature, that could be used at the planning level. Some formulation were given in [76]. However, an improved formulation was given by Sayadi et al in [77]. In this formulation, the important parameters at the system level can be applied to a regression formula in order to

generate the overall system level cost. These cost models cover the bare construction cost of the particle lift and not the life cycle cost that was not in the scope of this research.

The Sayadi cost model was found to be very beneficial but it was clear that a model with much more detail and flexibility is needed for further design analysis detail was needed since it does not take into factor the conditions of this special lift application. These conditions include higher temperature operation and shorter lift heights in comparison to most mining applications. This is especially true for the optimization of the skip used in the particle lift.

Therefore, two cost estimate procedures were developed and employed to the conceptual design. One procedure was based on using generic subsystem cost. The second procedure used the approach of modular cost for each major component allowing for a more accurate result, which is adaptable in its support for further design optimization.

In the generic subsystem model, module cost models for subsystems like the electric motor or gearing were taken from sources like [78], [79], or [80]. This cost model did not give us the desired ability to scale our system properly. Moreover, this cost model did not give us the ability to optimize or accurately estimate the cost of the skip. Cost models for skips tend to be propriety knowledge within the mining industry. Therefore, this cost model was abandoned in favor for the second cost model.

The second cost model approach resulted in a more desired modular cost model that had more of a resolution for cost when compared to a system level model but gave the speed and flexibility not seen in a detailed level cost model such as what is seen in the example [81]. The model was developed by conducting market surveys and obtained direct quotations for each component in the model over a wide range of ratings or capacities. From there, base cost factors and cost index were

determined, and scaling factors deduced through linear regression. More information on this cost model is detailed in Appendix A.

As an example of the direct quotation method conducted; various wire rope manufactures both in China and in the United States were contacted and direct quotes were obtained based on different wire materials and configurations. Following this, the cost model was developed as mentioned above. This method was used when no literature was available to use as initial base cost factor or initial scaling coefficients.

The market survey method started by referencing literature in which similar components had cost model developed. From there, component capacity or requirements were determined from the modeling. Cost were obtained from the suppliers, the lowest, median cost and higher cost values were determined. A cost model was then developed and compared to what was already available in literature.

Table 25 Example of cost model for Shaft bearings.

$C_c = C_O \left(\frac{R}{R_0}\right)^{\beta}$	(4)	C_0 = \$150,000	β = 0.8
		R_0 = 1864 kW (2500 HP)	

In Table 25, an example of the cost model as seen in Equation (4) was developed from a market survey. This example is for shaft bearings where the values are in 2017 dollars. The current cost C_c is evaluated from the base cost factor C_0, the motor sizing in kilowatts R, the base motor size R_0, and the scaling factor β.

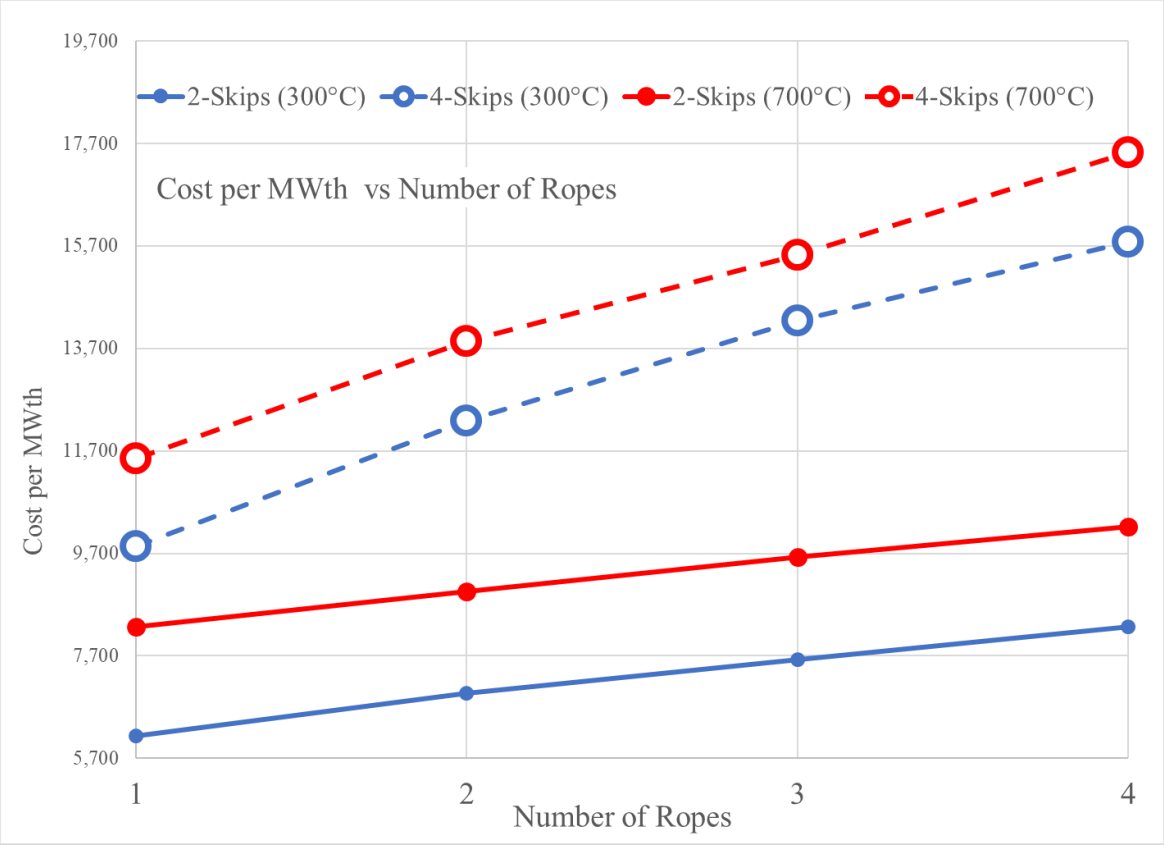

Figure 28 KEM results for Cost per MWth vs the Number of Ropes per skip.

By using the cost model in the KEM, the Cost per MWth could be determined and compared for multiples of skips installed and the number of wire ropes installed per skip. As seen in Figure 28, for the 300°C system, having only 2 skips installed in the system was always lower in cost. The lowest cost was for the 2-skip system with one rope installed per skip. However, this solution is not physically possible since the resulting diameter of the rope is 2.5 inches. Rope diameters above 2 inches and especially those approaching 3 inches are not recommended for hoisting use [38] since the flexibility of the rope greatly decreases. As expected with more ropes or more skips the cost of the system increases.

When considering the 700°C system, Figure 28 shows that a 4-skip system with one rope per skip (CB= 700°C) is lower in cost than the 2-skip system with 2 ropes per skip (CB= 700°C).

However, the 2-skip system with one rope per skip could not be considered since, as mentioned above, the wire rope diameter was 2.8 inches in diameter and this the wire rope would not be suitable for hoisting. With regards to other lower cost configurations, they were not considered since the customer wanted to have the ability in the future to upgrade from a 300°C system to a 700°C system. Therefore, the only configuration that could meet this customer need for the 700°C system would be the 2-skip system with 2 ropes per skip.

After taking the customer needs and system configuration into consideration for the 460 MWth Particle Lift design the modular cost approach was followed. It was found that the total estimated particle lift cost per MWth was $8,950 per MWth for the 700°C system and $6,970 per MWth for the 300°C system. These values were compared to the empirical estimated cost calculated from the Sayadi cost model. Sayadi cost model was found to be about $11,300 per MWth for the 700°C system and about $8,500 MWth for the 300°C system. All values have been adjusted to 2018 dollars.

In Table 26 and Table 27, the approximate total erected costs are presented for particle lift with reasonable provisions of construction overheads and integration. The cost brake down is based on methods used in the construction industry [80]. The installation cost is estimated to be close to 14% of the equipment cost unless otherwise stated. Also, average of 7% sales tax is taken to account and a conservation cost of labor of 115% due to possible overage is calculated into the estimate.

Table 26 Cost Analysis for Particle Lift Design (CB=300°C)

Description	Equipment Cost ($)	L&M Ratio	Materials & Labor ($)
Electric Motor	$290,000.00	0.14	$41,000.00
Reducer	$104,000.00	0.14	$15,000.00
Bearing	$56,000.00	0.14	$8,000.00
Hoist	$579,000.00	0.14	$81,000.00
Brakes	$16,000.00	0.14	$2,000.00
Rope	$91,000.00	0.14	$13,000.00
Skip	$362,000.00	0.14	$51,000.00
Variable Frequency Drive	$228,000.00	0.14	$32,000.00
Olds Elevator	$30,000.00	0.33	$10,000.00
Sub Total	**$1,756,000.00**		**$253,000.00**
Total Split - Material (60%)		0.60	$151,800.00
Total Split - Labor (40%)		0.40	$101,200.00
Instrumentation			
Material (30% of equipment)		0.30	$526,800.00
Installation (45% of instrument material)		0.45	$790,200.00
Subtotal	**$1,756,000.00**		**$1,468,800.00**
Sales Tax (7%)		0.07	$170,422.00
Indirect on Labor (115%)		1.15	$1,025,100.00
Bare Erected Total Cost			$3,204,500.00
Cost per Skip		2	**$1,602,250.00**
Total Estimated Particle Lift Cost per MWth		460	**$6,970.00**

Table 27 Cost Analysis for Particle Lift Design (CB=700°C)

Description	Equipment Cost ($)	L&M Ratio	Materials & Labor ($)
Electric Motor	$363,000.00	0.14	$51,000.00
Reducer	$245,000.00	0.14	$34,000.00
Bearing	$68,000.00	0.14	$10,000.00
Hoist	$492,000.00	0.14	$69,000.00
Brakes	$23,000.00	0.14	$3,000.00
Rope	$98,000.00	0.14	$14,000.00
Skip	$483,000.00	0.14	$68,000.00
Variable Frequency Drive	$457,000.00	0.14	$64,000.00
Olds Elevator	$30,000.00	0.33	$10,000.00
Sub Total	**$2,259,000.00**		**$323,000.00**
Total Split - Material (60%)		0.60	$193,800.00
Total Split - Labor (40%)		0.40	$129,200.00
Instrumentation			
Material (30% of equipment)		0.30	$677,700.00
Installation (45% of instrument material)		0.45	$1,016,550.00
Subtotal	**$2,259,000.00**		**$1,888,050.00**
Sales Tax (7%)		0.07	$219,135.00
Indirect on Labor (115%)		1.15	$1,318,000.00
Bare Erected Total Cost			$4,119,000.00
Cost per Skip		2	**$2,059,500.00**
Total Estimated Particle Lift Cost per MWth		460	**$8,950.00**

In this chapter, it was shown that even with advance solution-neutral design selection techniques certain key aspects of the design need to be address in a more refined form. By using the equation-based KEM, the overall optimized values of the particle lift characteristic were determined. While the DSM, contributes to a more detail efficiency analysis, what-if scenarios and technical specifications of the motor.

Moreover, the dimensions of the skip were modified based on the analysis for design for manufacturability and ease of transport and based on the parasitic heat loss analysis.

Lastly, a realistic cost model was developed for the particle lift that can give an accurate cost without the need to develop a very detailed design or bill of materials. It was also demonstrated that this cost model has an advantage over the traditional system level cost analysis that are not usually customized for extreme environments or non-typical operation conditions.

CHAPTER 5. CONCLUSIONS AND FUTURE WORK

To conclude, this thesis demonstrated innovations needed for design and optimization methods useful or even necessary to successfully develop energy intensive mechanical systems for challenging environments. These innovational methods have been applied to the critical component of a particle lift for a PHR system and have been shown to be useful in developing a feasible design. In particular the methods were successful for a test case of a power tower of 460 MWth. Moreover, the feasible design specifications and their cost models, were developed for two operational temperature ranges. There now exist kinematic and dynamic models in that academia and industry can use to improve particle lift designs, reduce cost and improve their operating efficiency.

These inovative methods were summarized in Figure 6 and in Figure 29. These methods show that a novel systematic process that entials flexibity in tool selection is feasible and needed for successfully design. This is also true especillay for the develpement of other applications needed for either challenging environments or for energy intenisve mechanical systems where relatively small improvement in performance can decide the success or failure of larger systems.

Novel methods, applied from the beginning of the design process where conventional design theory calls for patent searches and literature reviews, successfully showed the how quickly screening and filtering results can be conducted with the minmal use of time and resources.

These novel methods show demonstrated their greatest contribution to both academia and industry through the design process where functional requirements could be transformed and augmented with the addition of auxillary and temperoary Pseudo-Functional requirments for option comparison and selection. This is espcially true for the use of the cost indicator that gave

the ability of comparing more than one disimlar solution. Also, the process of using the Pugh method with major factor penalization, Pareto ordering and selection, and finally a pro/con analysis (as shown in Table 11) enables designers to focus on major factors that make the environment chanllegening. Most importanly, these methods enable built-in robustness in the design process to compensate for the unknown unknowns.

As for the optimization and modeling, academia and industry now have tools that can be used as stepping stones for more complex modeling and optiminzation for the design of similar application or other energy instensive systems. These tools includes a form of cost modeling somewhat familiar in thermal systems but possibly unusual in primarily mechanical systems. The cost model developed gives results that are on par to detail cost modeles without the need for detailed designs or bill of materials to have been completed.

This thesis also showed that not any one method for modeling, simulation or optimization is exculsive or independent of the other. By starting with the traditional method then moving to the SSM , then to the KEM and finally to the DSM, the development of the application can generate important information in quick procession with the minimal use of resources.

Through the development and use of these novel methods and their aid in the optimization and modeling of the energy intensive system design, key lessons have been learned and ideas developed, as seen in Figure 29. The key lessons learned are:

1. **Challenging projects tend to have non-typical conditions.** In this case, an extreme operating temperature prevails. Most designs in production can be improved and tested incrementally. However, in challenging projects, the non-typical conditions may mean that a minimal prototype may not be feasible. Instead, the initial unit must

be not only the prototype but also the operational service unit. This would also indicate iterative incremental improvement be cost prohibitive.

2. **All alternative solutions need to be considered especially since obvious solutions might not be the best suited solution.** As in the case of the particle lift, conveyor belts or bucket elevators seem to be self-evident solutions. However, by the accounting for the extreme temperatures of the particles and need to maintain these temperatures changed which solution should considered be the most suitable solution.

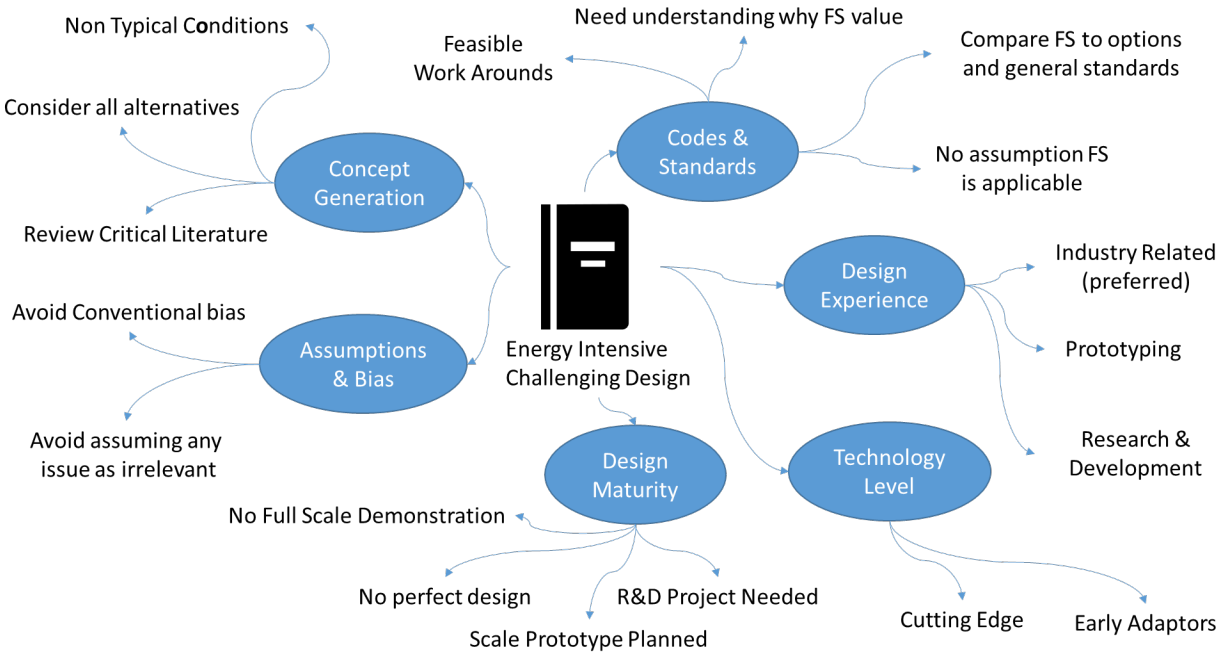

Figure 29 Mind Map showing aspects in an Energy Intensive Challenging Design.

3. **Avoid the fallacy of assuming conventional design and bias.** Would industry pick the Koepe friction hoist for the particle lift based on experience and accumulative knowledge resulting from its conventional use and bias? Probably this would be the default selection. However, by simply trying to fulfill the FR of maintaining the

particle temperature and thus minimizing heat loss, results in the disqualifying the conventional Koepe system. The reason is that the shaft temperature could greatly affect the friction needed by the hoist system to function or damage the wire rope. In addition to this, the unavoidable leakage of falling particles would easily compromise its tail ropes.

4. **Avoid the fallacy of assuming that any issue is minute or irrelevant.** It can be easy to assume that temperature plays an inconsequential role in the design since the particle temperatures do not reach the melting points of the skip materials or the shaft temperature with respect to the wire rope. By neglecting such information, a vital aspect of the design could be compromised especially since even a moderate rise in temperature can greatly reduce the strength of wire rope as seen in Figure 5. While the materials are to be used a temperature well below the operational limit, the somewhat elevated temperature is seen to have a significant effect. This situation was relatively well apparent in this design, but it is an example of how critical conditions must be identified early.
5. **Understanding the industry standard and codes and the reason "why" and "how" these values were determined.** In many cases, especially in the case of public access or life safety, a design must conform to a government regulation or an industry standard. However, it is important to understand the why the code was instituted or how the code guidelines were determined. Could the standard be a legacy value and not reflect current use and technology advancement? Or is it an essentially arbitrary value that greatly over compensates to ensure robustness is designed into the system.

6. **Do not assume the industry standards must apply to design solution and what is a more feasible standard to be applied.** As in the case of the particle lift the high safety value required by industry for elevator or hoist systems is due to the fact of possible loss of life would make the design unfeasible. In fact, this particle lift design is actually for a well-controlled industrial environment where no workers can possibly be present; therefore, the risk of loss of life is at a minimum, or if not possible during its normal intended use. By taking into consideration the why, how and intended use, a much lower safety factor can be successfully used.

With these lessoned learned and the novel methods developed; this thesis has extended the knowledge of advance design theory especially when related to extreme environment operation. The extent of which includes, a systematic approach of using different design tools earlier in the design process and relaxing the design theory procedures to better address customer needs. The systematic approach involves novel ways of using penalties in Pugh method comparisons, introducing Pseudo-Functional Requirements to Axiomatic Design evaluation and methods that can be used to quickly identify key aspects that influence a successful solution-neutral design earlier in the design cycle.

Future work would entail applying these design tools and guidelines to other extreme environment designs in order to refine this systematic multiple-tool approach to design. An obvious near-term example is the improved design of a continuous particle lift such as a high-temperature bucket elevator. Another longer-term example under consideration is the very challenging thermal control of a future Venus lander[82]. A general need is an improved and expanded cost model and associated data base. Currently, a scheme to automate the maintenance and updating of the data base is under consideration. Two more detailed improvements for the

current application are also needed: (1) The continuous improvement of the particle lift dynamic model so that it can incorporate AC induction motors without sacrificing simulation speed or drastically increasing computing resources, and (2) Further exercise and enhancement, if necessary, of the dynamic model to investigate the response of the system to other accident or failure modes. Overall, the research reported in this thesis should lead to further advances in design theory and practice and in advanced thermal and mechanical systems.

APPENDIX A: COST MODELS

The cost analysis was based on cost factors, scaling exponents and base rates that were developed using bracket values for each cost calculation, unless otherwise indicated. There are future plans to refine these values by using a range of values then use regression to determine the necessary values.

The cost calculation took the form of

$$C = C_0 \left(\frac{R}{R_0}\right)^{\beta} \tag{5}$$

Where,

C = Current cost of rated component

C_0 = Base cost for component

R = Rating Factor for component

R_0 = Base rating factor for component

β = Scaling factor for component

The scaling factor β was found using the following formulae by substituting known values for other coefficients or if the scaling factor was known in industry then the industry used value was taking as precedence.

$$ln\left(\frac{C}{C_0}\right) = \beta \cdot ln\left(\frac{R}{R_0}\right) \tag{6}$$

After component costs were determined, then a total bare erected cost was determined.

Component: Electric Motor

$C = C_0 \cdot \left(\frac{R}{R_0}\right)^{\beta}$	(7)	C_0 = \$150,000 R_0 = 1864 kW (2,500 HP) β = 0.8

Bracket Value	Cost Value	Rating Value
Lower	\$150,000	2,500 HP
Upper	\$1,000,000	20,000 HP

Source:
Kreith, Frank, and D. Yogi. Goswami. Energy Management and End Use Efficiency Handbook. Boca Raton, FL: CRC, 2006. Print. Pg 11-20

Coker, A. Kayode., and Ernest E. Ludwig. Ludwig's Applied Process Design for Chemical and Petrochemical Plants. Amsterdam: Elsevier Gulf Professional Pub., 2007. Print. Pg 71

Installed Cost (\$/hp)	Size Range (hp)
300–180	7.5–50
180–120	50–200
120–100	200–1000
100–60	1000–2500
60–50	2500–20,000

Kreith, Frank, and D. Yogi. Goswami. Energy Management and End Use Efficiency Handbook. Boca Raton, FL: CRC, 2006. Print. Pg 11-20

Component: Gear Reducer

$C = C_0 \cdot \left(\frac{R}{R_0}\right)^{\beta}$	(8)	C_0 = \$100,000 R_0 = 4200 kW β = 3.08

Bracket Value	Cost Value	Rating Value
Lower	\$100,000	4200 kW
Upper	\$300,000	6000 kW

Source:
http://www.alibaba.com/product-detail/H-series-high-power-heavy-duty_60275963234.html
http://www.alibaba.com/product-detail/Polygon-Hard-Tooth-Faced-Speed-Reducer_204531088.html

Component: Drum Brake

$C = C_0 \cdot \left(\frac{R}{R_0}\right)^{\beta}$ (9)	C_0 = \$2,286
	R_0 = 1 Brake Set
	β = 1

Value Determination
Based on values given on NREL/SR-500-33196 page 38 it was determined that each brake set could give 206,057 Nm of Torque. From there the number of brake sets was used to calculate cost.
Source: NREL/SR-500-33196 page 38

Component: Wire Rope

$C = C_0 \cdot \left(\frac{R}{R_0}\right)^{\beta}$ (10)	C_0 = \$46.22
	R_0 = 1 m
	β = 1

Value Determination
Source: Direct Quote from Hunan Baoxian Machinery Equipment Co, Ltd

Component: Skip

$\boldsymbol{C = C_0 \cdot \left(\frac{R}{R_0}\right)^{\beta}}$ (11)	C_0 = \$8.41
	R_0 = 1 kg
	β = 1

Value Determination
Source: Based on cost analysis in [65]

Component: Hoist Drum

$C = R_s \cdot C_0 \cdot \left(\frac{R}{R_0}\right)^{\beta}$ (12)	C_0 = $200,000
	R_0 = 5 m (Drum dia.)
	β = -1
	R_s = Number of Skips

Bracket Value	Cost Value	Rating Value
Lower	$500,000	2 m (drum dia.)
Upper	$200,000	5 m (drum dia.)
Source: http://www.alibaba.com/product-detail/Mine-Hoist-or-Mining-Hoist-Equipment_60033195793.html?s=p http://www.alibaba.com/product-detail/2JK-2-0X1-0-20-single_60207544552.html		

Component: Drum Bearing

$C = R_n \cdot C_0 \cdot \left(\frac{R}{R_0}\right)^{\beta}$ (13)	C_0 = $4,000 (2 bearings are used)
	R_0 = 0.180 m
	β = 1.13
	Rn = 2 x (Number of Skips)

Bracket Value	Cost Value	Rating Value
Lower	$3,25	150 mm (bore size)
Upper	$4,00	180 mm (bore size)
Source: http://www.ebay.com/itm/FAG-234430-M-SP-AXIAL-ANGULAR-CONTACT-BALL-BEARING-NTN-562030-GM-P4-/231403529689?pt=LH_DefaultDomain_0&hash=item35e0b9a5d9 http://www.ebay.com/itm/New-FAG-Bearing-7236B-MP-UA-Angular-Contact-Ball-Bearing-40-Degree-180mm-Bore-ID-/111657413257?pt=LH_DefaultDomain_0&hash=item19ff4cea89		

Component: Variable Frequency Drive

$C = R_s \cdot C_0 \cdot \left(\frac{R}{R_0}\right)^{\beta}$ (14)	C_0 = \$34,539
	R_0 = 2,000 kW
	β = 2.5

Bracket Value	Cost Value	Rating Value
Lower	\$34,539	2000 kW
Upper	\$301,333	7000KW
Source: http://www.alibaba.com/product-detail/Wanlida-medium-voltage-ac-motor-drive_60263599580.html?s=p		

Component: Foundry Style Skip (With Bail)

$C = C_0 \cdot \left(\frac{R}{R_0}\right)^{\beta}$ (15)	C_0 = \$6040
	R_0 = 1 m^3
	β = 1

Bracket Value	Cost Value	Rating Value
Lower	\$33,370	0.02 m^3
Upper	\$335,287	1 m^3
Source: Cost analysis done through market survey.		

APPENDIX B: KINEMATIC EES MODEL (KEM) CODE

The source code used in the EES environment for the kinematic model is presented below:

```
{Name: Kenzo Repole}
"Title: Particle Lift Kinematics Study"
"Log: Version 155 02-27-2019 "

{ ********************************************************************************
"Procedures Section"
 ******************************************************************************** }

Procedure  skipmovement(Deltat, A_x, V_0, H_0:  V_x, H_x, DeltaH)

t= Deltat
A_t = A_x
V_x = V_0 + (A_t)*t
H_x = H_0+V_0*t+0.5*(A_t)*t^2
DeltaH =V_0*t+0.5*(A_t)*t^2

End SkipMovement

Procedure  torquecalc(acc_rot, radius_d, moment_friction, Intertia_total, payload_wt, rope_force : Torque_applied,
InertiaPart)
 $common g, Rope_Number


//Torque_applied = ( (payload_wt*radius_d)+(Intertia_total*acc_rot))/(1-Factor_friction)
InertiaPart = Intertia_total*acc_rot
//InertiaPart =0
Torque_payload= payload_wt*radius_d
Torque_rope =( (rope_force*ROPE_NUMBER))*radius_d

Torque_applied = Torque_payload+Torque_rope + moment_friction+InertiaPart

End

Procedure  powercalc(Torque_applied, angular_velocity : Power_applied)

Power_applied = Torque_applied*angular_velocity

End

Procedure  angularvelcalc(velocity: angular_velocity )
 $common circumference_disk
 rad_m = 1 [rad]
angular_velocity = velocity/(CIRCUMFERENCE_DISK/(2*pi))*rad_m

End

Procedure  ropeforce( current_length: rope_force )
```

```
$common g_phys, rho_rope, H_design_total, Rope_CrossArea_EIPS

rope_mass_up  = RHO_ROPE*((H_DESIGN_TOTAL)-(2*current_length))*ROPE_CROSSAREA_EIPS
rope_mass_down  = RHO_ROPE*(current_length)*ROPE_CROSSAREA_EIPS
 rope_force = (rope_mass_up)*G_PHYS

End

Procedure  accelcalc(Deltat, V_i, V_f, radius_d : acc_rot)

rad_m  = 1 [rad]
//acc_rot = ((V_f-V_i)/(2*pi*radius_d*Deltat))*rad_m
  acc_rot = rad_m*((V_f-V_i)/(radius_d*Deltat))
End

Procedure  accelcalc2(Deltat, velocity: angular_acc)

angular_acc = velocity/Deltat

End

Procedure  wcalc( V_i,  : omega_rot)
$common Drum_Radius_EIPS, RadConvert

omega_rot = V_i/DRUM_RADIUS_EIPS*RADCONVERT

End

Procedure  findcost(C_0, R_0, Beta, R, Install_Ratio: C_cost, C_install)

C_cost = C_0*((R/R_0)^Beta)

C_install = Install_Ratio*C_cost

End

Procedure energy_input(Power_in_1, Power_in_2, Time_in_1, Time_in_2 : Energy_out)

delta_time = Time_in_2 - Time_in_1
 delta_power = (abs(Power_in_1)+abs(Power_in_2))/2
 Energy_out = delta_power*delta_time

End

Procedure energy_rms(Power_in_1, Power_in_2, Time_in_1, Time_in_2 : Energy_out_rms)

delta_time = Time_in_2 - Time_in_1
 rms_part = ((abs(Power_in_1))^2+(abs(Power_in_2))^2)/2
 Energy_out_rms = rms_part*delta_time

End
```

```
Procedure  skipconfig(SkipCase, Skip_Installed_in,Rope_Number_in, SafetyFactorCoff_in:
Temp_High_C,Temp_Low_C , Skip_Installed, Rope_Number, SafetyFactorCoff)

Case SkipCase

1::Temp_High_C = 1000 [C]   "From SunShot DOE SOPO"
    Temp_Low_C = 700 [C]      "From SunShot DOE SOPO"

2::Temp_High_C = 700 [C]   "From SunShot DOE SOPO"
    Temp_Low_C = 300 [C]      "From SunShot DOE SOPO"

Endcase

Skip_Installed = Skip_Installed_in "Number of Skips installed in tower"
Rope_Number = Rope_Number_in
SafetyFactorCoff = SafetyFactorCoff_in   "Working Safety Factor"

End  SkipConfig


{ ********************************************************************************
"End of Procedures"
 ********************************************************************************}


{ ********************************************************************************
"Program Control Config"
 ********************************************************************************}
SkipCase = 1
Skip_Installed_in = 2
Rope_Number_in =2
SafetyFactorCoff_in = 3
Shaft_Temp_in = 150[C]
//Heat_loss_elec = 1.291 " For 300 C"
  Heat_loss_elec = 4.735 " For 700 C"
Call  skipconfig(SkipCase, Skip_Installed_in,Rope_Number_in, SafetyFactorCoff_in: Temp_High_C,Temp_Low_C
, Skip_Installed, Rope_Number, SafetyFactorCoff)

{skipconfig(SkipCase, Skip_Installed_in,Rope_Number_in, SafetyFactorCoff_in: Temp_High_C,Temp_Low_C ,
Skip_Installed, Rope_Number, SafetyFactorCoff)

CASE 1::    Temp_High_C = 1000 [C]    "From SunShot DOE SOPO"
            Temp_Low_C = 700 [C]      "From SunShot DOE SOPO"

CASE 2::    Temp_High_C = 700 [C]     "From SunShot DOE SOPO"
            Temp_Low_C = 300 [C]      "From SunShot DOE SOPO"

}

//*******************************************************************************

"Defining Particulates Properties"
Particulate$ = 'ID-50'
     "From http://carboceramics.com.cn/attachments/wysiwyg/1/CARBOAccucast.pdf"

//C_p = 1.217543 [kJ/kg-K]
```

```
    {From http://carboceramics.com.cn/attachments/wysiwyg/1/CARBOAccucast.pdf}
//C_p_idk50 = 0.291 [cal/g-C]                                    {@1100 C}
//C_p =C_p_idk50*convert(cal/g-C,kJ/kg-K)
//C_p = 0.880 [kJ/kg-K]
Mw =101.9613 [g/mol]


CP_mid_mol = 119  [j/mol-K]
    "Extrapolated from data http://nvlpubs.nist.gov/nistpubs/jres/087/jresv87n2p159_A1b.pdf @500C"
CP_mid_k = Cp_mid_mol/Mw
//C_p =  CP_mid_k*Convert(j/g-K, kj/kg-K)
C_p = 1.175  [kJ/kg-K]
    "Ho, C.Physical properties of solid particle thermal energy storage media for concentrating solar power
applications Solar Paces 2013"


 "Density of Materials"
rho_idk50_imp = 113 [lb_m/ft^3]
rho_idk50 =  rho_idk50_imp*convert(lb_m/ft^3, kg/m^3)
rho_ss316 = 7990 [kg/m^3]
rho_steel = 8050 [kg/m^3] "wiki"
rho_rope = rho_steel*Rope_Crossection_Factor


"Temperature Change"
Temp_High =converttemp(C,K,Temp_High_C)
Temp_Low = converttemp(C,K,Temp_Low_C)

//Temp_Mid_C = 500 [C]
//Temp_Mid = converttemp(C,K,Temp_Mid_C)

DeltaTemp = Temp_High - Temp_Low

$ifnot parametrictable='TempVsRope_Diameter'
Temp_MaxShaft = 350 [C]              “Flashpoint on most lubricants is between 200 to 250 C"

$endif
Temp_MaxShaft_K = converttemp(C,K,Temp_MaxShaft)

//DeltaTemp = Temp_High

"Number of Skip"
//Skip_Installed = 2                                    "Number of Skips installed in tower"
Skip_Number = Skip_Installed /2                         "Number of Skips Operating At the same time"
"MassFlow rate over particle receiver"
//m_dot = Q_dot/(C_p*DeltaTemp)
//m_dot = (Q_dot/(C_p*DeltaTemp))/Skip_Number



"Rope Number"
//Rope_Number = 2  "ALTER"
//Rope_Number = 1  "ALTER"
//Rope_Number = 4  "For Validation"
//Rope_Number = 3  "ALTER"
```

```
"Overall Efficiency"
mu_cycle = 0.454348
mu_receiver = 0.4
mu_carnot =  1-(Temp_Low/Temp_High)
mu = mu_receiver*mu_carnot

 "Thermal Capacity of Power Station"
Q_dot =  460000 [kW]

"Power requirements"
Q_dot_elec = round( Q_dot/Mux)
W_dot_elec = round(Q_dot_elec*mu_cycle)


 //W_dot_elec = 10000 [kW]
//Q_dot_elec = round(W_dot_elec/mu_cycle)
//Q_dot = round(Q_dot_elec*Mux)



"Electrical Power"
//Q_dot_elec = 220000[kW] { mu*Q_dot}
 m_dot_ps =Q_dot_elec/(C_p*DeltaTemp)
Mux = 2.09                                                    "Solar Multiple based on Sandia Document"
 //m_dot_op = Mux*m_dot_ps
m_dot_op = Q_dot /(C_p*DeltaTemp)

m_dot= m_dot_op/Skip_Number
//m_dot= m_dot_op/Skip_Number/2


"Friction Factor"
Factor_friction = 0.0136                                      "From FLSmidth Report"
//Factor_friction = 0.075       "https://www.911metallurgist.com/mine-hoisting-equipment/#Load-Diagram"
//Factor_friction = 0.35
//Factor_friction = 0.18
"Chinese Paper The friction and wear properties of steel wire rope sliding against itself under impact load"

"Storage Times"
 Time_hotbin_hr = 9 [hr]
Time_hotbin = Time_hotbin_hr*convert(hr,s)

Time_coldbin_hr = 16[hr]
Time_coldbin = Time_coldbin_hr*convert(hr,s)

"Storage Bin Heights"
 mass_hotbin_storage = Time_hotbin*m_dot_ps
volume_hotbin_storage= mass_hotbin_storage/rho_idk50

mass_coldbin_storage = Time_coldbin*m_dot_ps
volume_coldbin_storage= mass_coldbin_storage/rho_idk50

Bin_diameter_desired = 20 [m]
Bin_area_desired = PI*(Bin_diameter_desired^2)*0.25

RemoveUnitsContstant =1 [m]
```

```
H_hotbin_desired_raw = (volume_hotbin_storage/Bin_area_desired)/RemoveUnitsContstant
H_hotbin_desired = ceil(H_hotbin_desired_raw)*RemoveUnitsContstant

H_coldbin_desired_raw = (volume_coldbin_storage/Bin_area_desired)/RemoveUnitsContstant
H_coldbin_desired = ceil(H_coldbin_desired_raw )*RemoveUnitsContstant



{*****************************************************************************************
                        POWER MODEL
*****************************************************************************************}

//Lift_Power = Lift_Torque/Total_Time
Lift_Torque = (torque_mass*g*Drum_Radius)
Stall_Torque=Lift_Torque
Lift_Torque_ftlbs = convert(N-m, ft-lb_f)* Lift_Torque
Drum_Circumference = 2*PI*Drum_Radius
Rev_per_min = 60 [s/min]
Lift_Rev = (V_BAIL[4]/ Drum_Circumference)*Rev_per_min
W_motor_max = Lift_Torque* (V_BAIL[4]/ (Drum_Circumference/(Pi*2)))
W_motor_maxKW = W_motor_max*convert(W,kW)
W_motor_maxHP = W_motor_maxKW*convert(kW,HP)
Power_conversion = 102 [kg-m/s*kW]
W_motor_Required = torque_mass*V_BAIL[4]/Power_conversion          "From SME Hand Book pg 1300 2014"
W_motor_Required_HP = W_motor_Required*convert(kW,HP)
Torque_Single_Drum = Lift_Torque
Torque_Double_Drum = ( (mass_sand
+(Rope_Number*H_design_total*rope_mass_length)*Skip_Number)*g*Drum_Radius)
SecondsPerHour = 3600 [s/hr]
Trips_per_hr = SecondsPerHour/Total_time
Mass_Sand_Tonne = Mass_Sand*convert(kg, tonne)
Tonnes_per_hr = Mass_Sand_Tonne*Trips_per_hr
Mass_per_hr = Mass_Sand*Trips_per_hr

//EIPS Drum Info
Drum_Circumference_EIPS = 2*PI*Drum_Radius_EIPS
RadConvert = 1 [rad]
//MaxRadsPerSecond = V_BAIL[4]/Drum_Circumference_EIPS*2*pi*RadConvert


{*****************************************************************************************
                                    COST MODEL
*****************************************************************************************}


"Electric Motor"
C_0_motor = 150000 [$]
R_0_motor = 1864 [kW]
beta_motor = 0.8
 R_motor =W_motor_maxKW
beta_install_motor = 0.14
Call  findcost(C_0_motor, R_0_motor, beta_motor, R_motor , beta_install_motor : C_cost_motor, C_install_motor)
```

"Gear Reducer"
C_0_gear = 100000 [$]
R_0_gear = 4200 [kW]
beta_gear = 3.08
R_gear =W_motor_maxKW
beta_install_gear = 0.14
Call findcost(C_0_gear, R_0_gear, beta_gear, R_gear, beta_install_motor: C_cost_gear, C_install_gear)

"Drum Brake"
C_0_brake = 2286 [$]
R_0_brake = 1 [-]
beta_brake = 1
base_torque = 206057 [N*m]
R_brake =round(Torque_Double_Drum/base_torque)
beta_install_brake = 0.14
Call findcost(C_0_brake, R_0_brake, beta_brake, R_brake, beta_install_brake: C_cost_brake, C_install_brake)

"Wire Rope"
C_0_wire = 46.22 [$]
R_0_wire = 1 [m]
beta_wire = 1
R_wire =round(length_rope_all)
beta_install_wire = 0.14
Call findcost(C_0_wire, R_0_wire, beta_wire, R_wire, beta_install_wire: C_cost_wire, C_install_wire)

"Skip"
C_0_skip = 8.41 [$]
R_0_skip = 1 [kg]
beta_skip = 1
R_skip =round(Skip_mass_est)
beta_install_skip = 0.14
Call findcost(C_0_skip, R_0_skip, beta_skip, R_skip, beta_install_skip: C_cost_skip, C_install_skip)

"Alternative Design Foundry Skip"
"C_0_foundry = 6040 [$]
R_0_foundry = 1 [m^3]
beta_foundry = 1
Volume_foundry = Skip_volume_metal/0.003*0.1
R_foundry =round(Volume_foundry)
beta_install_foundry = 0.14
Call findcost(C_0_foundry, R_0_foundry, beta_foundry, R_foundry, beta_install_foundry: C_cost_foundry, C_install_foundry)"
C_cost_foundry = C_cost_skip /5

"Hoist Drum"
C_0_hoist = 200000 [$]
R_0_hoist = 5 [m] "Drum Diameter"
beta_hoist = -1
R_s = Skip_Installed
//R_hoist =round(Drum_Diameter_EIPS)
R_hoist =(Drum_Diameter_EIPS)

```
beta_install_hoist = 0.14
Call  findcost(C_0_hoist, R_0_hoist, beta_hoist, R_hoist, beta_install_hoist: C_cost_hoist_s, C_install_hoist_s)

C_cost_hoist = R_s*C_cost_hoist_s
C_install_hoist =  R_s*C_install_hoist_s


 "Drum Bearing"

"https://www.nrel.gov/docs/fy07osti/40566.pdf"
 "Assuming Drum Bearing Cost included in Drum Cost"

C_0_bearing = 500 [$]
R_0_bearing = 0.180  [m]
beta_bearing = 1.13
R_n = 2*Skip_Installed
 //R_bearing =round(Drum_Diameter_EIPS)
R_bearing =(Drum_Diameter_EIPS)
beta_install_bearing = 0.14
Call  findcost(C_0_bearing, R_0_bearing, beta_bearing, R_bearing, beta_install_bearing: C_cost_bearing_n,
C_install_bearing_n)

C_cost_bearing = R_n*C_cost_bearing_n
C_install_bearing = R_n*C_install_bearing_n

  "Variable Frequency Drive"
C_0_vfd = 34539 [$]
R_0_vfd = 2000 [kW]
beta_vfd = 2.5
 R_vfd =W_motor_maxKW
beta_install_vfd = 0.14
Call  findcost(C_0_vfd, R_0_vfd, beta_vfd, R_vfd, beta_install_vfd: C_cost_vfd, C_install_vfd)

C_Cost_olds = 30000 [$]
C_install_olds = 10000 [$]

Cost_equipment= C_cost_motor
+C_cost_gear+C_cost_brake+C_cost_wire+C_cost_skip+C_cost_hoist+C_cost_bearing+C_cost_vfd+C_Cost_olds
 Cost_install= C_install_motor
+C_install_gear+C_install_brake+C_install_wire+C_install_skip+C_install_hoist+C_install_bearing+C_install_vfd
+C_install_olds

Material_Ratio = 0.60
Labor_Ratio = 0.40

Cost_Material  = Material_Ratio*Cost_install
Cost_Labor = Labor_Ratio*Cost_install

Instrument_Mat = 0.30
Instrument_Lab = 0.45

Cost_Instrument_Material  = Instrument_Mat*Cost_equipment
Cost_Instrument_Labor = Instrument_Lab*Cost_equipment

Sales_Tax = 0.07
```

```
Cost_SubTotal_Eqp = Cost_equipment
Cost_Sub_Total_Inst =  Cost_install + Cost_Instrument_Material + Cost_Instrument_Labor
Cost_Sale_Tax = Sales_Tax*(Cost_Material+Cost_Instrument_Material+Cost_equipment)

Indirect_Labor = 1.15
Cost_Indirect_Labor  = Indirect_Labor*(Cost_Instrument_Labor+ Cost_Labor)
Cost_Bare = Cost_SubTotal_Eqp + Cost_install + Cost_Sale_Tax+Cost_Indirect_Labor

Cost_PerSkip = Cost_Bare/Skip_Installed
OneMW = 1000 [kW]
Cost_PerMW = (Cost_Bare)*(OneMW/Q_dot)


{*****************************************************************************************
                                        COST MODEL SAYADI MODEL
*****************************************************************************************}


 Cost_Captial_Sayadi = (0.458*PR_S + 155323*DD_S + 135279*V_S+ 25.58*SL_S + 212.62*HP_S -
668373)*OneDollar

PR_S =  Mass_per_hr
HP_S = W_motor_maxHP
DD_S =Drum_Diameter_EIPS
SL_S = Mass_Sand
V_S = Avg_V
I_2007 = 207.342
I_now =  244.786
OneDollar = 1 [$]

Cost_Captial_SNOW = Cost_Captial_Sayadi*I_2007/I_now "$ 2018"
Cost_PerSkip_S = Cost_Captial_SNOW/Skip_Installed
Cost_PerMW_S =  (Cost_Captial_SNOW)*(OneMW/Q_dot)



{*****************************************************************************
                                        TOWER DEFINITION
*****************************************************************************}
"Defining Design Height"
H_pb = 10 [m]                                   "Height of Particulate Buffer and Chute above
Particle Receiver"
H_pc = 4 [m]                                    "Height of Particular Receiver"
//H_ht = 10 [m]                                 "Height of High Temp Bin"
H_ht = H_hotbin_desired                         "Height of High Temp Bin"
H_hx = 2 [m]                                    "Height of Heat Exchanger"
//H_lt = 10 [m]                                 "Height of Low Temp Bin"
H_lt = H_coldbin_desired                        "Height of Low Temp Bin"
H_lp =10[m]                                     "Height of Loading Pocket"

//H_design_total = H_pb+H_pc+H_ht+H_hx+H_lt+H_lp      "Height of Tower Design also distance Bail needs to
travel per cycle"
//H_design_total = 46 [m]
//H_design_total = 162 [m]
//H_design_total = 75 [m]
```

H_design_total = 138 [m]

{**********
****
SKIP DEFINITION
****
**********}

"Safety Factor"
//SafetyFactorCoff = 7.88 "For Validation"
//SafetyFactorCoff = 7.206
//SafetyFactorCoff = 5
//SafetyFactorCoff = 3 "Working Safety Factor"

"Gravity"
g_phys = 9.81 [m/s^2]
//
g_acc=0
//g_acc = 0.2
g = g_phys*(1+g_acc)

"Shaft Temperature for reduced heat loss"
Shaft_Temp = Shaft_Temp_in
//Shaft_Temp = 30 [C] "For Validation"

"Time for constant speed"
//DeltaT[4] = 1 [s]
Constant_Skip_Time = 25.88 [s]
//Time_ConstantVel = 1[s]

"Skip Factors"
Skip_Weight_Factor = 0.70 "SME Handbook Page 1300 Section 12.9"
//Skip_Weight_Factor = 0.833 "For Validation"

"Drum Dimensions"

Drum_Ratio = 80
Drum_Diameter = Rope_Diameter*Drum_Ratio
Drum_Radius = Drum_Diameter/2

Drum_Diameter_EIPS = Rope_Diameter_EIPS*Drum_Ratio
Drum_Radius_EIPS = Drum_Diameter_EIPS/2

Drum_Width_PerRope = drum_wall_thickness+drum_tube_length
Drum_Width_total =(Rope_Number* Drum_Width_PerRope) + drum_wall_thickness

Drum_mass_PerRope = mass_disk + mass_tube
Drum_mass_total = (Rope_Number* Drum_mass_PerRope) + mass_disk

Drum_inertia_PerRope = inertia_disk+interia_tube
Drum_inertia_total =((Rope_Number* Drum_inertia_PerRope) + inertia_disk)

```
"************************************************************"
"Drum design & inertia"
"************************************************************"

//Disk
thickness_disk = 2*Rope_Radius_EIPS
drum_wall_thickness = thickness_disk
diameter_disk = Drum_Diameter_EIPS
diameter_disk_inner = diamter_shaft
circumference_disk = pi*diameter_disk
area_disk =  (pi/4)*((diameter_disk)^2 - (diameter_disk_inner)^2)
volume_disk = area_disk*thickness_disk
mass_disk = rho_steel*volume_disk
inertia_disk =(mass_tube/2)*((diameter_disk)^2 + (diameter_disk_inner)^2)


//Tube
dead_turns_rope =10
number_turns_rope = (H_design_total /circumference_disk)+dead_turns_rope
//number_turns_rope =10
thickness_tube = 3*Rope_Radius_EIPS
diameter_tube = diameter_disk
diameter_tube_inner = diameter_disk - 2*thickness_tube
circumference_tube = pi*diameter_tube
length_tube = number_turns_rope*Rope_Radius_EIPS
drum_tube_length = length_tube
area_tube= (pi/4)*((diameter_tube)^2 - (diameter_tube_inner)^2)
volume_tube = area_tube*length_tube
mass_tube  = rho_steel*volume_tube
interia_tube = (mass_tube/2)*((diameter_tube)^2 + (diameter_tube_inner)^2)


//Shaft
meter_one = 1 [m]
diamter_shaft = meter_one/2
area_shaft = (pi*(diamter_shaft)^2)/4
length_shaft = 3*thickness_disk+2*length_tube+meter_one
volume_shaft = area_shaft*length_shaft
mass_shaft  = rho_steel*volume_shaft
//intertia_shaft = (mass_shaft*(diamter_shaft)^2)/8
intertia_shaft = 1000 [kg-m^2]

//Rope
 rope_mass_length = 15.5 [kg/m]
//length_rope_all = circumference_tube*number_turns_rope
//mass_rope_all = rho_rope*(length_rope_all+H_design_total)*Rope_CrossArea_EIPS
//intertia_rope_all = (mass_rope_all*(Rope_Radius_EIPS)^2)/2
length_rope_drum= circumference_tube*number_turns_rope*Skip_Installed
length_rope_all = length_rope_drum*Rope_Number*Skip_Installed
mass_rope_each =( length_rope_drum)*rope_mass_length
```

```
//Total Inertia Assembly
"BOM Assembly is 3xDisk + 2xTube+1xShaft+Motor+2xRope"
//total_vertical_mass = (Skip_Installed*mass_skip)+mass_sand +(Skip_Installed*Rope_Number*mass_rope_all)
total_vertical_mass = (Skip_Installed*mass_skip_skip)+mass_sand
+(Skip_Installed*Rope_Number*mass_rope_each)
torque_mass = mass_sand +(Rope_Number*H_design_total*rope_mass_length)*Skip_number +mass_skip

inertia_total_vertmass = total_vertical_mass*Drum_Radius_EIPS^2

inertia_motor = 211.1 [kg*m^2]
     "HV induction motors, technical catalog for IEC motors EN 07-2016 | BU Motors and Generators |
ABB  pg 124"

//intertia_drum_total = ((2*inertia_disk)+(interia_tube))*Skip_Installed*Rope_Number
intertia_drum_total=Drum_inertia_total*Skip_Installed    //2 skips mean one full drum or 4 skips means 2 full drums
 inertia_total = intertia_drum_total+intertia_shaft+inertia_motor +inertia_total_vertmass
interia_remain=intertia_shaft+inertia_total_vertmass
//inertia_total = 981443*0.88
moment_friction = total_vertical_mass*g*Factor_friction*Drum_Radius_EIPS
 //inertia_rotational =
((2*inertia_disk)+(1*interia_tube))*Skip_Installed*Rope_Number+intertia_shaft+inertia_motor
 //mass_drum_assembly =(3*mass_disk)+(2*mass_tube)+mass_shaft+mass_rope_all

"************************************************************"
"Gear Design"
"************************************************************"
Gear_Ratio = 50
Gear_eff = 0.95

"************************************************************"
"Skip Design"
"************************************************************"

"Define Internal Volume"
Vol_mass = m_volume
Vol_air = 1/8*Vol_mass
Vol_total = round( Vol_mass + Vol_air)

Dim_in_H = 3*Dim_in_T
Dim_in_W = Dim_in_T
Dim_in_vol  = Vol_total
Dim_in_vol = Dim_in_T*Dim_in_W*Dim_in_H

Fb_thickness = 0.063 [m]    "Thickness of Fire Brick"
Dim_fb_H = 3*Dim_fb_T
Dim_fb_W= Dim_fb_T
Dim_fb_T = Dim_in_T + 2*Fb_thickness
Vol_fb  = Dim_fb_H*Dim_fb_W*Dim_fb_T

Skip_metal_thickns = 0.003 [m]

Skip_Clearance = 0.5[m]
Skip_height = 3*Skip_width+ Skip_Clearance
Skip_Thickness = Skip_width
Skip_volume = Skip_height*Skip_width*Skip_Thickness
```

```
//Skip_volume = 8 [m^3]
Skip_volume = Vol_total

{
"Estimating Weight of Skip - Using Industry Standard for Weight Calculation"
"Skip_side = Skip_height*Skip_width*Skip_metal_thickns
Skip_bottom = Skip_width*Skip_Thickness*Skip_metal_thickns
Skip_top =  Skip_width*Skip_Thickness*Skip_metal_thickns
Skip_volume_metal = Skip_side*4 + Skip_bottom +Skip_top
Skip_mass_est = rho_ss316*Skip_volume_metal

//Skip_to_BaleRatio = 3.5
//Skip_Weight_FEST = Skip_mass_est*(1+Skip_to_BaleRatio)

//Skip_Weight_FEST = (Skip_mass_est/Mass_Sand )*1.05"
 }

Skip_mass_est = mass_skip

 {
//Skip_area = 4 [m^2]                                   "Internal Surface Area where particulate is located"
}

Time_load = 7.5 [s]                                     "From FLSmdith"
//Time_load = 10 [s]                                    "From Hard Rock Miner Hand Book for Automated
Filling of the Skip"
//Time_ConstantVel  =  2 [s]                            "For Optimization"

"Defining the different stages of one cycle of Balance 2 skip process"
"Height is the location of the Bail during the cycle"

{*****************************************************************************************
                                        SKIP OPERATION
*****************************************************************************************}

"Initial Conditions"
 STAGE$[0] ='Initial Condition'
H_BAIL[0] = 0 [m]
V_BAIL[0] = 0[m/s]
A_BAIL[0] = 0 [m/s^2]
M_SKIP[0] = 0 [kg]
T_start[0] = 0 [s]
DeltaT[0] = 0 [s]
DeltaH[0] = 0 [m]
T_end[0] = T_start[0] +DeltaT[0]
//Torque[0] = 0 [N*m]

//Time_Torque[0] = T_start[1]

//Call ropeforce( H_BAIL[0]: rope_force[0] )
Call wcalc( V_BAIL[0]  : omega[0])
```

"Charging Skip Stage"

{STAGE$[1] ='Filling Skip'
M_SKIP[1] = M_dot_fill *DeltaT[1]
V_BAIL[1] = 0[m/s]
A_BAIL[1] = 0[m/s]
H_BAIL[1] = 0 [m]
DeltaH[1] = 0 [m]
Call wcalc(V_BAIL[1] : omega[1])

T_start[1] = T_end[0]
DeltaT[1] = Time_load
T_end[1] = T_start[1] +DeltaT[1]
}

STAGE$[1] ='Filling Skip'
M_SKIP[1] = M_dot_fill *DeltaT[1]

A_BAIL[1] = A_BAIL[0]
Call wcalc(V_BAIL[1] : omega[1])

T_start[1] = T_end[0]
DeltaT[1] = Time_load
T_end[1] = T_start[1] +DeltaT[1]

Call skipmovement(DeltaT[1], A_BAIL[1], V_BAIL[0], H_BAIL[0]: V_BAIL[1], H_BAIL[1], DeltaH[1])

"Break Release"
STAGE$[2] ='Break Release'

M_SKIP[2] =M_SKIP[1]

V_BAIL[2] = 0.5 [m/s]
Call wcalc(V_BAIL[2] : omega[2])

T_start[2] = T_end[1]

DeltaT[2] = 1 [s]
T_end[2] = T_start[2] +DeltaT[2]

Call skipmovement(DeltaT[2], A_BAIL[2], V_BAIL[1], H_BAIL[1]: V_BAIL[2], H_BAIL[2], DeltaH[2])

"Creep In Stage"
STAGE$[3] ='Creep In Stage'
M_SKIP[3] =M_SKIP[1]

V_CI = 0.5 [m/s]
V_BAIL[3] = V_CI
Call wcalc(V_BAIL[3] : omega[3])

T_start[3] = T_end[2]

```
//DeltaT[3] = 5 [s]                                    "From Hard Rock Miner Hand Book"
DeltaT[3] = 3 [s]
T_end[3] = T_start[3] +DeltaT[3]


Call skipmovement(DeltaT[3], A_BAIL[3], V_BAIL[2], H_BAIL[2]:  V_BAIL[3], H_BAIL[3], DeltaH[3])


"Acceleration Stage"
STAGE$[4] ='Acceleration Stage'
M_SKIP[4] = M_SKIP[1]
 Call wcalc( V_BAIL[4]  : omega[4])

T_start[4] = T_end[3]
//DeltaT[4] = 15 [s]                                   "From Hard Rock Miner Hand Book"
DeltaT[4] = 7 [s]
T_end[4] = T_start[4] +DeltaT[4]
//A_BAIL[4] =  (V_BAIL[4] - V_BAIL[3])/DeltaT[4]

Call skipmovement(DeltaT[4], A_BAIL[4], V_BAIL[3], H_BAIL[3]:  V_BAIL[4], H_BAIL[4], DeltaH[4])


"Constant Speed Travel Stage"
STAGE$[5] ='Constant Speed Travel Stage'
M_SKIP[5] =M_SKIP[1]
A_BAIL[5] = 0 [m/s^2]
Call wcalc( V_BAIL[5]  : omega[5])
 {

V_BAIL[5] =Constant_Skip_Speed
 }

DeltaT[5]=Constant_Skip_Time

T_start[5] = T_end[4]
T_end[5] = T_start[5] +DeltaT[5]

Call skipmovement(DeltaT[5], A_BAIL[5], V_BAIL[4], H_BAIL[4]:  V_BAIL[5], H_BAIL[5], DeltaH[5])


"Deceleration Stage"
STAGE$[6] ='Deceleration Stage'
M_SKIP[6] =M_SKIP[1]
 Call wcalc( V_BAIL[6]  : omega[6])

T_start[6] = T_end[5]
//DeltaT[5] = 15 [s]                                   "From Hard Rock Miner Hand Book"
DeltaT[6] = 7 [s]
T_end[6] = T_start[6] +DeltaT[6]

V_BAIL[6] =  V_CO

Call skipmovement(DeltaT[6], A_BAIL[6], V_BAIL[5], H_BAIL[5]:  V_BAIL[6], H_BAIL[6], DeltaH[6])

// Call torquecalc(DeltaT[5], V_BAIL[5], V_BAIL[6], Rope_Radius_EIPS, Factor_friction, inertia_total,
Mass_Sand : Torque[5], Acc[5])
```

```
"Creep Out Stage"
STAGE$[7] ='Creep Out Stage'
M_SKIP[7] = M_SKIP[1]

V_CO= V_CI

V_BAIL[7] =  0.5 [m/s]

Call wcalc( V_BAIL[7]  : omega[7])

T_start[7] = T_end[6]
//DeltaT[6] = 5 [s]                                    "From Hard Rock Miner Hand Book"
DeltaT[7] = 3 [s]
T_end[7] = T_start[7] +DeltaT[7]


Call skipmovement(DeltaT[7], A_BAIL[7], V_BAIL[6], H_BAIL[6]:  V_BAIL[7], H_BAIL[7], DeltaH[7])

"Break Engage"
STAGE$[8] ='Break Engage'

M_SKIP[8] =M_SKIP[1]


V_BAIL[8] = 0.0 [m/s]
Call wcalc( V_BAIL[8]  : omega[8])

T_start[8] = T_end[7]
//DeltaT[2] = 5 [s]                                    "From Hard Rock Miner Hand Book"
DeltaT[8] = 1 [s]
T_end[8] = T_start[8]+DeltaT[8]

Call skipmovement(DeltaT[8], A_BAIL[8], V_BAIL[7], H_BAIL[7]:  V_BAIL[8], H_BAIL[8], DeltaH[8])


"Discharging Skip Stage"
STAGE$[9] ='Discharging Skip'
M_SKIP[9] = 0 [kg]


V_BAIL[9] = 0 [m/s]
A_BAIL[9] =0 [m/s^2]
DeltaH[9] = H_BAIL[9] - H_BAIL[8]
 H_BAIL[8]=H_BAIL[9]
T_start[9] = T_end[8]
DeltaT[9] =Time_load                                   " From Hard Rock Miner Hand Book for Automated
Filling of the Skip"
T_end[9] = T_start[9] +DeltaT[9]

Call wcalc( V_BAIL[9]  : omega[9])


m_dot*T_end[9] = M_SKIP[1]
H_design_total= H_BAIL[9]
```

```
m_volume =  M_SKIP[1]/rho_idk50

Total_Time = T_end[9]


{*****************************************************************************************
                              TORQUE CALCULATIONS
*****************************************************************************************}

"Calculating Required Torque at each stage"
 "Start of Charging"

 Time_Torque[0] = T_start[0]
Torque[0] = 0 [N*m]
Acc[0] =  0 [rad/s^2]
Constant_Acc = Acc[0]
//Time_Torque[0] = T_start[1]
Call ropeforce( H_BAIL[0]: rope_force[0] )

Call angularvelcalc(V_BAIL[0]: angular_velocity[0] )
Call  powercalc(Torque[0], angular_velocity[0] : Power_applied[0])


 "End of Charging"
"Start of Break Release"
Time_Torque[1] =  T_end[1]
Torque[1] = 0 [N*m]
Acc[1] =  0 [rad/s^2]
Call ropeforce( H_BAIL[0]: rope_force[1] )

Call angularvelcalc(V_BAIL[1]: angular_velocity[1] )
Call  powercalc(Torque[1], angular_velocity[1] : Power_applied[1])

{Time_Torque[1] = T_end[1]
Call ropeforce( H_BAIL[1]: rope_force[1] )
//Torque[1] = 0 [N*m]
Acc[1] =  0 [rad/s^2]
Call torquecalc( Acc[1], Drum_Radius_EIPS, moment_friction, inertia_total, load_sand, rope_force[1] : Torque[1])
Call angularvelcalc(V_BAIL[1]: angular_velocity[1] )
Call  powercalc(Torque[1], angular_velocity[1] : Power_applied[1])}



 "End of Break Release"

 "Start of Creep"
Time_Torque[2] = T_start[2]
Call ropeforce( H_BAIL[1]: rope_force[2] )
//Acc[1] = 0
Call accelcalc(DeltaT[2], V_BAIL[1], V_BAIL[2], Drum_Radius_EIPS : Acc[2])
 Call torquecalc( Acc[2], Drum_Radius_EIPS, moment_friction, inertia_total, load_sand, rope_force[2] : Torque[2],
InertiaPart[2])

Call angularvelcalc(V_BAIL[1]: angular_velocity[2] )
Call  powercalc(Torque[2], angular_velocity[2] : Power_applied[2])
```

"End of Creep"
Time_Torque[3] = T_end[2]
Call ropeforce(H_BAIL[2]: rope_force[3])
//Acc[2] = Acc[1]
Call accelcalc(DeltaT[2], V_BAIL[1], V_BAIL[2], Drum_Radius_EIPS : Acc[3])
Call torquecalc(Acc[3], Drum_Radius_EIPS, moment_friction, inertia_total, load_sand, rope_force[3] : Torque[3], InertiaPart[3])

Call angularvelcalc(V_BAIL[2]: angular_velocity[3])
Call powercalc(Torque[3], angular_velocity[3] : Power_applied[3])

"Start of Acceleration"
Time_Torque[4] = T_start[3]
Call ropeforce(H_BAIL[2]: rope_force[4])
Call accelcalc(DeltaT[3], V_BAIL[2], V_BAIL[3], Drum_Radius_EIPS : Acc[4])
//Call accelcalc2(DeltaT[3], angular_velocity[4]: angular_acc)
Call torquecalc(Acc[4], Drum_Radius_EIPS, moment_friction, inertia_total, load_sand, rope_force[4] : Torque[4], InertiaPart[4])

Call angularvelcalc(V_BAIL[2]: angular_velocity[4])
Call powercalc(Torque[4], angular_velocity[4] : Power_applied[4])

"End of Acceleration"
Time_Torque[5] = T_end[3]
Call ropeforce(H_BAIL[3]: rope_force[5])
//Acc[4] = Acc[3]
Call accelcalc(DeltaT[3], V_BAIL[2], V_BAIL[3], Drum_Radius_EIPS : Acc[5])
Call torquecalc(Acc[5], Drum_Radius_EIPS, moment_friction, inertia_total, load_sand, rope_force[5] : Torque[5], InertiaPart[5])

Call angularvelcalc(V_BAIL[3]: angular_velocity[5])
Call powercalc(Torque[5], angular_velocity[5] : Power_applied[5])

"Start of Constant Speed"
Time_Torque[6] = T_start[4]
Call ropeforce(H_BAIL[3]: rope_force[6])
Call accelcalc(DeltaT[4], V_BAIL[3], V_BAIL[4], Drum_Radius_EIPS : Acc[6])
//Acc[5] = Constant_Acc
Call torquecalc(Acc[6], Drum_Radius_EIPS, moment_friction, inertia_total, load_sand, rope_force[6] : Torque[6], InertiaPart[6])

Call angularvelcalc(V_BAIL[3]: angular_velocity[6])
Call powercalc(Torque[6], angular_velocity[6] : Power_applied[6])

"End of Constant Speed"
Time_Torque[7] = T_end[4]
Call ropeforce(H_BAIL[4]: rope_force[7])
//Acc[7] = Constant_Acc
Call accelcalc(DeltaT[4], V_BAIL[3], V_BAIL[4], Drum_Radius_EIPS : Acc[7])
Call torquecalc(Acc[7], Drum_Radius_EIPS, moment_friction, inertia_total, load_sand, rope_force[7] : Torque[7], InertiaPart[7])

Call angularvelcalc(V_BAIL[4]: angular_velocity[7])
Call powercalc(Torque[7], angular_velocity[7] : Power_applied[7])

```
 "Start of Deceleration"
Time_Torque[8] = T_start[5]
Call ropeforce( H_BAIL[4]: rope_force[8] )
Call accelcalc(DeltaT[5], V_BAIL[4], V_BAIL[5], Drum_Radius_EIPS : Acc[8])
 Call torquecalc( Acc[8], Drum_Radius_EIPS, moment_friction, inertia_total, load_sand, rope_force[8] : Torque[8],
InertiaPart[8])

Call angularvelcalc(V_BAIL[4]: angular_velocity[8] )
Call  powercalc(Torque[8], angular_velocity[8] : Power_applied[8])

"End of Deceleration"
Time_Torque[9] = T_end[5]
Call ropeforce( H_BAIL[5]: rope_force[9] )
Call accelcalc(DeltaT[5], V_BAIL[4], V_BAIL[5], Drum_Radius_EIPS : Acc[9])
Call torquecalc(Acc[9], Drum_Radius_EIPS, moment_friction, inertia_total, load_sand, rope_force[9] : Torque[9],
InertiaPart[9])

Call angularvelcalc(V_BAIL[5]: angular_velocity[9] )
Call  powercalc(Torque[9], angular_velocity[9] : Power_applied[9])


 "Start of Creep Out"
Time_Torque[10] = T_start[6]
Call ropeforce( H_BAIL[5]: rope_force[10] )
Call accelcalc(DeltaT[6], V_BAIL[5], V_BAIL[6], Drum_Radius_EIPS : Acc[10])
 Call torquecalc( Acc[10], Drum_Radius_EIPS, moment_friction, inertia_total, load_sand, rope_force[10] :
Torque[10], InertiaPart[10])

Call angularvelcalc(V_BAIL[5]: angular_velocity[10] )
Call  powercalc(Torque[10], angular_velocity[10] : Power_applied[10])

"End of Creep Out"
Time_Torque[11] = T_end[6]
Call ropeforce( H_BAIL[6]: rope_force[11] )
Call accelcalc(DeltaT[6], V_BAIL[5], V_BAIL[6], Drum_Radius_EIPS : Acc[11])
Call torquecalc(Acc[11], Drum_Radius_EIPS, moment_friction, inertia_total, load_sand, rope_force[11] :
Torque[11],InertiaPart[11])

Call angularvelcalc(V_BAIL[6]: angular_velocity[11] )
Call  powercalc(Torque[11], angular_velocity[11] : Power_applied[11])

 "Start of Discharging"
Time_Torque[12] = T_start[7]
Call ropeforce( H_BAIL[6]: rope_force[12] )
Call accelcalc(DeltaT[7], V_BAIL[6], V_BAIL[7], Drum_Radius_EIPS : Acc[12])
//Acc[12] =Constant_Acc
 Call torquecalc( Acc[12], Drum_Radius_EIPS, moment_friction, inertia_total, load_sand, rope_force[12] :
Torque[12], InertiaPart[12])
//Torque[12] = 0 [N*m]

Call angularvelcalc(V_BAIL[6]: angular_velocity[12] )
Call  powercalc(Torque[12], angular_velocity[12] : Power_applied[12])

"End of Discharging"
Time_Torque[13] = T_end[7]
```

```
Call ropeforce( H_BAIL[7]: rope_force[13] )
// Acc[13] = Constant_Acc
Call accelcalc(DeltaT[7], V_BAIL[6], V_BAIL[7], Drum_Radius_EIPS : Acc[13])
Call torquecalc(Acc[13], Drum_Radius_EIPS, moment_friction, inertia_total, load_sand, rope_force[13] :
Torque[13], InertiaPart[13])
//Torque[13] = 0 [N*m]

Call angularvelcalc(V_BAIL[7]: angular_velocity[13] )
Call  powercalc(Torque[13], angular_velocity[13] : Power_applied[13])

 "End of Discharging"
Time_Torque[14] = T_start[8]
Call ropeforce( H_BAIL[8]: rope_force[14] )
// Acc[13] = Constant_Acc
Call accelcalc(DeltaT[8], V_BAIL[7], V_BAIL[8], Drum_Radius_EIPS : Acc[14])
Call torquecalc(Acc[14], Drum_Radius_EIPS, moment_friction, inertia_total, load_sand, rope_force[14] :
Torque[14], InertiaPart[14])
//Torque[13] = 0 [N*m]

Call angularvelcalc(V_BAIL[7]: angular_velocity[14] )
Call  powercalc(Torque[14], angular_velocity[14] : Power_applied[14])

  "Start of Break Engage"
Time_Torque[15] = T_end[8]
Call ropeforce( H_BAIL[8]: rope_force[15] )
Call accelcalc(DeltaT[8], V_BAIL[7], V_BAIL[8], Drum_Radius_EIPS : Acc[15])
//Acc[12] =Constant_Acc
 Call torquecalc( Acc[15], Drum_Radius_EIPS, moment_friction, inertia_total, load_sand, rope_force[15] :
Torque[15], InertiaPart[15])
//Torque[12] = 0 [N*m]

Call angularvelcalc(V_BAIL[8]: angular_velocity[15] )
Call  powercalc(Torque[15], angular_velocity[15] : Power_applied[15])

   "Start of Discharging"
"End of Break Engage"
Time_Torque[16] = T_start[9]
Call ropeforce( H_BAIL[9]: rope_force[16] )
//Call accelcalc(DeltaT[9], V_BAIL[8], V_BAIL[9], Rope_Radius_EIPS : Acc[17])
Acc[16] =Constant_Acc
 //Call torquecalc( Acc[17], Drum_Radius_EIPS, moment_friction, inertia_total, load_sand, rope_force[17] :
Torque[17])
Torque[16] = 0 [N*m]
 angular_velocity[16] = 0 [rad/s]
Power_applied[16] = 0 [W]
//Call angularvelcalc(V_BAIL[9]: angular_velocity[17] )
//Call  powercalc(Torque[17], angular_velocity[17] : Power_applied[17])

   "End of Discharging"
Time_Torque[17] = T_end[9]
Call ropeforce( H_BAIL[9]: rope_force[17] )
Acc[17] =Constant_Acc
Torque[17] = 0 [N*m]
 angular_velocity[17] = 0 [rad/s]
Power_applied[17] = 0 [W]
```

```
//***************Input Energy ******************************

Call energy_input(Power_applied[2], Power_applied[3], Time_Torque[2] , Time_Torque[3] : Energy_out[0])
"Brake Release"
Call energy_input(Power_applied[4], Power_applied[5], Time_Torque[4] , Time_Torque[5] : Energy_out[1])
"Creep Out"
Call energy_input(Power_applied[6], Power_applied[7], Time_Torque[6] , Time_Torque[7] : Energy_out[2])
"Acceleration"
Call energy_input(Power_applied[8], Power_applied[9], Time_Torque[8] , Time_Torque[9] : Energy_out[3])
"Constant Speed"
Call energy_input(Power_applied[10], Power_applied[11], Time_Torque[10] , Time_Torque[11] : Energy_out[4])
"Deceleration"
Call energy_input(Power_applied[12], Power_applied[13], Time_Torque[12] , Time_Torque[13] : Energy_out[5])
"Creep In"
Call energy_input(Power_applied[14], Power_applied[15], Time_Torque[14] , Time_Torque[15] : Energy_out[6])
"Creep In"

 { dc = 93% https://www.alibaba.com/product-detail/Heavy-duty-dc-motor-
manufacturer_60568729971.html?spm=a2700.7724857.normalList.9.36d31762FmQCRu&s=p }
eta_motor =0.97 {https://en.wikipedia.org/wiki/Induction_motor#Efficiency}
eta_vfd = 0.96
eta_gear =0.95
eta_drum =0.98
Total_energy_In
=(Energy_out[0]+Energy_out[1]+Energy_out[2]+Energy_out[3]+Energy_out[4]+Energy_out[5]+Energy_out[6])/(et
a_motor*eta_gear){*eta_drum)}
 Total_energy_win =( Total_energy_In/(Time_Torque[14]-Time_Torque[2]))*convert(J/s, kW)
 Total_energy_potential = Mass_Sand*g*H_BAIL[7]
 Total_energy_wpotential  = (Total_energy_potential /( Time_Torque[14]-Time_Torque[2]))*convert(J/s, kW)
eta_particlelift_motor = Total_energy_potential /Total_energy_In

eta_particlelift = (Total_energy_wpotential)/ (Total_energy_win+Heat_loss_elec)

 //***************RMS*****************************************


 Call energy_rms(Power_applied[2], Power_applied[3], Time_Torque[2] , Time_Torque[3] : Energy_out_rms[0])
"Brake Release"
Call energy_rms(Power_applied[4], Power_applied[5], Time_Torque[4] , Time_Torque[5] : Energy_out_rms[1])
"Creep Out"
Call energy_rms(Power_applied[6], Power_applied[7], Time_Torque[6] , Time_Torque[7] : Energy_out_rms[2])
"Acceleration"
Call energy_rms(Power_applied[8], Power_applied[9], Time_Torque[8] , Time_Torque[9] : Energy_out_rms[3])
"Constant Speed"
Call energy_rms(Power_applied[10], Power_applied[11], Time_Torque[10] , Time_Torque[11] :
Energy_out_rms[4]) "Decceleration"
Call energy_rms(Power_applied[12], Power_applied[13], Time_Torque[12] , Time_Torque[13] :
Energy_out_rms[5]) "Creep In"
Call energy_rms(Power_applied[14], Power_applied[15], Time_Torque[14] , Time_Torque[15] :
Energy_out_rms[6]) "Creep In"

Power_RMS = sqrt(
(Energy_out_rms[0]+Energy_out_rms[1]+Energy_out_rms[2]+Energy_out_rms[3]+Energy_out_rms[4]+Energy_ou
t_rms[5]+Energy_out_rms[6])/ ( (Time_Torque[14]-Time_Torque[2]) +( Time_Torque[1]-
Time_Torque[0])/3))*convert(W,kW){/eta_motor}
```

```
//***************AC Motor Values ***************************

//motor_voltage = 2200 [V]
motor_voltage = 10000 [V]
motor_z = motor_voltage^2/(25*power_rms*convert(kW, W))

motor_freq = 60 [Hz]
motor_L= motor_Z / motor_freq


"https://www.mathworks.com/help/physmod/sps/powersys/ug/simulating-a-dc-motor-drive.html"

//Skip_height = m_volume/Skip_Area
//Skip_volume = m_volume
{T_hb_cycle  = H_design/V_BAIL[4]+ 15 +  DeltaT[1]
T_end[7] = T_hb_cycle}

Avg_V = H_BAIL[7]/T_end[8]

"Rope Safety Limit"
//M_TOTAL = M_SKIP[1]*(1+Skip_Weight_Factor)          "From SME Mining Handbook"
M_TOTAL_SKIP = (mass_sand_skip+mass_skip_skip)
M_TOTAL = M_TOTAL_SKIP*Skip_Number
//M_TOTAL = M_SKIP[1]+Skip_Weight_FEST
//M_TOTAL = 55000 [kg]                                "Calculated"
//M_TOTAL_TONNE = M_TOTAL/1000
M_TOTAL_TONNE = M_TOTAL*convert(kg,Tonne)
M_TOTAL_TON_US = M_TOTAL*convert(kg,Ton)

mass_sand_skip = M_SKIP[1]
load_sand_skip = mass_sand_skip*g
mass_skip_skip=mass_sand_skip*Skip_Weight_Factor
Load_Total_skip = (mass_sand_skip+mass_skip_skip)*g

Mass_Sand = mass_sand_skip*Skip_Number
load_sand = mass_sand*g
 mass_skip = Mass_Sand*Skip_Weight_Factor
//mass_skip = Skip_Weight_FEST
Load_Total = (Mass_Sand+mass_skip)*g

//Data_Yield_300C = INTERPOLATE2('YieldStress', 'Temp_C', 'Yield', Temp_C= Temp_Low)
//Data_Tensile_300C = INTERPOLATE2('TensileStrength', 'Temp', 'TensileStrength', Temp = Temp_Low_C)
//Data_Yield_Shaft_Temp = interpolate('YieldStress', 'Temp_C', 'Yield', Temp_C= Shaft_Temp)
//Data_Tensile_Shaft_Temp = interpolate('TensileStrength', 'Temp', 'TensileStrength', Temp = Shaft_Temp)
//Data_Tensile_Shaft_Temp = interpolate('TensileStrengthModified', 'Temp', 'TensileStrength', Temp =
Shaft_Temp)

//Data_Tensile_Shaft_Temp = 1206 [MPa]
//Data_Tensile_Shaft_Temp_EIPS = 1760 [MPa]
```

```
//***************Defining Steel Strength*******************************
Steel_Tensile_IPS =  1206 [MPa]
Steel_Yield_IPS = 500[MPa]
Steel_Tensile_EIPS =  1760 [MPa]

//**************Using Temperature Factor Tables*****************
Data_Tensile_Shaft_Temp_IPS = interpolate('HighTempReductionFactors', 'Temp_Steel_C', 'Factor_limit',
Temp_Steel_C = Shaft_Temp)*Steel_Tensile_IPS
Data_Yield_Shaft_Temp = interpolate('HighTempReductionFactors', 'Temp_Steel_C', 'Factor_yield', Temp_Steel_C
= Shaft_Temp)*Steel_Yield_IPS
Data_Tensile_Shaft_Temp_EIPS  = interpolate('HighTempReductionFactors', 'Temp_Steel_C', 'Factor_limit',
Temp_Steel_C = Shaft_Temp)*Steel_Tensile_EIPS
Data_Tensile_Shaft_Temp = Data_Tensile_Shaft_Temp_IPS

//Rope_Load_YieldStrength = Data_Yield_Shaft_Temp
//Rope_Load_Allowable =  Rope_Load_YieldStrength/SafetyFactorCoff

//****************FOR STEEL EIPS*****************************************************************
 Rope_failure_load_EIPS = convert(MPa, kN/m^2)*Data_Tensile_Shaft_Temp*Rope_CrossArea_EIPS
Rope_Load_Allowable_EIPS=  Data_Tensile_Shaft_Temp_EIPS/SafetyFactorCoff
Rope_Load_Allowable_PA_EIPS = Rope_Load_Allowable_EIPS*convert(MPa,Pa)

//Rope_Load =  Load_Total/Rope_Number
Rope_Load =  Load_Total_skip/Rope_Number                    "Load experienced by each rope"
//Rope_Crossection_Factor = 0.55                            "From Hanson Manual - For Fiber Core Rope"
Rope_Crossection_Factor = 0.62                              "For IWRC Rope Includes Strand 7"
Rope_Crossection_Prelim_EIPS = (Rope_Load/Rope_Load_Allowable_PA_EIPS)
        "Rope Cross section without correction factor"

Rope_CrossArea_EIPS = Rope_Crossection_Prelim_EIPS/Rope_Crossection_Factor
Rope_Radius_EIPS_m = (Rope_CrossArea_EIPS/PI)^0.5

Rope_Diameter_EIPS_m = 2*Rope_Radius_EIPS_m
Rope_Diameter_mm_EIPS =round( Rope_Diameter_imp_EIPS*convert(in,mm),0.1)
Rope_Diameter_imp_EIPS = round(Rope_Diameter_EIPS_m*convert(m,in), 0.1)
Rope_Radius_EIPS = 0.5*Rope_Diameter_imp_EIPS*convert(in,m)
Rope_Diameter_EIPS=  Rope_Diameter_mm_EIPS*convert(mm,m)

//***************************FOR STEEL IPS*************************************************

 Rope_failure_load = convert(MPa, kN/m^2)*Data_Tensile_Shaft_Temp*Rope_CrossArea
Rope_Load_Allowable =  Data_Tensile_Shaft_Temp/SafetyFactorCoff
Rope_Load_Allowable_PA = Rope_Load_Allowable*convert(MPa,Pa)

Rope_Crossection_Prelim = (Rope_Load/Rope_Load_Allowable_PA)
                        "Rope Cross-section without correction factor"
Rope_CrossArea = Rope_Crossection_Prelim/Rope_Crossection_Factor
//T, my precious
//Salmah,  my free spirit
//Sumayyah, most like me, tenacity
//Abdurahman, inventor and kind at heart
//Abdullah, loving, brilliant, charismatic
//Maysoon. exacting, brilliant, caring
//Way cool Zach! Mini me.
Rope_Radius = (Rope_CrossArea/PI)^0.5
```

```
Rope_Diameter = Rope_Radius*2
Rope_Diameter_mm = Rope_Diameter*convert(m,mm)
Rope_Diameter_imp = Rope_Diameter*convert(m,in)

 Rope_Load_Allowable2 =  (Data_Yield_Shaft_Temp)/SafetyFactorCoff
Rope_Load_Allowable_PA2 = Rope_Load_Allowable2*convert(MPa,Pa)

Rope_CrossArea2 = (Load_Total/Rope_Number)*0.5/Rope_Load_Allowable_PA2/Rope_Crossection_Factor
Rope_Radius2 = (Rope_CrossArea2/PI)^0.5
Rope_Diameter2 = Rope_Radius2*2
Rope_Diameter_imp2 = Rope_Diameter2*convert(m,in)

"Taking into account flashpoint of lubricants using lower temp"

Data_Yield_Flashpoint = interpolate1('YieldStress', 'Temp', 'Yield', Temp= Temp_MaxShaft_K)
Data_Tensile_Flashpoint = interpolate1('TensileStrength', 'Temp', 'TensileStrength', Temp = Temp_MaxShaft)

Rope_Load_YieldStrength_fp =Data_Yield_Flashpoint
Rope_Load_Allowable_fp = Data_Yield_Flashpoint/SafetyFactorCoff
Rope_Load_Allowable_PA_fp = Rope_Load_Allowable_fp*convert(MPa,Pa)

Rope_CrossArea_flashpoint = (Load_Total/Rope_Number)/Rope_Load_Allowable_PA_fp
Rope_Radius_flashpoint = (Rope_CrossArea_flashpoint)^0.5/PI
Rope_Diameter_flashpoint = Rope_Radius_flashpoint*2
Rope_Diameter_imp_flashpoint = Rope_Diameter_flashpoint*convert(m,in)


"Energy Decrease for Braking"

DeltaU = (0.5*M_TOTAL*V_BAIL[4]^2)*convert(kg-m^2/s^2,kJ) "For One skip but must be used in 2 skip
design"

"Torque"

Torque_Drum =  Drum_Radius * Mass_Sand* g_phys

{$if parametrictable= 'Test'
//DummyCOF =1
Data_Temp = DataLoad[1]*DataTemp[1]/DataLoad[1]*DummyCOF
$endif}
```

APPENDIX C: DYNAMIC SIMULINK MODEL (DSM)

This appendix contains the Level 1 and Level 2 Schematics for the DSM.

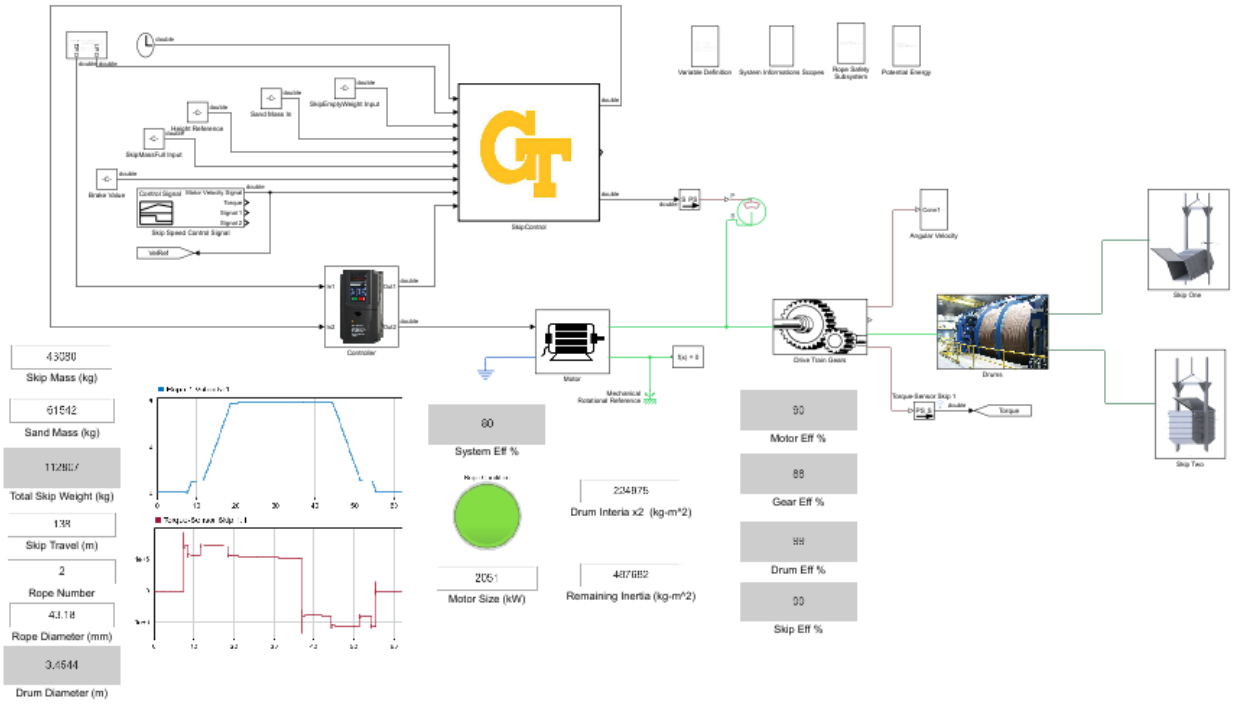

Figure 30 DSM Level 1 Schematic showing overall model

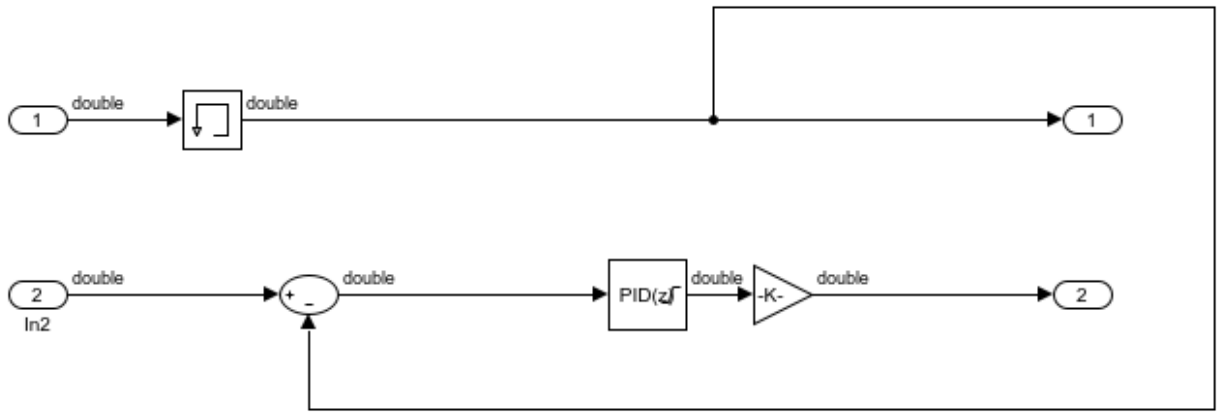

Figure 31 Level 2 Schematic of the DSM speed controller

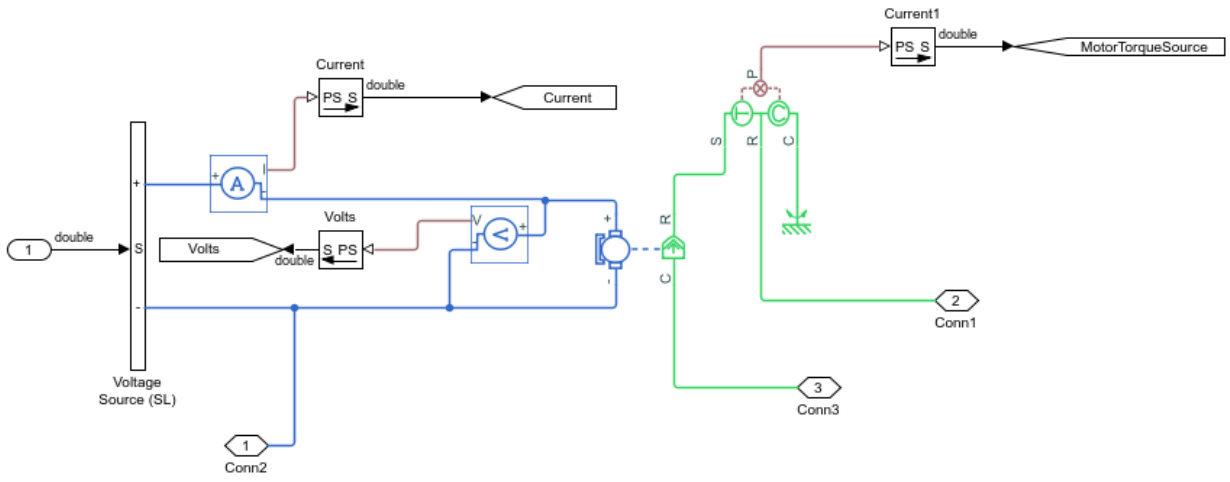

Figure 32 Level 2 Schematic of DSM motor model

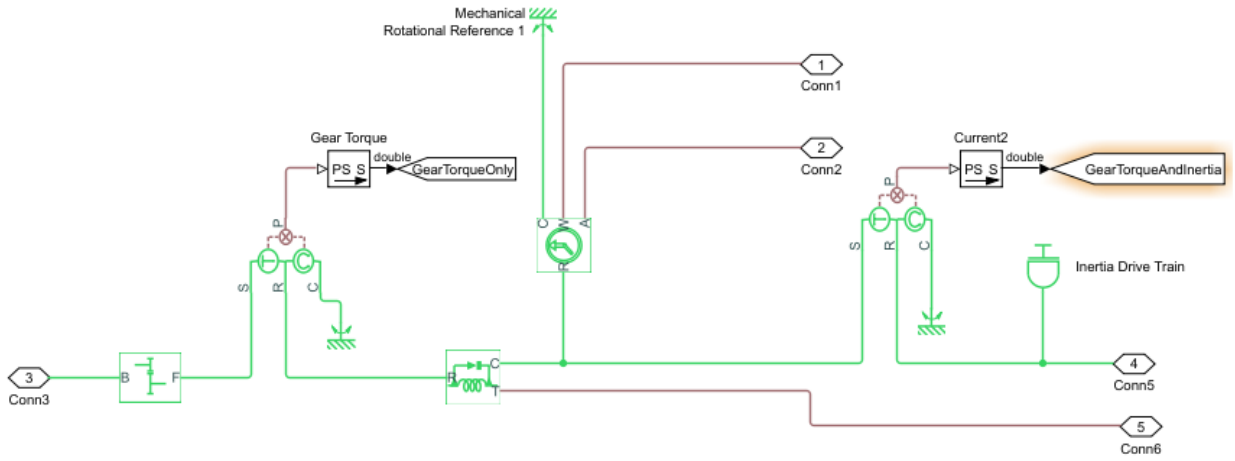

Figure 33 Level 2 Schematic of DSM Gear Train Model

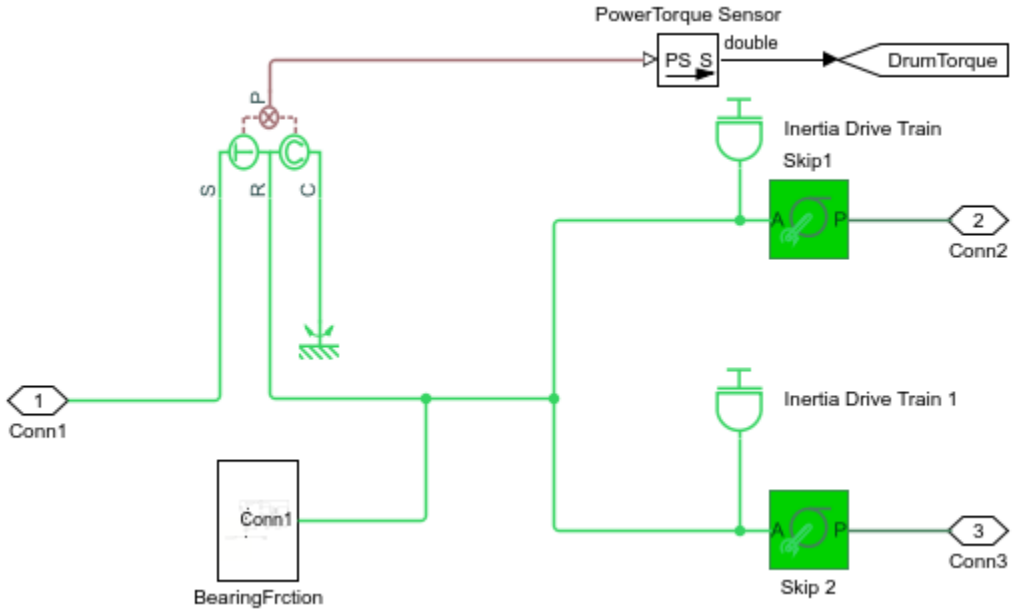

Figure 34 Level 2 Schematic of DSM Mine Hoist and Drums model

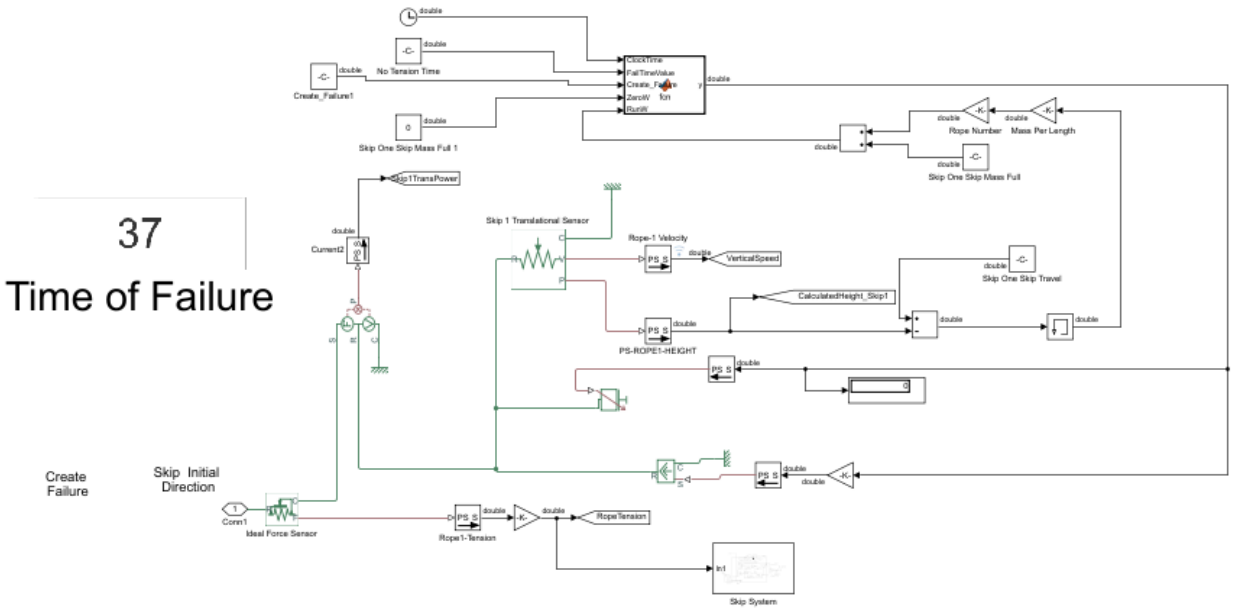

Figure 35 Level 2 Schematic of DSM Skip One Model with Failure Controls

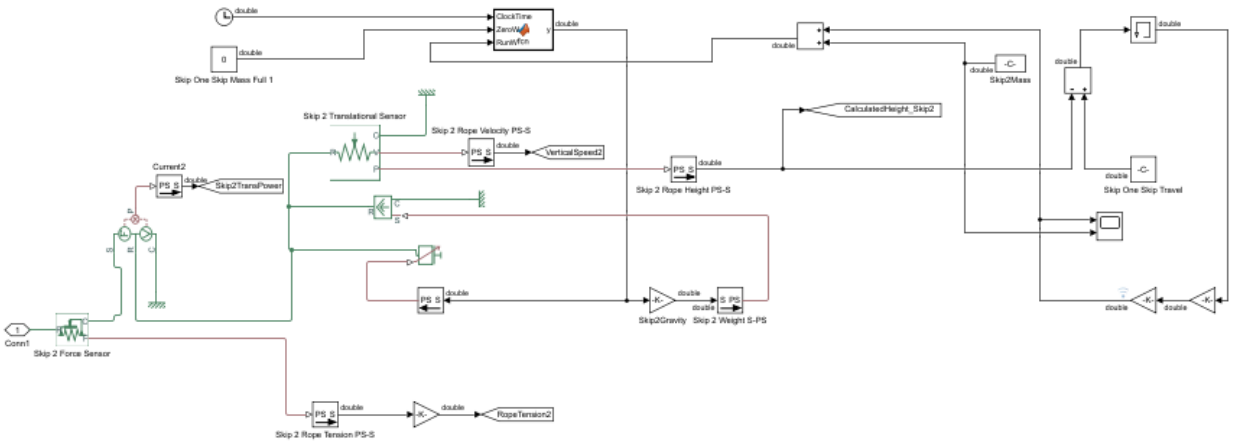

Figure 36 Level 2 Schematic of DSM Skip Two Model

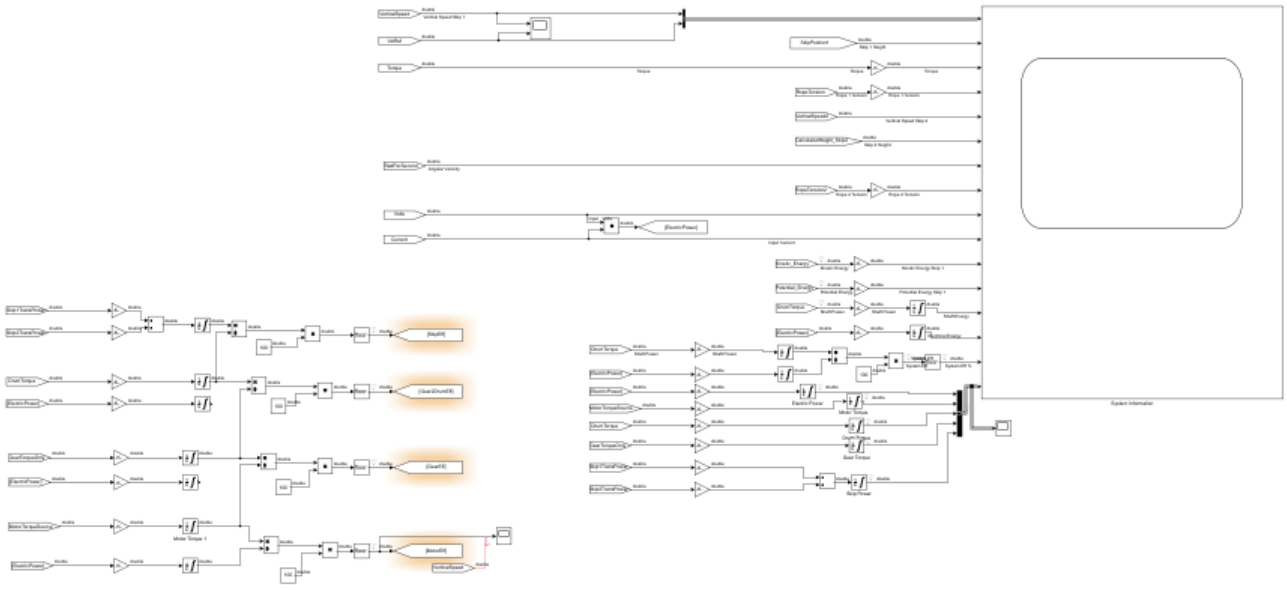

Figure 37 Level 2 Schematic of DSM Signal Monitoring Subsection

REFERENCES

[1] A. C. Ferreira, M. L. Nunes, J. C. F. Teixeira, L. A. S. B. Martins, and S. F. C. F. Teixeira, "Thermodynamic and economic optimization of a solar-powered Stirling engine for micro-cogeneration purposes," *Energy,* vol. 111, pp. 1-17, 9/15/2016 2016.

[2] P. J. Mago and R. Luck, "Potential reduction of carbon dioxide emissions from the use of electric energy storage on a power generation unit/organic Rankine system," *Energy Conversion and Management,* vol. 133, pp. 67-75, 2/1/2017 2017.

[3] A. P. Muroyama, A. J. Schrader, and P. G. Loutzenhiser, "Solar electricity via an Air Brayton cycle with an integrated two-step thermochemical cycle for heat storage based on Co3O4/CoO redox reactions II: Kinetic analyses," *Solar Energy,* vol. 122, pp. 409-418, 2015/12/01/ 2015.

[4] C. Ho *et al.*, "Technology Advancements for Next Generation Falling Particle Receivers," *Energy Procedia,* vol. 49, pp. 398-407, 2014/01/01/ 2014.

[5] J. Vidal, "Molten Salt Technology, Debrief Overview," in *CSP Gen 3 Road Map*, ed: Department of Energy, 2016.

[6] J. M. Hruby, "Technical feasibility study of a solid particle solar central receiver for high temperature applications,"; Sandia National Labs., Livermore, CA (USA)SAND-86-8211; Other: ON: DE86008793 United States Other: ON: DE86008793 NTIS, PC A04/MF A01; 1. SNL English, 1986.

[7] P. K. Falcone, J. E. Noring, and J. M. Hruby, "Assessment of a solid particle receiver for a high temperature solar central receiver system,"; Sandia National Labs., Livermore, CA (USA)SAND-85-8208; Other: ON: DE85008028 United States Other: ON: DE85008028 NTIS, PC A05/MF A01. SNL English, 1985.

[8] M. Murray, "Total System Efficiency," *Power Transmission Engineering,* vol. Feburary 2010, pp. 16-23, 2010.

[9] R. Poore and T. Lettenmaier, "Alternative Design Study Report: WindPACT Advanced Wind Turbine Drive Train Designs Study," National Renewable Energy Laboratory, Kirkland, Washington2003.

[10] R. E. Westney, *The Engineer's Cost Handbook : Tools for Managing Project Costs*. Baton Rouge, UNITED STATES: CRC Press, 1997.

[11] K. Repole and S. Jeter, "Design and Analysis of a High Temperature Particulate Hoist for Proposed Particle Heating Concentrator Solar Power Systems," (in English), *Proceedings of the Asme 10th International Conference on Energy Sustainability, 2016, Vol 1,* 2016.

[12] W. Corp. (2016). *Mining Skip Image*. Available: http://www.wabicorp.com/mine-equipment-division/skips/

[13] C. Prieto, L. Miró, G. Peiró, E. Oró, A. Gil, and L. F. Cabeza, "Temperature distribution and heat losses in molten salts tanks for CSP plants," *Solar Energy,* vol. 135, pp. 518-526, 10/ 2016.

[14] N. Siegel, M. Gross, C. Ho, T. Phan, and J. Yuan, "Physical Properties of Solid Particle Thermal Energy Storage Media for Concentrating Solar Power Applications," *Energy Procedia,* vol. 49, pp. 1015-1023, 2014/01/01 2014.

[15] A. C. Iniesta, M. Diago, T. Delclos, Q. Falcoz, T. Shamim, and N. Calvet, "Gravity-fed Combined Solar Receiver/Storage System Using Sand Particles as Heat Collector, Heat Transfer and Thermal Energy Storage Media," *Energy Procedia,* vol. 69, pp. 802-811, 2015/05/01 2015.

[16] I. Perez Lopez *et al.*, "On-sun operation of a 150 kWth pilot solar receiver using dense particle suspension as heat transfer fluid," *Solar Energy,* vol. 137, pp. 463-476, 11/1/ 2016.

[17] R. C. Knott, D. L. Sadowski, S. M. Jeter, S. I. Abdel-Khalik, H. A. Al-Ansary, and A. El-Leathy, "High Temperature Durability of Solid Particles for Use in Particle Heating Concentrator Solar Power Systems," no. 45868, p. V001T02A041, 2014.

[18] J. Christian and C. Ho, "System Design of a 1 MW North-facing, Solid Particle Receiver," *Energy Procedia,* vol. 69, pp. 340-349, 2015/05/01 2015.

[19] H. Al-Ansary, E. Djajadiwinata, A. El-Leathy, S. Danish, and Z. Al-Suhaibani, "Modeling of Transient Cyclic Behavior of a Solid Particle Thermal Energy Storage Bin for Central Receiver Applications," *Energy Procedia,* vol. 69, pp. 716-725, 2015/05/01 2015.

[20] G. Pahl, K. Wallace, L. n. Blessing, and G. Pahl, *Engineering design : a systematic approach*, 3rd ed. London: Springer, 2007, pp. xxi, 617 p.

[21] K. T. Ulrich and S. D. Eppinger, *Product Design and Development*. McGraw-Hill Education (India) Pvt Limited, 2003.

[22] K. Fu, J. Murphy, M. Yang, K. Otto, D. Jensen, and K. Wood, "Design-by-analogy: experimental evaluation of a functional analogy search methodology for concept generation improvement," (in English), *Research in Engineering Design,* vol. 26, no. 1, pp. 77-95, Jan 2015.

[23] M. K. Thompson, "Improving the requirements process in Axiomatic Design Theory," (in English), *Cirp Annals-Manufacturing Technology,* vol. 62, no. 1, pp. 115-118, 2013.

[24] N. E. Seghedin and D. F. Chitariu, "Software System for the Development of Morphological Matrixes Used in Technical Creation," (in English), *Let's Build the Future through Learning Innovation!, Vol Iv,* pp. 377-383, 2014.

[25] P. G and B. K.H., "Lagebericht. Erfahrungen mit dem methodischen Konstruieren," *Werkstatt und Betrieb,* vol. 114, pp. 773-782, 1981.

[26] B. Rohrbach, "Kreativ nach Regeln eMethode 635, eine neue Technik zum Losen von Problemen," *Absatzwirtschaft,* vol. 12, pp. 73-75, 1969.

[27] J. Beel and S. Langer, "An exploratory analysis of mind maps," presented at the Proceedings of the 11th ACM symposium on Document engineering, Mountain View, California, USA, 2011.

[28] W. Wang, L. Aichmayer, B. Laumert, and T. Fransson, "Design and Validation of a Low-cost High-flux Solar Simulator using Fresnel Lens Concentrators," *Energy Procedia,* vol. 49, pp. 2221-2230, 2014/01/01/ 2014.

[29] N. P. Suh, "Designing-in of quality through axiomatic design," *IEEE Transactions on Reliability,* vol. 44, no. 2, pp. 256-264, 1995.

[30] A. M. Gonçalves-Coelho, G. Neştian, M. Cavique, and A. Mourão, "Tackling with redundant design solutions through axiomatic design," *International Journal of Precision Engineering and Manufacturing,* journal article vol. 13, no. 10, pp. 1837-1843, October 01 2012.

[31] N. P. Suh, *Complexity: Theory and Applications*. Oxford University Press, 2005.

[32] M. M. Tseng and J. Jiao, "A module identification approach to the electrical design of electronic products by clustering analysis of the design matrix," *Computers & Industrial Engineering,* vol. 33, no. 1, pp. 229-233, 1997/10/01/ 1997.

[33] D. E. Whitney, "Manufacturing by Design," (in English), *Harvard Business Review,* vol. 66, no. 4, pp. 83-91, Jul-Aug 1988.

[34] P. Darling, "SME Mining Engineering Handbook," 3rd ed. ed. Littleton :: SME, 2011. [Online]. Available: Ebook Library: https://ebookcentral.proquest.com/lib/swb/detail.action?docID=655790.

[35] *RR-W-410G : "Federal Specifications: Wire Rope and Strand"*, 2007.

[36] A. N. S. LTD., "Section 02 Wire Rope and Strand," ed: A. Noble & Sons LTD., 2016, p. 26.

[37] N. A. Stainless, "Flat Product Stainless Steel Grade Sheet," ed: North American Stainless 2016.

[38] H. S. Inc, "Wire Rope 101,"

[39] U. M. Group, "Wire Rope User Manual," U. M. Group, Ed., ed. Italy: Usha Martin Group, 2015.

[40] CIMAF, "CIMAF Wire Rope Technical Manual," ed, 2013.

[41] *Eurocode 3: Design of steel structures - Part 1-2: General rules - Structural fire design* 2005.

[42] J. Outinen and P. Makelainen, "Mechanical properties of structural steel at elevated temperatures and after cooling down," (in English), *Fire and Materials,* vol. 28, no. 2-4, pp. 237-251, Mar-Aug 2004.

[43] Z. P. Bažant and Q. Yu, "Relaxation of Prestressing Steel at Varying Strain and Temperature: Viscoplastic Constitutive Relation," *Journal of Engineering Mechanics,* vol. 139, no. 7, pp. 814-823, 2013.

[44] K. Repole and S. Jeter, "Application of a Sequence of a Design Methodologies to the Problem of Transporting Warm Particles in Particle Heating Receiver Solar Energy Systems," in *Proceedings, Fifteenth Annual Early Career Technical Conference*, Birmingham, AL, 2015, p. 89.

[45] W. contributors., "Bulk material handling," in *Wikipedia, The Free Encyclopedia*, ed, 2018.

[46] M. M. Tseng and J. Jiao, "A variant approach to product definition by recognizing functional requirement patterns," *Computers & Industrial Engineering,* vol. 33, no. 3, pp. 629-633, 1997/12/01/ 1997.

[47] M. Golob, S. Abdel-Khalik, R. Gill, S. Jeter, and C. Nguyen, "Solar Simulator Test Of Wire Mesh Particle Heating Receiver To Measure Receiver Efficiency," in *Proceedings, Fourteenth Annual Early Career Technical Conference*, Birmingham, AL, 2014, p. 56.

[48] O. E. LLC. (2014). *Product Brochure Olds Elevator LLC*. Available: www.oldsusa.com

[49] Rexnord. (2007). *Rexnord High Performance Bucket Elevators*. Available: www.rexnord.com

[50] R. Koch, *The 80/20 manager : the secret to working less and achieving more*, 1st North American ed.. ed. (Eighty twenty manager). New York: New York : Little, Brown, 2013.

[51] J. Luft and H. Ingham, "The Johari window, a graphic model of interpersonal awareness," *Proceedings of the western training laboratory in group development,* vol. 246, 1955.

[52] H. Courtney, J. Kirkland, and P. Viguerie, "Strategy under uncertainty," *Harvard business review,* vol. 75, no. 6, p. 66, 1997.

[53] J. A. Nelder and R. Mead, "A simplex method for function minimization," *The computer journal,* vol. 7, no. 4, pp. 308-313, 1965.

[54] M. A. Luersen and R. Le Riche, "Globalized Nelder–Mead method for engineering optimization," *Computers & structures,* vol. 82, no. 23-26, pp. 2251-2260, 2004.

[55] B. Selman and H. A. Kautz, "An empirical study of greedy local search for satisfiability testing," in *AAAI*, 1993, vol. 93, pp. 46-51.

[56] B. Schwartz, "Analysis of Sand Lift (Internal Report)," Georgia Institute of Technology, Atlanta GA2014.

[57] W. Corp. (2015). *Ore Skips, Mine Haulage Systems and Other Foundry Products in Ontario*. Available: http://www.wabicorp.com

[58] J. D. l. Vergene, *Hard Rock Miner's Handbook*, 3 ed. Ontario, Canada.: McIntosh Engineering, 2003.

[59] J. E. Shigley and C. R. Mischke, *Mechanical engineering design*, 5th ed. (McGraw-Hill series in mechanical engineering). New York: McGraw-Hill, 1989, pp. xxv, 779 p.

[60] *29 CFR 1926.251: "Safety and Health Regulations for Construction"* 2010.

[61] *30 CFR 57.19019: "Regulation on Guide Ropes."*, 2014.

[62] J. Shao, F. Lu, C. Zeng, and M. Xu, "Research Progress Analysis of Reliability Design Method Based on Axiomatic Design Theory," *Procedia CIRP,* vol. 53, pp. 107-112, 01/ 2016.

[63] B. P. Nepal, O. P. Yadav, L. Monplaisir, and A. Murat, "A framework for capturing and analyzing the failures due to system/component interactions," *Quality and Reliability Engineering International,* vol. 24, no. 3, pp. 265-289, 2008.

[64] M. Sy and C. Mascle, "Product design analysis based on life cycle features," *Journal of Engineering Design,* vol. 22, no. 6, pp. 387-406, 2011/06/01 2011.

[65] K. Repole and S. Jeter, "Preliminary Commercial Design For Transporting Low Temperature Particles for Use in Particle Solar Receivers Using Lifting Skips," in *Proceedings, Fourteenth Annual Early Career Technical Conference*, Birmingham, AL, 2014, p. 63.

[66] *49 CFR 192.111 : "Design Factor for Steel Pipe."*, 2014.

[67] F. Company, "Personal Communication," ed: FLSmidth Company, 2016.

[68] Y. X. Wu, C. J. Zhang, H. B. Huo, and C. Q. Zhou, "Design and Simulation of Fuzzy-PID DC Governor System Based on Mine Hoist," *Applied Mechanics and Materials,* vol. 341-342, pp. 834-838, 2013.

[69] Q. Yi-bin, W. Xiao-jie, and L. Xiang-chao, "Digital distance control system research and implementation," *Procedia Earth and Planetary Science,* vol. 1, no. 1, pp. 1375-1379, 2009/09/01/ 2009.

[70] R. Automation, "AC and DC Variable Speed Drives Application Consideration," no. Publication D-7725, 04/2000 2000.

[71] M. Lee, T. Kim, H.-K. Jung, U.-K. Lee, H. Cho, and K.-I. Kang, "Green construction hoist with customized energy regeneration system," *Automation in Construction,* vol. 45, pp. 66-71, September 2014 2014.

[72] S. Tominaga, I. Suga, H. Araki, H. Ikejima, M. Kusuma, and K. Kobayashi, "Development of energy-saving elevator using regenerated power storage system," in *Power Conversion Conference, 2002*, Osaka, 2002, vol. 2, pp. 890-895.

[73] S. Acquaviva, "Energy Storage and Recovery System for Lift," in *Elevcon 2014*, Paris, 2014, pp. 168-178.

[74] K. K. D. Repole and S. M. Jeter, "Design and Analysis of a High Temperature Particulate Hoist for Proposed Particle Heating Concentrator Solar Power Systems," (in English), *Proceedings of the Asme 10th International Conference on Energy Sustainability, 2016, Vol 1,* 2016.

[75] U. S. D. o. E. O. o. E. Efficiency, R. Energy, U. S. D. o. E. O. o. Scientific, and T. Information, *Improving Motor and Drive System Performance: A Sourcebook for Industry*. United States. Department of Energy. Office of Energy Efficiency and Renewable Energy, 2010.

[76] USBM, "Mining and beneficiation of metallic and nonmetallic minerals expected fossil fuels in the United States and Canada," pp. Open file report 10-87, 1987.

[77] A. Sayadi, A. Lashgari, K. Oraee, and M. Yavari, "Hoisting Equipment Cost Estimation in Underground Mines," in *SME International Conference on Hoisting and Haulage*, Las Vegas, USA., 2010.

[78] M. S. Peters, *Plant design and economics for chemical engineers*, 5th ed. / Max S. Peters, Klaus D. Timmerhaus, Ronald E. West.. ed. New York: New York : McGraw-Hill, 2003.

[79] D. E. Garrett, *Chemical engineering economics*. New York: New York : Van Nostrand Reinhold, 1989.

[80] R. S. Means. (2015). *Construction Cost Guides*. Available: http://www.rsmeans.com

[81] C. W. S. J.F. Britt, H. L. Davey, *GM Transportation Systems Center: Heliostat production evaluation and cost analysis: executive summary*. Department of Energy, Solar Energy Research Institute, General Motors Corporation, 1979.

[82] M. T. Pauken, C. J. Fernandez, and S. M. Jeter, "Expendable Cooling for a One-Day Venus Lander," in *11th International Planetary Probe Workshop*, 2014, vol. 1795.